*Report of Investigations No. 132*

DOE/ET/27111--T2

DE84 004396

# *CONTINUITY AND INTERNAL PROPERTIES OF GULF COAST SANDSTONES AND THEIR IMPLICATIONS FOR GEOPRESSURED FLUID PRODUCTION*

*R. A. Morton,*
*T. E. Ewing,*
*and N. Tyler*

*Assisted by*
*B. E. Bullock*





*1983*

*BUREAU OF ECONOMIC GEOLOGY*

*W. L. Fisher, Director*
*The University of Texas at Austin*
*Austin, Texas 78712*

*Research funded by the U.S. Department of Energy,*
*Division of Geothermal Energy,*
*Contract No. DE-AC08-79ET27111*

## DISCLAIMER

# CONTENTS

## *FIGURES*

# TABLES

# ABSTRACT

*Continuity of sandstone reservoirs is controlled by various factors, including faults, sand-body geometry, and the distribution of framework grains, matrices, and interstices within the sand body. Except for faults, these factors are largely inherited from the depositional environment and modified during sandstone compaction and cementation. Regional and local continuity of Gulf Coast sandstone reservoirs depends on a four-level depositional and structural hierarchy: (1) genetically related sandstones commonly associated with a single depositional system, (2) areally extensive fault blocks, (3) individual sandstones within a fault block, and (4) isolated reservoirs within a fault-bounded sandstone.*

*Published and unpublished data on Tertiary and late Quaternary Gulf Coast sandstones of fluvial, deltaic, barrier-strandplain, and submarine channel and fan origins suggest that volumes of sand systems (first hierarchical level) are about $10^{11}$ to $10^{13}$ $ft^3$, whereas volumes of individual sand bodies are about $10^9$ to $10^{11}$ $ft^3$. The continuity and productive limits of ancient sandstones are substantially reduced by faults and internal heterogeneities, which further subdivide sand bodies into individual compartments. In the Wilcox Group and Frio Formation trends of Texas, fault blocks (second hierarchical level) vary greatly in size, most being between 0.3 and 52 $mi^2$; however, the distribution of fault blocks is strongly skewed toward small areas (<10 $mi^2$). Volumes of individual reservoirs (fourth hierarchical level) determined from engineering production data range from 50 percent less to 200 percent more than volumes estimated by geologic mapping. In general, mapped volumes are less than production volumes for reservoirs in which faults are nonsealing and are greater than production volumes for reservoirs in which laterally continuous shale breaks cause reductions in permeability.*

*Gross variations in the pore properties (porosity and permeability) of a reservoir can be predicted by examining its internal stratification and its sandstone facies if original sedimentological properties are not masked by diagenetic alterations. Six patterns are recognized that describe, in general, the vertical variations in pore properties within a sand body at a well site. Core analyses show (1) upward increases, (2) upward decreases, (3) central increases, (4) central decreases, (5) uniformly low values, and (6) irregular changes in porosity and permeability with depth. Within these trends, porosity and permeability are generally highest in large-scale crossbedded intervals and lowest in contorted, bioturbated intervals and intervals of small-scale ripple cross-laminations.*

*Sandstone facies models and the regional structural fabric of the Gulf Coast Basin both suggest that large and relatively continuous reservoirs should be found where barrier-strandplain and delta-front sandstones parallel regional faults. These conditions should optimize the yield and rate of fluid production from geopressured geothermal aquifers and maximize the efficiency of primary and enhanced recovery of conventional hydrocarbons. Thick fluvial-channel deposits trending roughly normal to regional faults are laterally less continuous than barrier and delta-front sandstones, but they may also be significant targets for exploration and production of unconventional and conventional energy resources.*

*Keywords: Texas, Gulf Coastal Plain, Tertiary, sediments, structure contour maps, stratigraphic maps, reservoir properties, sand bodies, geothermal energy.*

# INTRODUCTION

Sandstone reservoirs are confined by lateral and vertical changes in primary rock properties such as grain size, porosity, and permeability, which are largely inherited from the depositional environment. Equally important in reservoir characterization are postdepositional events, including structural deformation and diagenetic alteration; these events cause major reductions in reservoir transmissivity. Studies of modern clastic environments and their ancient counterparts have resulted in conceptual models of the most common sandstone facies. These models have established criteria for interpreting genetic depositional systems from well cuttings, cores, and geophysical logs (Fisher and Brown, 1972; Fisher and others, 1969) and for predicting the geometry and continuity of many sandstone reservoirs (LeBlanc, 1977; Sneider and others, 1977).

In the Gulf Coast Basin, the common sandstone facies are products of deposition in fluvial, deltaic, barrier-strandplain, transgressive marine, and shelf-slope systems. These sandstone systems, which are major hydrocarbon reservoirs and which commonly form aquifers in the geopressured zone, exhibit certain predictable properties. Studies of reservoir continuity that jointly examine sedimentological characteristics and engineering data on sandstone reservoirs should improve our capabilities for predicting those properties and thereby enhance development of our energy resources. Toward that aim, this report systematically investigates, classifies, and differentiates the intrinsic properties of the genetic sandstone units that typify many geopressured geothermal aquifers and hydrocarbon reservoirs in the Gulf Coast region.

## *QUANTIFICATION OF INHOMOGENEITIES*

Identifying geological factors suitable for reservoir discrimination requires (1) compilation of selected geologic data on ancient sandstones and modern analogs and (2) examination of production data from selected reservoirs. The first type of data was reported by Pryor (1973), who analyzed nearly 1,000 sediment samples taken from three modern depositional environments. Pryor concluded that point-bar and beach sands have directional permeabilities, whereas porosity and permeability in eolian dunes vary little and exhibit no discernible trends.

Investigations of the internal properties of sandstones from cores and outcrops permit relative ranking of the production potential of sandstone aquifers and hydrocarbon reservoirs. Results identify

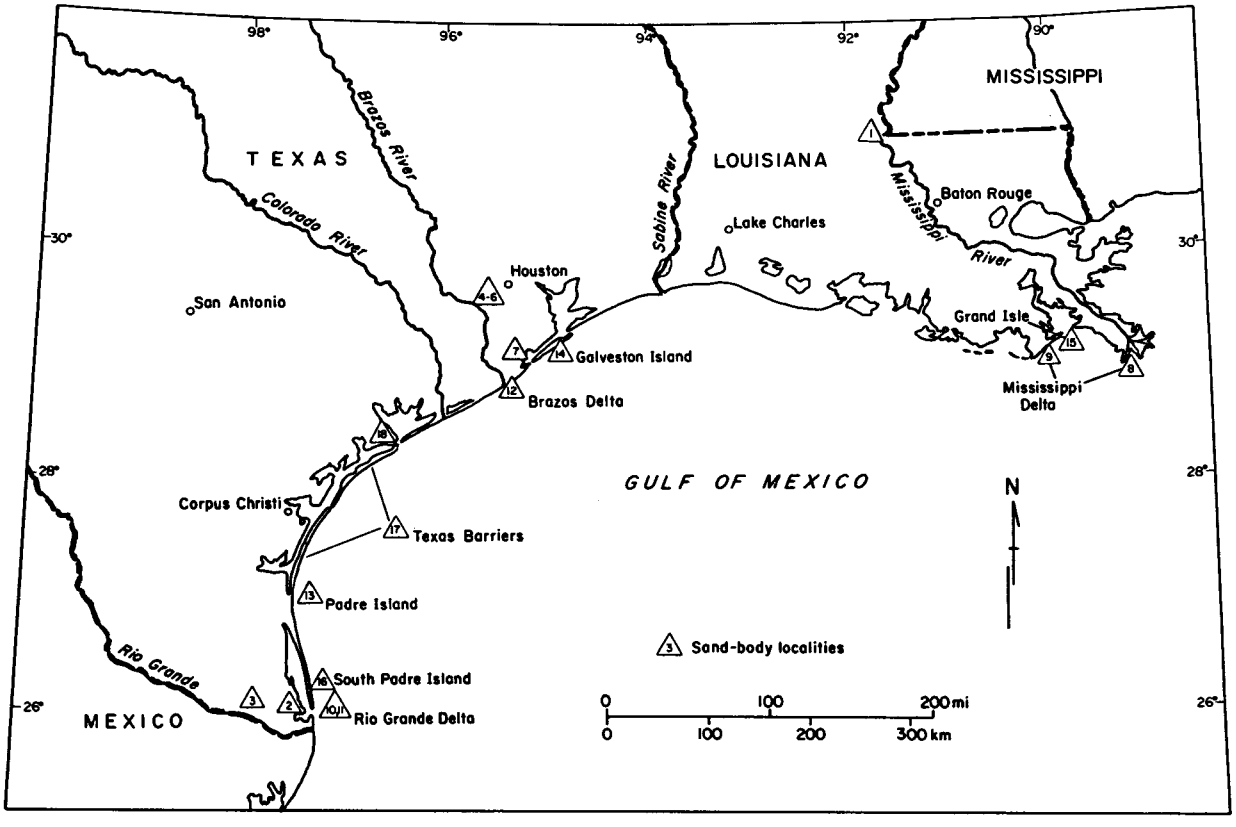


*Figure 1.* Locations of sand bodies listed in table 1.

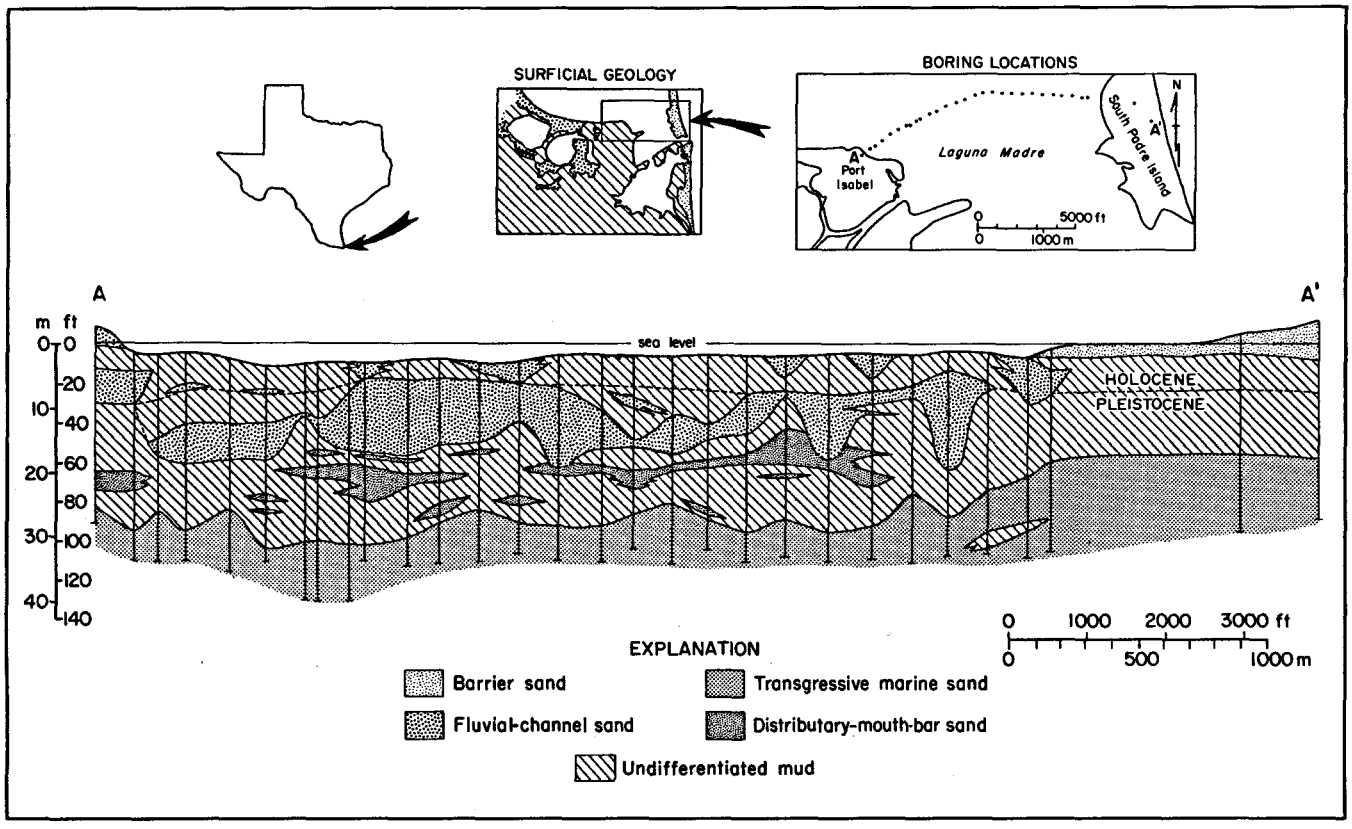


*Figure 2.* Stratigraphic section of late Quaternary Rio Grande deltas near South Padre Island. Interpreted from descriptions of borings provided by the Texas Department of Highways and Public Transportation.

the sandstone facies that are likely to exhibit less variability because of their internal stratification and other physical qualities, such as pore-space distribution and frequency and position of shale breaks. Most studies based on outcrop samples and subsurface cores (for example, Polasek and Hutchinson, 1967) recognize that reservoir heterogeneity is related to internal stratification but do not address the broader issue of how to apply this knowledge to the construction of sandstone models in order to improve predictive capabilities.

Attempts to quantify sand-body geometry and reservoir inhomogeneities have been unsuccessful because of difficulties inherent in subsurface correlations, lack of precise geological boundaries, and spatially discontinuous data. However, at least two ways to quantify reservoir continuity and internal heterogeneity have been proposed.

Fulton (1975) used a continuity index to describe spatial variations in sandstones of the ancestral Rio Grande delta (fig. 1). He defined horizontal continuity as the ratio of sand-body length to cross-section length, and vertical continuity as the ratio of maximum thickness of continuous sand to total sand thickness. The numerical values reported in that study are not necessarily accurate because the boundaries and dimensions used to calculate the index were constrained by the cross sections themselves. Nevertheless, Fulton's study demonstrates, as do many others, that (1) fluvial sands are more continuous in directions parallel to progradation than in directions perpendicular to progradation, (2) delta-front sands are widely distributed and are nearly continuous both along strike and in updip and downdip directions, and (3) prodelta sands are thin and highly discontinuous, having greatest continuity in directions parallel to progradation. Although not evaluated by Fulton (1975), the transgressive marine sand (a reworked meanderbelt deposit) underlying the progradational sequence (fig. 2) represents the most continuous and areally extensive sand within his study area.

Polasek and Hutchinson (1967) used a heterogeneity factor to quantify the layering and abundance of shaly material in sand sequences. In that study, heterogeneity factors were determined empirically for several producing reservoirs but were not related to sandstone facies or depositional environment. Because geological factors were not included, the predictive capabilities of this method are unknown.

Reservoir heterogeneities have also been statistically treated to explain the high variability in numerical evaluations. Normal and log-normal distributions that characterize porosity and permeability measurements grouped by depth (Law, 1944; Polasek and Hutchinson, 1967) are adequate for summarizing general reservoir properties; however, as predictors they are less useful than the geological models that explain spatial variability of pore-space properties within and among sandstone units.

# STRUCTURAL AND STRATIGRAPHIC LIMITS OF SANDSTONE RESERVOIRS

## *SAND-BODY AND RESERVOIR HIERARCHY*

Depositional and structural conditions within a four-level hierarchy control the volume and areal extent of sandstone reservoirs. The first level includes the entire reservoir interval, or aquifer system, which spans several hundred to several thousand feet of interbedded sand and shale. Commonly, sandstones within the reservoir interval are genetically related and are associated with a single depositional system. Large fault blocks encompassing the reservoir interval make up the second hierarchical level. Third and fourth levels are individual sandstones within a fault block and isolated reservoirs within an individual fault-bounded sandstone, respectively.

Modern and ancient sandstones of regional and local scale can be grouped and measured according to the first and third levels of the hierarchy (genetically related sequences and individual sandstones, respectively). This makes distinction between local sand features and the sand trends of regional or continental proportion important to predicting the size and arrangement of prospective sand bodies. The fourth hierarchical level comprises those conditions in which interbedded shales or other permeability barriers within the sandstones reduce the effective reservoir volume. This level does not include potential increases in reservoir energy or capacity resulting from external contributions, such as shale dewatering or nonsealing faults.

## *POSSIBLE EXTERNAL CONTRIBUTIONS*

Marked decreases in permeability define the reservoir boundaries and limit the volume of sediment from which fluids can be produced. These permeability changes usually occur along the margins of a sand body; therefore, fluid withdrawal is chiefly from a single sand (simple or composite) within a fault block. Fluids might enter producing reservoirs across faults or from surrounding shales; however, generally these influxes are either regarded as minor or are ascribed to unique circumstances that would not affect cumulative production from most reservoirs. At present, the importance of nonsealing faults and the extent of shale dewatering are unknown in all but a few fields; hence, faults and shales should not be eliminated as potential sources of fluid.

Theoretical studies and field observations have demonstrated that some faults do not prevent lateral migration of fluids; migration occurs, for example, when correlative sand bodies are juxtaposed across the fault (Smith, 1980). Although this theory primarily deals with entrapment of hydrocarbons in the hydropressured zone, it also applies to water movement in the geopressured zone.

Structure maps of several Tertiary sandstone reservoirs in Louisiana (Smith, 1980) suggest that minor faults may not be complete barriers to flow because lithologies and capillary properties across the faults are similar. These observations suggest that if sand thickness exceeds fault displacement, effective volumes of hydrocarbon reservoirs and geopressured aquifers may not be limited by minor faults.

The areal limits of water production from reservoirs and associated aquifers are usually uncertain. A significant reduction in reservoir pressure during production might cause an influx of water from shales surrounding the aquifer. In addition to minimizing pressure decline in the reservoir, shale recharging could substantially increase the effective reservoir volume beyond the sand-body limits. Theoretically, the vast surface area along sand margins and along interbedded shales would provide many pathways for fluid invasion despite the low permeabilities at these boundaries. Field data (Wallace, 1969) and reservoir simulations (Chierici and others, 1978; Garg, 1980) indicate that only reservoirs having long life expectancies would be noticeably enhanced by shale compaction and fluid expulsion. Even under ideal circumstances, it appears doubtful that substantial volumes of shale water would flow to the well bore, given the anticipated high flow rates and rapid drawdown of most geopressured reservoirs.

The vertical permeability of shale is a prime factor controlling the influx of shale-derived water (Garg, 1980). Because in situ shale permeabilities are poorly documented and production data are sparse, the reliability of dewatering predicted by model studies is uncertain. Undoubtedly, new knowledge will be gained by production from several design wells. A major objective of the Dow-Department of Energy L. R. Sweezy No. 1 well in the Parcperdue field (Vermilion Parish, Louisiana) is to determine the magnitude of shale dewatering in an areally limited geopressured reservoir.

# CHARACTERISTICS AND DIMENSIONS OF GULF COAST SANDSTONES

The northwest margin of the Gulf of Mexico has been an area of active sedimentation for millions of years; it is also the site of exploration and production of hydrocarbons contained in the thick clastic sequences of the Gulf Coast Basin. The near-surface geology of the Gulf Coast has been documented in detail because the

area is accessible, the depositional environments are diverse, and the research is applicable to energy resource exploration elsewhere. Studies of modern and ancient depositional systems along the Gulf Coast have improved our capabilities for predicting the external geometry and internal properties of sandstone reservoirs.

## *LIMITATIONS OF DATA*

Reservoir studies that integrate surface exposures, electric logs, seismic sections, and subsurface cores provide a more complete picture than any single data base of rock properties inherited from the original depositional environment and added by subsequent diagenetic modifications. In the Gulf Coast region, modern sand-rich environments are commonly analogous to ancient sedimentary deposits; therefore, surficial exposures of sand bodies provide excellent control on textures, directional properties, bed continuities, and spatial relationships with surrounding sediments. Analyses of modern sand bodies, however, tend to overestimate certain reservoir properties (volume, porosity, and permeability) because compaction, cementation, and structural deformation have not occurred. In contrast, studies of ancient sandstones yield more realistic approximations of reservoir conditions because they examine what is actually preserved over broad areas.

Common disadvantages of subsurface studies are (1) the lack of dense subsurface control, (2) the necessity of indirectly measuring geological parameters, and (3) the uncertainty of log correlations in structurally complex areas. These factors greatly influence stratigraphic interpretations and paleogeographic reconstructions, which in turn affect general characterizations and volumetric estimates of particular sand bodies (tables 1, 2, and 3). Volumetric estimates are only accurate within an order of magnitude because (1) sandbody dimensions are averaged and (2) at least one dimension is usually either an arbitrary truncation (dip direction for channels, strike direction for barriers) or the limit of available data. Despite these discrepancies, data show that individual sand bodies (third hierarchical level) contain about $10^9$ to $10^{11}$ $ft^3$ of sand, whereas sand systems (first hierarchical level) contain about $10^{11}$ to $10^{13}$ $ft^3$ (tables 1, 2, and 3). (Metric conversion factors are given in appendix A.)

## *LATE QUATERNARY SEDIMENTS*

Most sands deposited during the late Quaternary Period remain unconsolidated, exhibiting characteristics established when they were initially deposited. By studying these geologically young sand bodies, we can begin to understand the physical and chemical changes that occur during burial. It should be noted, however, that some Holocene sand systems (table 1) are smaller than their ancient counterparts (table 2) because changes in relative sea level and vertical stacking of sand bodies have been minimal during the past few thousand years.

## Fluvial Sandstones

Along the Gulf Coastal Plain, fluvial channels commonly meander, whereas distributary channels are relatively stable because of lower gradients and mud-rich delta-plain deposits, which inhibit lateral migration of the channels. Either channel type may contain clay plugs as abandoned-channel fill. The locations of such major discontinuities are usually unpredictable unless well control is fairly dense. However, as shown by Galloway (1968) and others, clay plugs are easily distinguished on electric logs and are well documented. Within a fluvial system, grain size generally decreases downstream; but at the scale of most reservoirs, vertical and cross-channel changes in grain size are more important to reservoir performance.

### *Mississippi River*

Point-bar deposits of the Mississippi River were described by Frazier and Osanik (1961), who reported that sedimentary structures within the middle and lower point-bar deposits of this major river were mainly festoon crossbeds or large-scale scour and fill features. The fluvial sands thin rapidly and are replaced by silts and clays deposited as natural levees and abandoned-channel fill. These fine-grained discontinuities would disrupt fluid flow across the sand body but would not necessarily interfere with fluid movement parallel to the channel axis.

The Mississippi River point-bar deposit described by Frazier and Osanik (1961) is 75 ft thick and about 4 mi wide; it contains approximately 41 Bcf (billion $ft^3$) of sand. As expected, the size and volume are greater than those of other individual fluvial sands (table 1).

### *Rio Grande*

Frequent discontinuities in fluvial sands were also recognized by Fulton (1975), who used numerous borings and electric logs to delineate the geometry of sandstone facies of the Rio Grande fluvial system. A cross section (fig. 2) through the same stratigraphic interval studied by Fulton (1975) illustrates the thickness and continuity of fluvial sands in a downstream (dip) direction.

Channels of the Holocene Rio Grande average 15 to 30 ft thick (table 1); progressively younger channels are thinner. Such chronological relationships are common where thin but areally extensive alluvial-plain and upper delta-plain sediments were deposited over older, more stable fluvial deposits. Channel sands of late Pleistocene age vary widely in thickness (fig. 2) because of the abundance of clay plugs. Channel deposits up to 65 ft thick and containing about 800 Bcf of sand

*TABLE 1. Approximate dimensions of late Quaternary Gulf Coast sand bodies.*

| FEATURE | SAND | AGE | THICK-NESS (ft) | LENGTH (ft x $10^3$) | WIDTH (ft x $10^3$) | SAND VOLUME ($ft^3$ x $10^9$) | REFERENCE |
|---|---|---|---|---|---|---|---|
| FLUVIAL | | | | | | | |
| 1. Mississippi River | point bar | Holocene | 75 | 26 | 21 | 41 | Frazier and Osanik (1961) |
| 2. Rio Grande | fluvial channel | Holocene | 15 | 40 | 10 | 6 | Fulton (1975) |
| 3. Rio Grande | fluvial system | Pleistocene | 65 | 237 | 53 | 816* | Brown and others (1980) |
| 4. Brazos River | point bar | Holocene | 55 | 6 | 3 | <1 | Bernard and others (1970) |
| 5. Brazos River | fluvial channel | Holocene | 40 | 53 | 8 | 17 | Bernard and others (1970) |
| 6. Brazos River | fluvial system | Holocene | 40 | 264 | 63 | 665* | Bernard and others (1970) |
| 7. Brazos River | fluvial system | Pleistocene | 25 | 316 | 158 | 1,248* | Winker (1979) |
| DELTAIC | | | | | | | |
| 8. Mississippi delta | distributary-mouth bar | Holocene | 100 | 21 | 5 | 11 | Fisk (1961) |
| 9. Mississippi delta | delta-front system | Holocene | 40 | 317 | 80 | 1,014* | Fisk (1955) |
| 10. Rio Grande delta | distributary-mouth bar | Pleistocene | 10 | 17 | 15 | 3 | figure 2 and Fulton (1975) |
| 11. Rio Grande delta | transgressive marine | Holocene | 30 | 53 | 16 | 25 | Fulton (1975) |
| 12. Brazos delta | delta system | Holocene | 25 | 8 | 10 | <2* | figure 3 and Bernard and others (1970) |
| BARRIER STRANDPLAIN | | | | | | | |
| 13. Padre Island | barrier | Holocene | 40 | 105 | 26 | 109 | Fisk (1959) |
| 14. Galveston Island | barrier | Holocene | 30 | 137 | 13 | 53 | Bernard and others (1970) |
| 15. Grand Isle | barrier | Holocene | 20 | 20 | 4 | 2 | Conatser (1971) |
| 16. South Padre Island | barrier | Holocene | 12 | 105 | 5 | 6 | Morton and McGowen (1980) |
| 17. Texas barrier islands | barrier system | Holocene | 40 | 1,056 | 15 | 633* | Morton and McGowen (1980) |
| 18. Ingleside strandplain | strandplain system | Pleistocene | 60 | 528 | 53 | 1,679* | Winker (1979) |

*Numbers keyed to figure 1.* **system scale*

represent a major river system that built a relatively large delta (70 to 160 ft thick) extending more than 50 mi along strike and more than 20 mi across the inner shelf. Because of their depositional setting, the late Pleistocene channels are probably analogous to many of the Tertiary fluvial sandstones associated with stable platform deposits.

## *Brazos River*

The Blasdel point bar of the Brazos River (Bernard and others, 1970) displays an upward-fining sequence accompanied by an upward decrease in scale of primary sedimentary structures. The vertical succession of structures from lower point-bar to floodbasin deposits is (1) large-scale trough cross-stratified sand having some minor clay partings separating foreset units, (2) horizontally stratified sand having interlaminated silt and clay, (3) small-scale trough cross-stratified sand and silt having clay drapes, and (4) laminated sandy clay and silt. The Blasdel point bar and the Wallis point bar, described by Morton and McGowen (1980), show that the thickness and frequency of mud partings increase toward the top of the deposit, and the proportion

*TABLE 2. Approximate dimensions of Tertiary Gulf Coast sand bodies.*

| AREA | FORMATION | POROSITY (%) | PERMEABILITY (md) | THICKNESS (ft) | LENGTH (ft x $10^3$) | WIDTH (ft x $10^3$) | SAND VOLUME ($ft^3$ x $10^9$) | REFERENCE |
|---|---|---|---|---|---|---|---|---|
| FLUVIAL | | | | | | | | |
| East Texas | Wilcox | – | – | 300 | 106 | 53 | 1,685* | Fisher and McGowen (1967) |
| Seeligson, Tex. | Frio | – | – | 40 | 40 | 13 | 21 | Nanz (1954) |
| Central Texas coast | Miocene | – | – | 200 | 106 | 185 | 3,922* | Solis Iriarte (1980) |
| Central Texas coast | Miocene | – | – | 150 | 211 | 37 | 1,171* | Doyle (1979) |
| Austin Bayou, Tex. | Frio | 21 | 211 | 60 | 26 | 26 | 42 | Morton and others (1980) |
| Central Louisiana | Wilcox | – | – | 130 | 32 | 8 | 33 | Galloway (1968) |
| Main Pass, La. | Miocene | 34 | 3,000 | 35 | 16 | 2 | 1 | Hartman (1972) |
| DELTAIC | | | | | | | | |
| Cook field, Tex. | Wilcox | 25 | 242 | 60 | 74 | 16 | 71 | Bebout and others (1982) |
| Austin Bayou, Tex. | Frio | 20 | 40 | 60 | 106 | 37 | 235 | Bebout and others (1978) |
| Austin Bayou, Tex. | Frio | – | – | 400 | 106 | 53 | 2,247* | Bebout and others (1978) |
| Central Texas coast | Miocene | – | – | 500 | 317 | 79 | 12,522* | Solis Iriarte (1980) |
| Central Texas coast | Miocene | – | – | 300 | 686 | 105 | 21,609* | Doyle (1979) |
| South Texas | Wilcox | – | – | 100 | 211 | 79 | 1,667* | Edwards (1980) |
| E. White Point field, Tex. | Frio | – | – | 300 | 20 | 15 | 90 | Martyn and Sample (1941) |
| Upper Texas coast | Vicksburg | – | – | 30 | 700 | 150 | 3,150* | Gregory (1966) |
| Louisiana onshore | Miocene | – | – | 300 | 370 | 105 | 11,655* | Curtis (1970) |
| BARRIER AND STRANDPLAIN | | | | | | | | |
| SW. Lake Arthur, La. | Frio | 30 | 2,000 | 15 | 40 | 8 | 5 | Gotautas and others (1972) |
| Chandeleur Sound, La. | Miocene | 33 | 1,680 | 60 | 7 | 5 | 2 | Woltz (1980) |
| Milbur, Tex. | Wilcox | 34 | 600 | 15 | 35 | 10 | 5 | Chuber (1972) |
| Hardin County, Tex. | Yegua | 27 | 2,200 | 35 | 10 | 1 | <1 | Casey and Cantrell (1941) |
| Jim Hogg County, Tex. | Jackson | – | – | 35 | 158 | 53 | 292 | Freeman (1949) |
| Central Texas coast | Wilcox | – | – | 400 | 400 | 158 | 25,280* | Fisher and McGowen (1967) |
| Central Texas coast | Frio | – | – | 1,000 | 317 | 68 | 21,556* | Boyd and Dyer (1966) |
| Central Texas coast | Miocene | – | – | 450 | 211 | 53 | 5,032* | Solis Iriarte (1980) |
| NE. Thompsonville field, Tex. | Wilcox | 20 | 140 | 75 | 32 | 4 | 10 | Young (1966) |
| SUBMARINE CHANNEL AND FAN | | | | | | | | |
| Katy, Tex. | Wilcox | 12 | ~1 | 100 | 32 | 25 | 80 | DePaul (1980) |
| McAllen Ranch, Tex. | Vicksburg | 15 | ~1 | 60 | 30 | 15 | 27 | Berg and others (1979) |
| Port Acres/Port Arthur, Tex. | Hackberry | 29 | 275 | 450 | 23 | 16 | 165* | Halbouty and Barber (1961) |
| NE. Thompsonville field, Tex. | Wilcox | 15 | 28 | 50 | 22 | 15 | 17 | Berg and Tedford (1977) |
| Port Acres/Port Arthur, Tex. | Hackberry | – | – | 300 | 32 | 11 | 105* | Weise and others (1981) |

**system scale*

*TABLE 3. Approximate dimensions of non-Gulf Coast sand bodies.*

| AREA | AGE | POROSITY (%) | PERMEABILITY (md) | THICKNESS (ft) | LENGTH (ft x $10^3$) | WIDTH (ft x $10^3$) | SAND VOLUME (ft$^3$ x $10^9$) | REFERENCE |
|---|---|---|---|---|---|---|---|---|
| FLUVIAL | | | | | | | | |
| Elk City field, Okla. | Pennsylvanian | 10-15 | 75-1,500 | 50 | 10 | 4 | 2 | Sneider and others (1977) |
| Rhône River, France | Holocene | -- | -- | 7 | 10 | 8 | <1 | Oomkens (1970) |
| Clinton delta, Ohio | Silurian | -- | -- | 20 | 16 | 2 | <1 | Overbey and Henniger (1971) |
| Coyote Creek field, Wyo. | Cretaceous | 15 | 200 | 50 | 20 | 4 | 4 | Berg and Davies (1968) |
| Fry area, Ill. | Pennsylvanian | 14-25 | 10-1,200 | 30 | 12 | 3 | 1 | Hewitt and Morgan (1965) |
| DELTAIC | | | | | | | | |
| Clinton delta, Ohio | Silurian | -- | -- | 35 | 64 | 11 | 25 | Overbey and Henniger (1971) |
| Rhône delta, France | Holocene | -- | -- | 33 | 163 | 65 | 350* | Oomkens (1970) |
| Bartlesville sandstone, Okla. | Pennsylvanian | -- | -- | 50 | 475 | 158 | 3,752* | Visher and others (1971) |
| BARRIER | | | | | | | | |
| Elk City field, Okla. | Pennsylvanian | 16-24 | 10-1,000 | 40 | 8 | 7 | 2 | Sneider and others (1977) |
| Bell Creek field, Mont. | Cretaceous | 32 | 50-13,000 | 20 | 60 | 7 | 8 | Berg and Davies (1968) |

**system scale*

of mud to sand increases downstream. Correlation of SP (spontaneous potential) responses in these deposits (Bernard and others, 1970) indicates that most of the shale breaks are discontinuous, but a few extend as far as several thousand feet normal to the channel axis.

Although individual point-bar deposits contain less than 1 Bcf of sand, the channel segments of which they are a part contain considerably more sand, primarily because of the greater length of the channel segment. One channel segment of the modern Brazos River contains about 17 Bcf of sand, whereas the fluvial system contains about 665 Bcf of sand (table 1). By comparison, a part of the Pleistocene Brazos River system contains nearly twice as much sand (1,200 Bcf) because of greater meanderbelt width and slightly greater length (table 1).

## Deltaic Sandstones

Sediment dispersal within a delta system is primarily controlled by the interaction of tides, fluvial processes, oceanic waves, and littoral currents. Water depth and the composition of underlying sediments also control the lateral extent of deltaic sand bodies. For example, sheetlike sand bodies are typical of shallow-water deltas (Fisk, 1955) deposited on shelf platforms having relatively stable substrates. Shallow-water deltas are also characterized by thin prodelta muds and relatively thick delta-plain sequences that contain numerous alluvial and distributary channels. These fluvial facies account for the greatest volume of sand preserved in shallow-water deltas (Morton and Donaldson, 1978).

In contrast, sandstones deposited by deep-water deltas typically are highly elongate and parallel the fluvial axes. Thick bar-finger sands (Fisk, 1961) are protected from lateral reworking as they subside into the underlying prodelta-shelf and slope muds, which are unstable because of their great thickness, high water content, and relatively steep gradient. Under these conditions, sandstone continuity is disrupted by slumping, growth faulting, shale diapirism, and

sediment deformation within the sand itself (Coleman and Garrison, 1977).

Patterns of sedimentation and their control on the distribution of sandy sediments within modern deltas are well known. Periods of active delta growth are interrupted by intervals of either nondeposition or local mud deposition as distributaries become inactive and minor reworking of abandoned lobes begins. Subsequent reactivation of distributaries or renewed outbuilding marks the beginning of another delta-construction cycle. The largest deltas of the northwestern Gulf of Mexico (Mississippi, Brazos-Colorado, and Rio Grande) are lobate to elongate, attesting to fluvial dominance, abundant sediment supply, and relatively low wave energy. Except for the Mississippi bird's-foot delta, which is building into deep water near the shelf edge, these deltas were deposited in shallow water after the Holocene transgression. Each of these fluvial-deltaic systems is fed by a large drainage area. These systems are analogous to the high-constructive deltas that prograded basinward throughout the Tertiary Period. They are also substantially larger than the coastal-plain rivers and deltas located between major depocenters.

### *Mississippi Delta*

The primary subdeltas of the Mississippi River are among the most intensively studied deltaic deposits in the world. Areally extensive and closely spaced borings (Fisk, 1955, 1961; Scruton, 1960; Frazier, 1967, 1974) provide excellent control on the thickness, lateral extent, and texture of major deltaic sand bodies. Delta-front sands of the shoal-water Lafourche subdelta are relatively thin (25 to 50 ft) but widespread (>15 mi) along depositional strike and contain about 1 Tcf (trillion $ft^3$) of sand (table 1). Delta-front sands grade upward from prodelta clayey silts having sand laminae to well-sorted sands. They are typically crossbedded, bioturbated, and interlaminated with thin layers of organic detritus, silt, and clay (Gould, 1970).

In contrast, distributary-mouth bars of the bird's-foot delta are relatively thick (100 to 200 ft) but narrow (1 mi) ribbons of sand that parallel the distributary channel. Upward, distributary-mouth bars coarsen, and thickness and frequency of silt and clay interbeds decrease. Bar sands grade from interlaminated silts and sands having organic detritus to clean, crossbedded sands near the bar crest (Gould, 1970). As shown by Frazier (1967, 1974), the offlapping arrangement of deltaic facies causes physical disruptions in sand continuity even though delta-front and distributary-mouth-bar sands appear at the same stratigraphic horizon.

### *Rio Grande Delta*

Similar disruptions in sand continuity occur in the ancestral Rio Grande delta complex. However, sand bodies within the elongate-lobate Rio Grande delta are thinner and less extensive than those in the Mississippi delta. The largest distributary-mouth-bar sands are 5 to 15 ft thick and up to 15,000 ft wide (table 1), whereas other lenticular sands are less than 5 ft thick and 500 ft wide (fig. 2).

The underlying transgressive marine sand is thicker and laterally more continuous than any of the deltaic sands. It extends a minimum of 3 mi in a dip direction (fig. 2) and 10 mi along strike and contains about 25 Bcf of sand (table 1). This widespread unit may be partly a marine deposit and partly a reworking of the sandy fluvial facies of the preceding progradational cycle. Regardless of its origin, this sand body exhibits the greatest continuity of any individual sandstone within the Rio Grande system.

### *Brazos Delta*

Although naturally occurring wave-dominated deltas are absent in the northwestern Gulf of Mexico, the recently formed Brazos delta (fig. 3) embodies many of the properties that are attributed to intensive marine reworking. The delta, which formed after the Brazos River was diverted in 1929, exhibits an upward-coarsening sequence of textures beginning with shelf and prodelta muds and ending with shoreface and beach-ridge sands; the latter are products of winnowing by waves. On close examination, the SP curves and grain-size analyses of Bernard and others (1970) show upward-coarsening sediments in the lower progradational facies followed by upward-fining aggradational sediments deposited in natural levee, marsh, and back-bar subenvironments. Ponds and swales between the beach ridges also trap mud, which covers the delta plain during coastal flooding. Along some segments of the delta margin, a thin, upward-coarsening sequence overlies the fine-grained delta-plain deposits, where transgressive beach and wash-over sands were laid down during shoreline retreat. In plan view, the delta-plain environments occur in parallel, broadly arcuate to cuspate patterns that characterize wave-dominated deltas (Fisher and others, 1969).

Successive periods of rapid sediment influx followed by wave reworking and sediment sorting give rise to clean, well-sorted sands that are interlaminated and interbedded with muds, which disrupt overall sand continuity. Because of the orderly arrangement of beach ridges and intervening swales, these zones of lower permeability may be laterally persistent, especially near the river mouth. Influence of high silt and clay concentrations introduced by riverine flooding progressively diminishes away from the river mouth, where marine processes dominate over fluvial processes.

Although the Brazos delta is small, it contains nearly 2 Bcf of sand. Naturally occurring wave-dominated deltas are substantially larger, having sand volumes that are several orders of magnitude greater. The Rhône delta, for example, contains about 350 Bcf of sand (table 3).

## Barrier and Strandplain Sandstones

Barriers and strandplains are similar in environmental setting; one exception is that lagoons separate barriers from the mainland shoreline. These

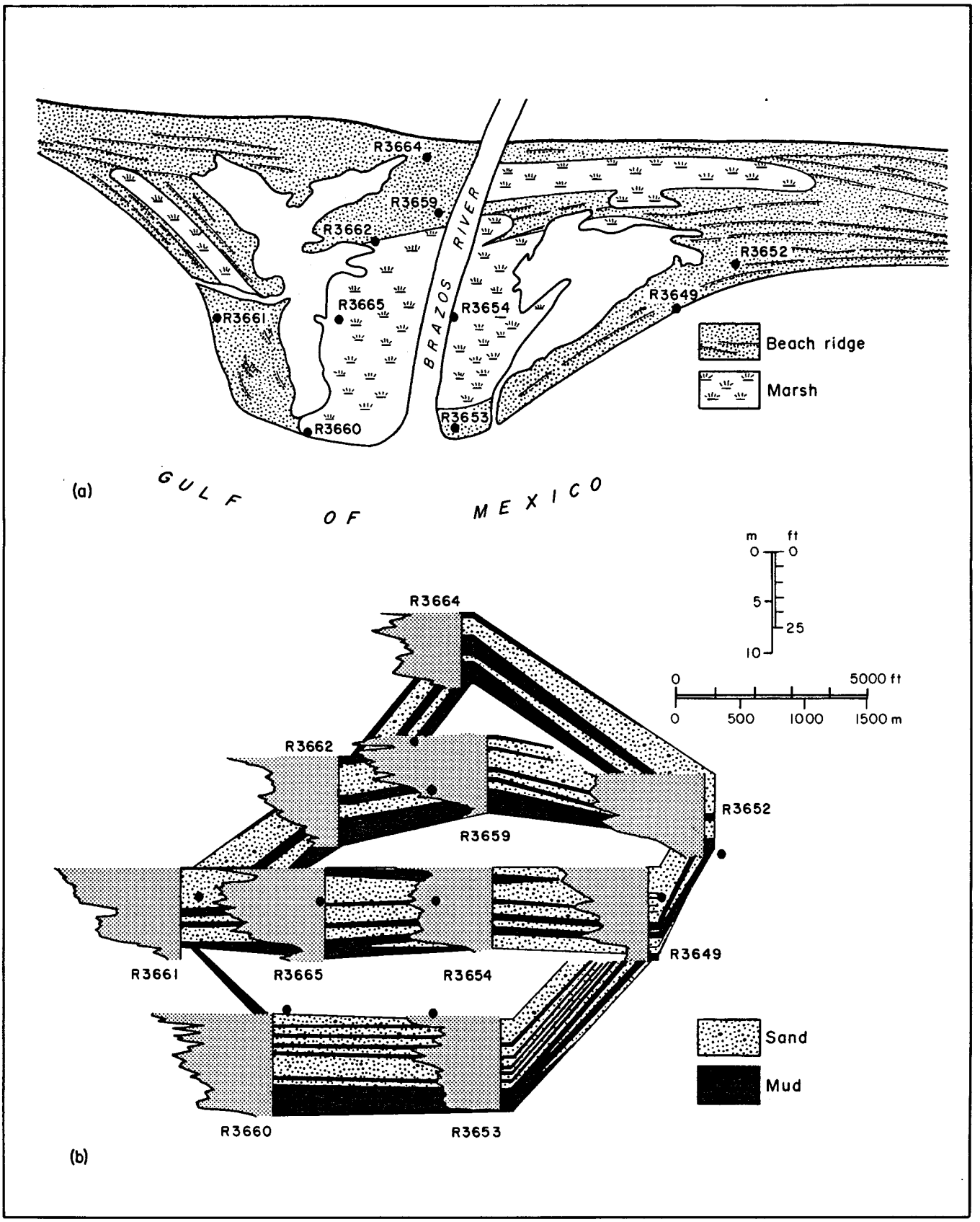


*Figure 3.* Distributions of (a) subaerial environments and (b) subsurface sediment types in the recently formed Brazos delta. Boring locations and spontaneous potential patterns from Bernard and others (1970).

delta-flank or interdeltaic deposits are composed of sediments reworked from active and abandoned deltas and transported by littoral currents away from the delta headlands and distributary mouths. Hence, barrier and strandplain sands are composed of well-sorted sands that grade seaward into shoreface sands and muds and landward into either washover sands and lagoonal muds (barriers) or delta-plain sands and muds (strandplains). An upward-coarsening shoreface profile of textures and sedimentary structures is common to barriers, strandplains, and wave-dominated deltas. Apart from this shared feature, barriers and strandplains are morphologically different landforms, although one may grade into the other.

Barrier and strandplain sediments having the greatest potential for preservation are those deposited on the shoreface that extends from submarine depths of 30 to 45 ft to the intertidal zone. Landward increases in physical energy across the shoreface are reflected in sediment textures, slope, and morphology. The seafloor of the lower shoreface is composed of muds and sandy muds that are featureless and merge seaward with muddy slopes of the inner continental shelf. The upper shoreface, however, is a dynamic area where bars are constructed and then destroyed or driven landward by wave processes and currents driven by tides and winds. Upper shoreface sediments are typically composed of fine-grained to very fine grained sand having local shell concentrations. If preserved, the sedimentary structures are either low-angle, parallel-inclined laminations, irregular scour and fill, or structures formed by vertical accretion and migration of breaker bars and troughs. These include horizontal parallel laminations of the bar crest, ripple cross-laminations, and foresets. On high-energy coasts that experience seasonal changes, physical structures are commonly preserved; however, on low-energy coasts, such as the Gulf Coast, abundant nearshore infauna effectively rework the sediments and destroy much of the stratification.

Along many coastal areas, erosional (transgressive) and accretionary (regressive) barriers occupy orderly positions relative to active and abandoned delta lobes. More often than not, delta headlands grade laterally into transgressive barriers, which in turn grade into regressive barriers. The transition from transgressive to regressive landforms can cover a shoreline distance of a few thousand feet to tens of miles. Transgressive and regressive barriers can be distinguished on the basis of geologic history, surficial morphology, and lateral facies relationships. This distinction is important to predicting the sedimentary properties and reservoir characteristics of preserved barrier deposits. The spectrum of barrier settings and associated sand facies is represented by Padre Island, Galveston Island, and South Padre Island in Texas and by Grand Isle in Louisiana.

## *Padre Island*

Barrier sands of Padre Island stretch unbroken from the Rio Grande to the central Texas coast, a distance of more than 100 mi. The central and northern parts of the barrier are 3 to 10 mi wide. Sand thicknesses of 35 to 60 ft have been reported (Fisk, 1959; Dickinson and others, 1972) from areas where the barrier has been stable for the past few thousand years. According to Fisk (1959), Padre Island grew vertically as sea level rose and grew seaward after sea level stabilized. Despite vertical aggradation, total thickness of the Padre Island barrier sands is close to that of Gulf Coast barriers that accreted much farther seaward.

A large volume of laterally continuous sand comprises Padre Island and the other barrier islands between the Holocene Brazos-Colorado and the Rio Grande deltas (table 1). Barrier chains of comparable length occur elsewhere, but the Texas barriers are probably unsurpassed in content of clean, well-sorted sands. Recurrence of a barrier system in the same relative geographic position throughout much of the Tertiary is attributed to the San Marcos Arch, across which minimal sedimentation and subsidence between the Rio Grande and Houston Embayments occurred.

## *Galveston Island*

Borings and SP logs through Galveston Island (Bernard and others, 1970) show distinctly different vertical sequences for eastern (regressive) and western (transgressive) segments. A typical offlap sequence is preserved on east Galveston Island, where accretion ridges are prominent. Along this segment, lower shoreface and shelf deposits of bioturbated and interlaminated shelly sand and mud grade laterally and upward into horizontal and low-angle, cross-stratified barrier and upper shoreface sand containing thin shell beds. On west Galveston Island, the Pleistocene-Holocene unconformity is overlain by Brazos River prodelta mud which, in turn, is overlain by a thin interval of barrier-island and shoreface sands and muds.

Barrier sands beneath Galveston Island range in thickness from 15 to 50 ft (table 1). Sand thickness increases progressively eastward from the Holocene Brazos delta. The lenticular sand body is 1 to 2.5 mi wide and about 26 mi long (Bernard and others, 1970). Bernard and others (1970) estimated that about 50 Bcf of the total volume of sand in the barrier is clean. The depositional model of Galveston Island suggests that barrier sands are best developed progressively farther away from the delta with which they are associated. This model is supported by field evidence along the Texas coast and elsewhere (Morton and McGowen, 1980).

## *Grand Isle*

Like Galveston Island, Grand Isle is a delta-margin barrier that has both transgressive and regressive features. Moreover, the lens of fine-grained sand beneath Grand Isle thickens eastward from 10 to nearly 60 ft (Fisk, 1955) in a pattern remarkably similar to that seen at Galveston Island (Bernard and others, 1970). However, the greatest thicknesses of sand beneath Grand Isle are actually composites of individual sand lenses, each between 20 and 30 ft thick (Conatser, 1971).

Individual sand lenses each contain about 2 Bcf of sand; aggregate volume of sand of the vertically stacked lenses is about 8 Bcf.

### *South Padre Island*

Barrier islands fronting the Rio Grande delta were formed by delta destruction and transgressive marine deposition that followed delta abandonment. On South Padre Island, barrier sands 10 to 15 ft thick overlie delta-plain deposits (fig. 2). The subaerial part of the barrier is 2,000 to 15,000 ft wide and extends at least 20 mi along depositional strike.

Typical sedimentary structures of the barrier sands are horizontal and low-angle parallel laminations having subordinate scour and fill, rare foresets, and small-scale ripple cross-laminations. Sands are mainly fine grained to very fine grained, and textural changes within the sands are primarily related to the presence or absence of shell fragments. The thin sand facies interfingers with and overlies lagoonal muds and interbedded algal-bound sands and muds deposited on wind-tidal flats and washover fans.

### *Ingleside Strandplain*

During the late Quaternary Period, abundant sand was supplied to the Texas coast by coalescing deltas having broad, sand-rich, meandering streams. Accumulation of the sand along a stable, aggrading coastline formed a 10-mi-wide strandplain system that extended more than 100 mi along strike and contained slightly more than 1.5 Tcf of sand (table 1). The Ingleside strandplain occupied an area that is currently the site of several modern barrier islands that are separated from the Pleistocene strandplain by lagoons. This present-day occurrence of stratigraphically juxtaposed or stacked barrier sequences produces a sand body more than 60 ft thick beneath some of the central Texas barriers (fig. 1). The Ingleside strandplain is of comparable thickness where it is buried and unmodified by surficial erosion, suggesting that it may be a composite of vertically aggraded and laterally accreted barrier-strandplain deposits (Winker, 1979).

## Shelf and Slope Sandstones

Unlike those of the other sandstone facies, sedimentary models of shelf and slope sandstones were not developed from the northwestern Gulf Coast region because submarine canyons and fans are not currently active along the continental margin. Short cores from the Mississippi fan and deeper parts of the central Gulf of Mexico contain mostly mud; the few sands exhibit turbidite characteristics (Bouma, 1968). Typical turbidites described by Bouma (1962) have been interpreted by Walker (1979) as outer suprafan deposits. The sand sequences are usually widespread but thinly bedded (1 to 3 ft) and upward fining. The sands themselves either are well sorted by high-velocity turbidity currents or contain considerable mud because of gravity-induced slumping and a high concentration of suspended sediment. Thick sand sequences deposited by coalescing and aggrading submarine channels provide the best reservoirs in deep-water sediments. Although they are well documented in the rock record, these channel sands have not been cored in Quaternary sediments of the Gulf of Mexico.

# *TERTIARY SEDIMENTS*

Direct comparison of modern sand bodies with ancient ones is difficult because of the paucity of detailed core descriptions and the lack of data on other sedimentological properties of the Tertiary sandstones. Nearly all published studies rely principally on either stratigraphic cross sections or isopach maps, or both. Some also have fence diagrams or grain-size analyses, but remarkably few include core descriptions or plots of sedimentary structures and pore properties.

The environmental groupings of Tertiary sandstones in table 2 are tentative. For example, Wilcox sands in the Katy field have been interpreted both as delta fronts (Fisher and McGowen, 1967; Williams and others, 1974) and as turbidites (Berg and Findley, 1973; DePaul, 1980). Likewise, Wilcox sands in Northeast Thompsonville field have been interpreted both as barriers (Young, 1966) and as submarine fans (Berg and Tedford, 1977). Hackberry sands in the Port Acres/Port Arthur area have been interpreted both as deltaic deposits (Halbouty and Barber, 1961) and as submarine channels (Berg and Powers, 1980). The interpreted deep-water origin of the Hackberry sandstones appears valid on the basis of regional depositional setting (Paine, 1971); however, recent work (Edwards, 1980, 1981) confirms the interpretation of Fisher and McGowen (1967) that sandstones of the Wilcox Group were deposited primarily in shallow water.

Although the depositional environment of the Tertiary sandstones is uncertain, reasonable estimates of ancient sandstone dimensions and volumes can be made (table 2). Volumetric estimates agree with estimates of modern analogs at the same hierarchical level. Individual sand bodies (third level) contain about $10^9$ to $10^{11}$ $ft^3$ of sand, and sand systems (first level) contain about $10^{11}$ to $10^{13}$ $ft^3$ of sand.

## Fluvial Sandstones

Tertiary sandstones interpreted as fluvial deposits characteristically have dendritic and elongate isopach patterns oriented normal to depositional strike. Many of these sand bodies exhibit upward-fining textures and upward increases in shale content, as indicated by SP log patterns. In plan view, grain size also tends to decrease toward the channel axis (Nanz, 1954), probably reflecting the presence of fine-grained abandoned-channel fill.

Individual fluvial channels are a few thousand feet to a few miles wide, 3 to 8 mi or more long, and 35 to 60 ft thick (table 2). Greater thicknesses may develop near distributary mouths, where unstable prodelta muds promote sandstone subsidence and vertical aggradation (Fisk, 1961). Apparently, sand volumes of 20 to 40 Bcf are typical of meandering alluvial channels, whereas smaller coastal-plain streams or minor, laterally restricted distributary channels are smaller by an order of magnitude. The few dimensional data on fluvial systems suggest that differences in volume (1 to 4 Tcf) result mainly from differences in meanderbelt widths, which range from 7 to 16 mi.

## Deltaic Sandstones

Despite their importance as hydrocarbon reservoirs in the Gulf Coast Basin, only a few individual Tertiary sandstones of deltaic origin have been described. Most published studies of deltaic sandstones examine partial or complete delta systems (table 2) rather than individual sandstones. Progradational sequences recorded on electric logs are 10- to 40-percent sandstone. The sandstones are arranged in elongate to lobate patterns that reflect sediment dispersal by fluvial and marine processes. The sandstones grade updip and laterally into shales and thin sandstones deposited in delta-plain and interdistributary-bay environments. They also grade downdip into prodelta shales. Upward increases in sand-bed thickness and upward decreases in shale content are typical of these regressive deposits. The sandstones are laminated and crossbedded, and carbonaceous material is commonly disseminated throughout the sand body.

Individual sandstones deposited in delta-front and delta-fringe environments are typically 3 to 7 mi wide and 14 to 20 mi long (table 2); corresponding sand volumes are 100 to 200 Bcf. In contrast, deltaic systems are 100 to 500 ft thick, 10 to 30 mi wide, and 20 to 130 mi long. Sand volumes of these deltaic systems range from 2 to 20 Tcf, a range similar to that of the barrier-strandplain systems. The similarity in range results from the depositional similarities between barrier-strandplain systems and wave-dominated deltas.

## Barrier and Strandplain Sandstones

Tertiary barrier and strandplain sandstones are identified mainly by elongate and lenticular isopach patterns that parallel depositional strike. Other corroborating evidence includes well-sorted sands of uniform or upward-coarsening textures and concomitant upward or central increases in permeability. Some sand bodies interpreted as barriers grade landward into fine-grained sandstones and carbonaceous mudstones and shales, probably representing marsh deposits. These same sand bodies grade seaward into fine-grained shelf deposits.

The dimensions of individual barrier and strandplain sands cover a broad range, even though the volumes of both sands are 10 Bcf or less (table 2). Barrier sands are 15 to 75 ft thick, a few thousand feet to a few miles wide, and 2 to 8 mi long (the latter dimension is arbitrary because of map boundaries). Barrier systems are 450 to 1,000 ft thick, about 10 mi wide, and 40 to 60 mi long, containing 5 to 25 Tcf of sand. Varying thicknesses of the barrier system are largely responsible for the differences in sandstone volume.

## Shelf and Slope Sandstones

Outer shelf and upper slope sediments formed by turbidity currents are widely distributed in deep-water deposits such as the Hackberry sandstones. These submarine channel and fan deposits typically have narrow, dip-trending, elongate to digitate patterns in areas of maximum net sandstone. Over the entire depositional interval, sandstone thickness diminishes upward and shale-bed frequency and thickness increase upward. The sandstones also grade downdip into shale; thinly interbedded sandstones and siltstones make up the fan deposits. Both massive sands having abrupt bases and thin-bedded sandstones show textural gradations. Grain sizes of sands range from coarse to fine; the average sand is fine grained. Internal stratification varies greatly; the sandstones are typically laminated, rippled, or contorted and, occasionally, bioturbated. These sedimentary structures are not unique to deep-water deposits; hence, turbidite interpretations should be supported by faunal evidence.

Outer shelf and upper slope sandstones are remarkably uniform in size, according to the limited data available (table 2). The individual sandstones are 3 to 5 mi wide, 4 to 6 mi long, and 50 to 100 ft thick; corresponding sand volumes are 30 to 80 Bcf. Thickness distinguishes shelf-slope systems from individual sandstone units. Genetically related turbidite systems are 300 to 450 ft thick and contain about 100 to 150 Bcf of sand-size sediment. These volumes are 2 to 3 orders of magnitude less than sand volumes estimated in other depositional systems (table 2).

# *SEDIMENTS IN OTHER BASINS*

A brief examination of previous studies indicates that some sandstones of the Appalachian, Rocky Mountain, and mid-continent regions of the United States are similar to Tertiary Gulf Coast sandstones. In fact, sandstones of Paleozoic and Mesozoic age have dimensions (table 3) and sedimentary properties that are similar to Cenozoic sandstones of comparable origin (tables 1 and 2). Sand volumes of individual sandstones and sandstone systems are within the lower end of the range of Tertiary examples, suggesting that the other sand bodies are somewhat smaller; however, the number of examples is too small to determine this conclusively.

# FAULT-COMPARTMENT AREAS

The volumes of Gulf Coast reservoirs, as mentioned previously, are determined by depositional sand-body geometries, by the areas of fault compartments, and by internal permeability barriers. The second of these factors, the size and geometry of fault compartments, can be considered a function of position within the Gulf Coast geopressure trends.

To examine data on the second hierarchical level (fault area), published and unpublished regional structure maps of geopressured sediments at depths of interest were assembled. For the Wilcox fairways of South and Central Texas, the structure maps presented by Bebout and others (1982) of the top of the Wilcox (Zapata, Duval, and Live Oak fairways) and the top of the lower Wilcox (De Witt and Colorado fairways) were used with slight modification. A structure map of the Bee delta system (top of the Wilcox) was taken from Weise and others (1981). For the Frio fairways of the central Gulf Coast (Nueces, Matagorda, and Brazoria fairways), commercial structure maps of the top of the Frio and published structure maps of the Brazoria fairway (Bebout and others, 1978) were used. On each of these regional structure maps, fault-compartment areas of all the fault compartments shown were measured by planimetry. This totaled 90 compartments in the Wilcox fairways and 116 compartments in the Frio fairways.

The Wilcox data are presented in table 4 and figure 4a. A wide range of compartment areas is represented, from 0.4 to 80 $mi^2$. Seventy percent of all the compartments lie between 1.5 and 29 $mi^2$. Distribution of areas is strongly skewed toward small areas, but the log distribution of areas is nearly uniform. Median area is 9.3 $mi^2$ and mean is 15 $mi^2$. Distribution of fault-compartment areas along the growth-fault trend shows no distinct variations. The percentage of large compartments seems to be greater south of the Bee delta than in the De Witt and Colorado fairways, but this may result from the smaller scale and the different datum of the structure maps of South Texas. Distribution of areas in each Wilcox fairway is skewed toward small areas, the mean area being greater than the median in all except the Duval and Colorado fairways. Range of areas is generally similar; the higher limit is greatly dependent on definition of the closure of large fault blocks.

The Frio data are presented in table 5 and figure 4b. Again, there is a wide range of values, from 0.3 to 69 $mi^2$. Overall distribution is skewed toward small areas, and the mean area of 12 $mi^2$ is significantly greater than the median area of 5.7 $mi^2$. The histogram of plotted log areas (fig. 4b) shows that the distribution is close to log-normal. Like the Wilcox data, Frio data show no distinct variations in position on the growth-fault trend within the area studied. Percentages of large fault compartments fluctuate widely because of the problems of defining closure. Areal distribution in each part of the trend is skewed toward small areas and is probably log-normal.

*TABLE 4. Areas of fault compartments in Wilcox geopressured fairways.*

| | ZAPATA FAIRWAY | DUVAL FAIRWAY | LIVE OAK FAIRWAY | BEE DELTA | DE WITT FAIRWAY | COLORADO FAIRWAY | OVERALL |
|---|---|---|---|---|---|---|---|
| SMALL | | | | | | | |
| Number | 3 | 2 | 8 | 2 | 13 | 1 | 29 |
| % of all | 21 | 11 | 42 | 18 | 59 | 17 | 32 |
| Mean area | 2.0 | 1.7 | 1.5 | 3.1 | 1.5 | 0.8 | 1.7 |
| MEDIUM | | | | | | | |
| Number | 6 | 7 | 8 | 4 | 7 | 5 | 37 |
| % of all | 43 | 39 | 42 | 36 | 32 | 83 | 41 |
| Mean area | 9.7 | 8.6 | 10.4 | 13.1 | 7.0 | 16.5 | 10.4 |
| LARGE | | | | | | | |
| Number | 5 | 9 | 3 | 5 | 2 | 0 | 24 |
| % of all | 36 | 50 | 16 | 45 | 9 | 0 | 27 |
| Mean area | 43.8 | 28.3 | 26.4 | 38.8 | 29.0 | - | 36.9 |
| OVERALL | | | | | | | |
| Number | 14 | 18 | 19 | 11 | 22 | 6 | 90 |
| Mean area | 20.2 | 17.6 | 24.1 | 23.0 | 5.8 | 13.9 | 14.7 |
| Median area | 13.0 | 18.1 | 6.1 | 16.7 | 2.6 | 16.3 | 9.3 |
| 84% of blocks > | 2.5 | 3.7 | 1.2 | 3.3 | 0.8 | 0.8 | 1.5 |
| 84% of blocks < | 44.0 | 32.3 | 17.5 | 29.2 | 7.8 | 18.5 | 28.6 |

*All areas are in square miles. Small blocks are less than 4 $mi^2$, medium blocks are 4 to 20 $mi^2$, and large blocks are more than 20 $mi^2$.*

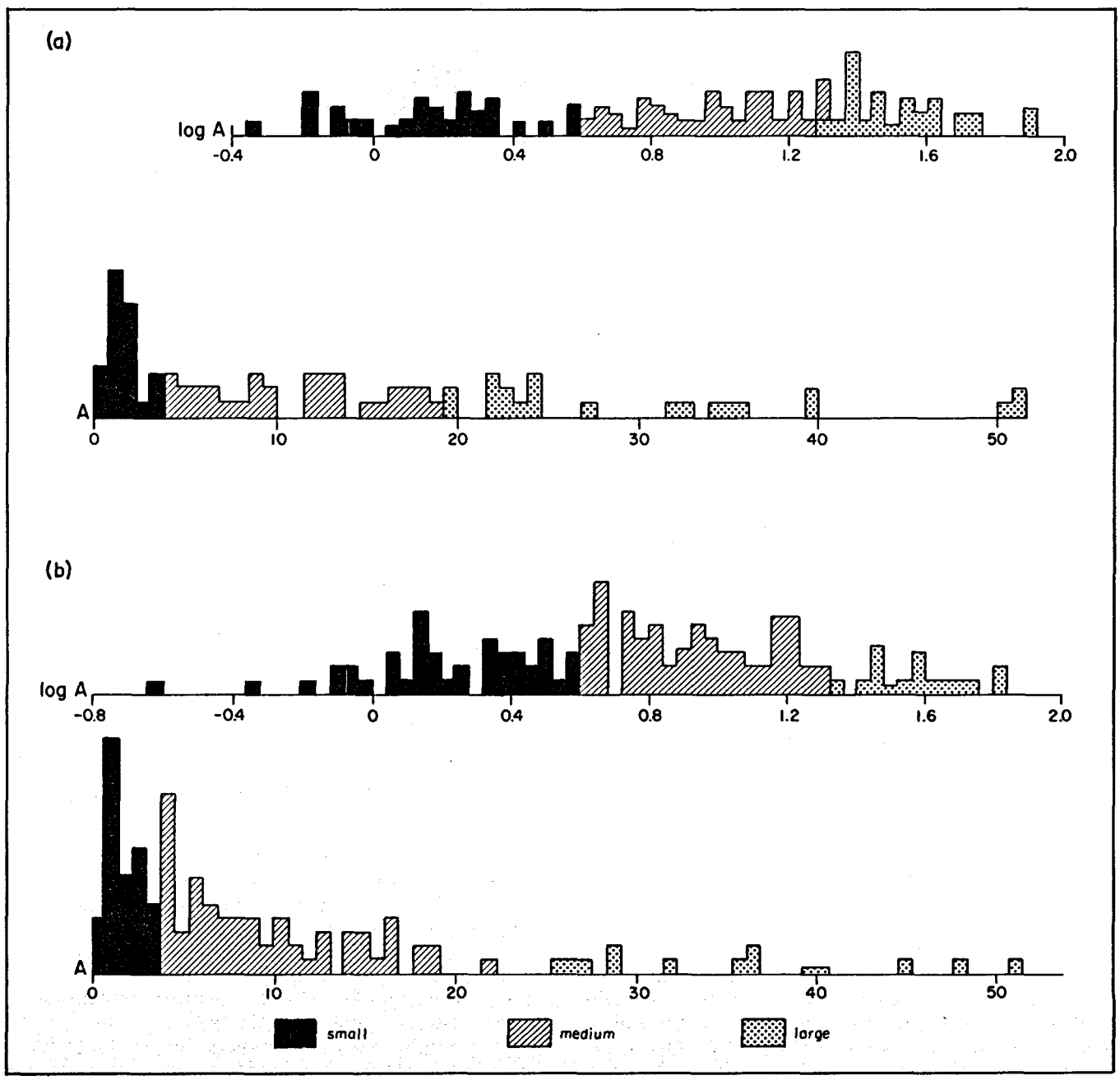


*Figure 4.* Histograms of fault-compartment areas showing the distribution on both log and arithmetic scales of (a) Wilcox compartments, Lower and Middle Texas Gulf Coast, and (b) Frio compartments, Middle Texas Gulf Coast (between Corpus Christi and Brazoria fairways). Areas are in square miles.

Overall values for Wilcox and Frio fault-compartment areas are similar; the median is 9.3 $mi^2$ for the Wilcox and 5.7 $mi^2$ for the Frio. The somewhat smaller size of Frio compartments is in part caused by the smaller scale of most of the Wilcox structure maps that were used.

The methods used here to estimate areal distribution are limited because construction of the structure maps determines which compartment areas are measured. This is an uncertain process, and accuracy depends on adequate well control. Moreover, some of the small-scale maps show only the large fault blocks. Finally, the largest fault blocks are not closed but, rather, are part of sizeable areas of unfaulted terrain. However, the mean and median values derived here approximate the most probable size of fault compartments to be found in the Texas Gulf Coast geopressure trends. Note that these fault compartments are of the same order of magnitude as the areas covered by typical sand bodies.

*TABLE 5. Areas of fault compartments in Frio geopressured fairways.*

| | KLEBERG COUNTY | NUECES COUNTY | SAN PATRICIO COUNTY | REFUGIO/ ARANSAS COUNTIES | CALHOUN/ JACKSON COUNTIES | MATAGORDA COUNTY | BRAZORIA COUNTY | OVERALL |
|---|---|---|---|---|---|---|---|---|
| SMALL | | | | | | | | |
| Number | 3 | 5 | 5 | 8 | 0 | 3 | 8 | 32 |
| % of all | 30 | 33 | 62 | 50 | 0 | 10 | 27 | 28 |
| Mean area | 3.0 | 2.2 | 1.2 | 2.0 | -- | 2.6 | 2.2 | 2.2 |
| MEDIUM | | | | | | | | |
| Number | 6 | 7 | 3 | 8 | 7 | 19 | 17 | 67 |
| % of all | 60 | 47 | 38 | 50 | 86 | 66 | 56 | 58 |
| Mean area | 11.1 | 9.3 | 4.9 | 5.9 | 11.2 | 9.7 | 9.0 | 9.3 |
| LARGE | | | | | | | | |
| Number | 1 | 3 | 0 | 0 | 1 | 7 | 5 | 17 |
| % of all | 10 | 20 | 0 | 0 | 13 | 24 | 17 | 15 |
| Mean area | 40.0 | 41.5 | -- | -- | 64.9 | 34.7 | 42.1 | 42.7 |
| OVERALL | | | | | | | | |
| Number | 10 | 15 | 8 | 16 | 8 | 29 | 30 | 116 |
| Mean area | 11.5 | 13.4 | 2.6 | 3.9 | 18.0 | 15.6 | 12.7 | 11.9 |
| Median area | 10.6 | 6.5 | 1.5 | 3.9 | 12.8 | 10.9 | 6.3 | 5.7 |
| 84% of blocks > | 2.9 | 1.4 | 0.7 | 1.1 | 4.5 | 4.1 | 2.3 | 1.5 |
| 84% of blocks < | 15.6 | 21.9 | 4.5 | 6.7 | 18.9 | 27.7 | 20.7 | 17.6 |

*All areas are in square miles. Small blocks are less than 4 mi², medium blocks are 4 to 20 mi², and large blocks are more than 20 mi².*

# COMPARISON OF PRODUCTION AND GEOLOGIC ESTIMATES OF AQUIFER FLUID VOLUME

Nine geopressured gas reservoirs in eight fields were studied in detail to obtain volumetric estimates of reservoirs and contiguous aquifers within a fault-bounded sandstone (fourth hierarchical level) and to gain additional insight into reservoir continuity in the geopressure zone. Eight of these reservoirs were previously analyzed by Boardman (1980) to estimate aquifer volume and area from gas production and pressure data. Similar calculations were made for a ninth reservoir (Mobil-David L reservoir, Nueces County). The fields represent three water-drive and four pressure-depletion reservoirs in the Wilcox Group and two pressure-depletion reservoirs in the Frio Formation.

The areal distribution of these nine reservoirs (fig. 5) is less than ideal for a regional study of reservoir parameters. The reservoirs were chosen primarily because they contain a small number of producing wells and are close to geothermal prospect areas. Five of the nine are from a single Wilcox fairway, the De Witt. Given this erratic distribution, studies of the reservoirs can serve mainly to suggest factors that might affect reservoir continuity and to verify geologic estimates of reservoir volume.

## *CALCULATION OF AQUIFER FLUID VOLUME FROM PRODUCTION DATA*

Steps for calculating aquifer volume from production data have been briefly summarized by Boardman (1980). Information for that study was obtained from 24-hour shut-in wellhead pressures taken semiannually; only annual readings were used. Whether the reservoir is driven by water or pressure depletion was determined through consultation with the operating companies.

For a water-drive reservoir (typically, a large reservoir having a gas-water contact), the technique developed by Stuart (1970) was used to calculate water volume (fig. 6a). In this method, the produced gas volume is first converted to gas in place. Then, assuming a gas saturation of 25 $ft^3$/bbl of water at a standard temperature and pressure and a porosity of about 20 percent (needed to determine rock compressibility), the aquifer fluid volume is calculated.

For a pressure-depletion reservoir (a smaller reservoir having no water contact that is produced by gas pressure only [fig. 6b]), the decline in BHP/z (bottom-hole pressure as corrected for compressibility) with gas production should be linear. An extrapolation to zero pressure gives an estimate of total gas volume in the reservoir. This volume is converted to gas in place. Then, assuming a water saturation of 25 percent, the aquifer fluid volume is calculated (Craft and Hawkins, 1959).

The estimates obtained by these methods (table 6) are sensitive to the assumptions and values used; if

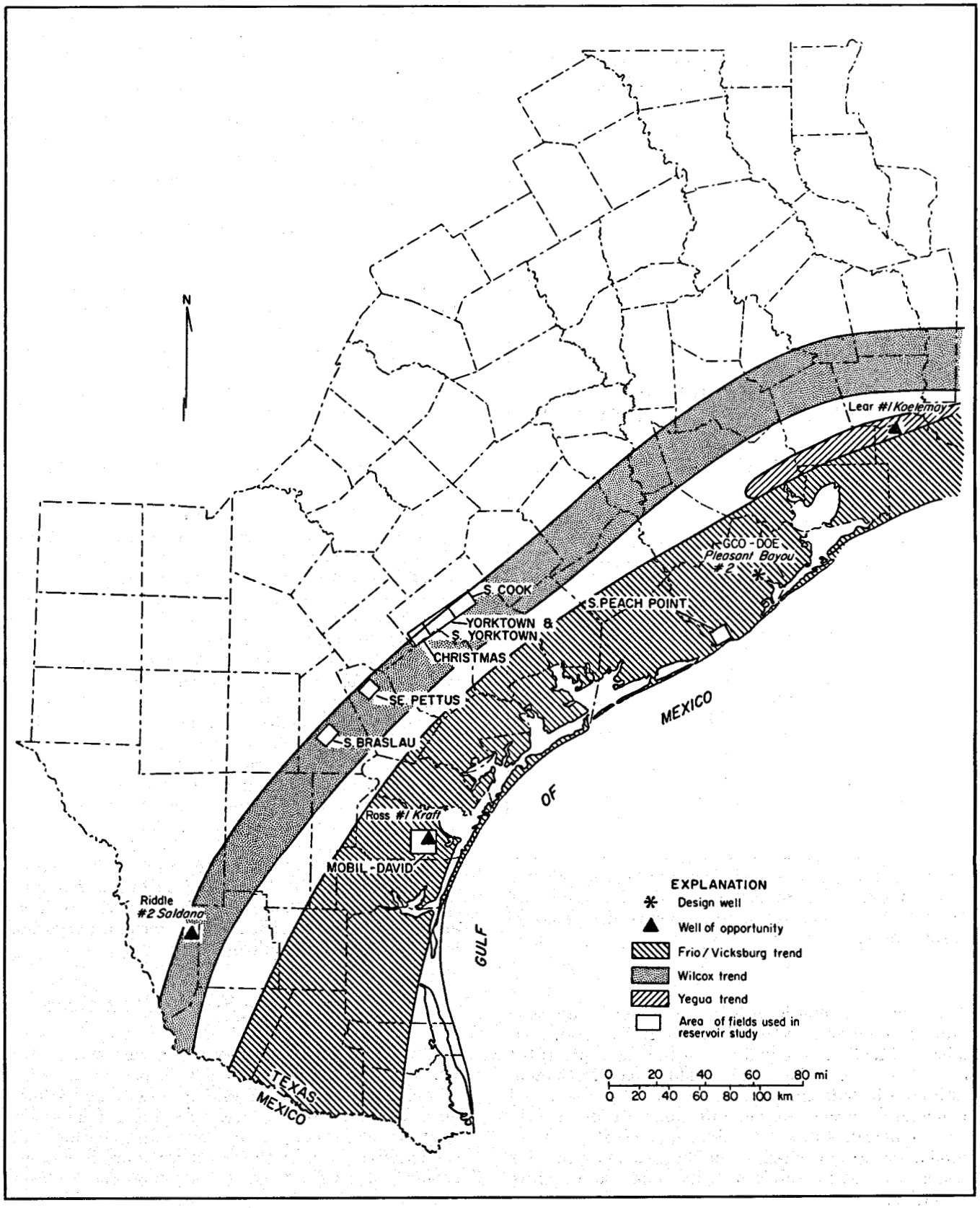


*Figure 5.* Locations of hydrocarbon and geothermal trends, geothermal test wells, and Texas Gulf Coast areas studied in this report.

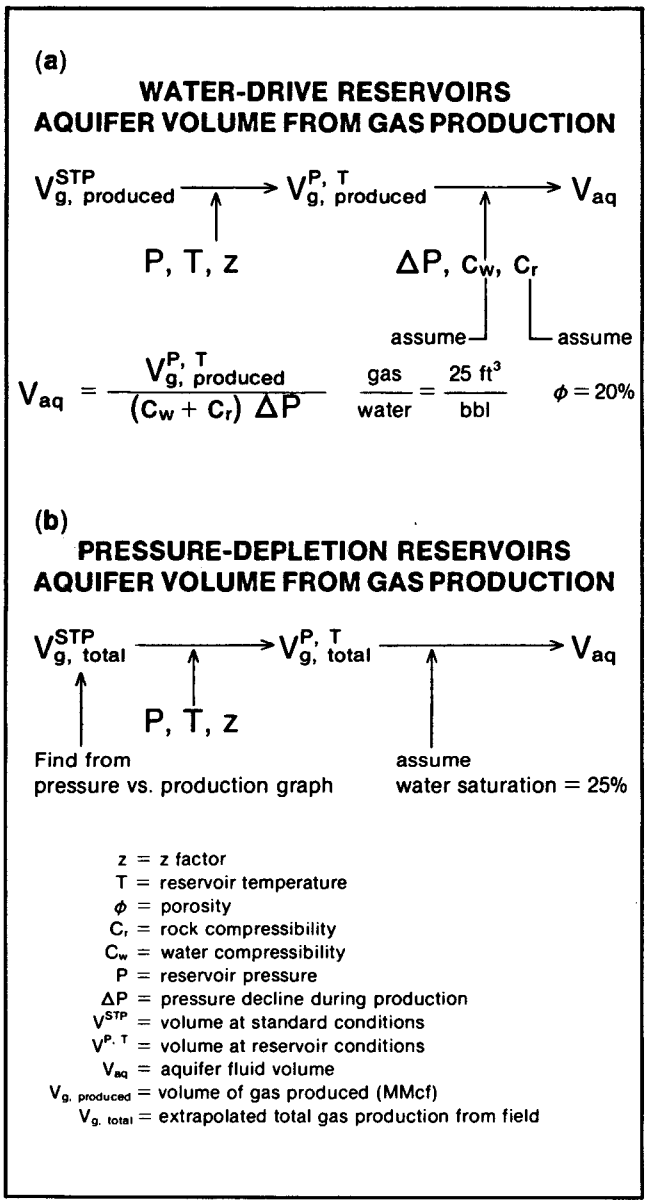


*Figure 6.* Calculations for estimating aquifer volume from production data for (a) water-drive reservoirs (Stuart, 1970) and (b) pressure-depletion reservoirs (Craft and Hawkins, 1959).

a reservoir is misclassified, an order-of-magnitude difference in aquifer volume can result. However, such misclassifications are unlikely in the cases presented here. Other variations that could affect production estimates include inaccurate estimates of pressure and temperature of the reservoir (affecting the conversion to gas in place), scatter of points on a BHP/z-versus-production graph, changes in the gas-water ratio or water saturation, and porosity and permeability variations.

The production estimates reported by Boardman (1980) for pressure-depletion reservoirs (for six of the nine reservoirs studied) were recalculated for several reasons: (1) to incorporate all the semiannual shut-in data reported since 1972, thus providing a fairly accurate picture of pressure decline; (2) to study the behavior of individual wells in the fields; (3) to use porosity values more appropriate to the reservoirs considered; and (4) to provide error limits on the projected total gas in the reservoir, as derived from a least-squares linear regression on the data points. All the results presented in this report for pressure-depletion reservoirs (table 6) are recalculated values.

# *SOUTH COOK FIELD*

South Cook field produces from the B and C correlation intervals of the lower Wilcox Group (Bebout and others, 1982). Temperature in the reservoirs is about 275° F. Shut-in pressure was originally 7,100 psi, yielding a pressure gradient of 0.65 psi/ft. Porosity in the reservoir is about 20 percent (Bebout and others, 1982), as measured in Atlantic No. 1 C. A. Schorre well (fig. 7).

## Stratigraphy of Producing Sands

The B and C sands (10,850 and 10,900 ft) occur at the top of the lower Wilcox Group and form the upper units of the Rockdale delta system in the area. Geometry of the sand facies is influenced by syndepositional faulting. In the fault block of interest, the sands are dip oriented and were deposited by distributary channels extending southeast from the delta plain.

Four dip-oriented sand thicks in the B sand can be identified (fig. 7). The westernmost, which is the producing sand in South Cook field, runs nearly north to south across the southwestern part of the fault block. Interpretation of whole core from Atlantic No. 1 Schorre well suggests that the sand formed in a distributary-channel setting (Winker and others, in press).

There are two dip-oriented depocenters in the C sand (fig. 7); only the western one is included in South Cook field. Cores from Atlantic No. 1 Schorre well suggest that the lower part of the sand formed in a distributary-channel setting and the upper part in a distributary-channel and distributary-mouth-bar setting (Winker and others, in press). The two sand facies are separated by a thin (2 to 3 ft) shale break.

## Structure of the South Cook Area

The South Cook area lies within the trend of lower Wilcox growth faulting. The field is located on a slight rollover anticline within an elongate fault compartment up to 25 $mi^2$ in area. Large, well-defined faults to the northwest, south, and southeast isolate the compartment; the northeastern boundary is less well determined. The eastern extremity of the compartment, as shown on figure 7, may be separated from the rest of the South Cook compartment by a smaller fault (not shown). More information on the structure of the area is given in Bebout and others (1982) and Winker and others (in press).

*TABLE 6. Volume estimates of geopressured gas reservoirs, Texas Gulf Coast.*

| NAME, COUNTY, SAND, DEPTH | PRIMARY GEOLOGIC ESTIMATES | | | | PRODUCTION ESTIMATES | | COMPARISON | |
|---|---|---|---|---|---|---|---|---|
| | AREA ($mi^2$) | $V_{res}$ (Bcf) | $V_{aq}$ (million bbl) | POROSITY (%) | $V_{aq}$ (million bbl) | DRIVE | % INTER-CONNECTION | COMMENTS |
| *SE. Pettus,* Bee Co., First Massive, 9,000 ft | 2.04-4.26 | 4.56-9.52 | 130-270 | 16 | 28±2 | pd | 23-10 | thin shale breaks; $V_{aq}$ = 60-120 million bbl |
| *S. Braslau,* Live Oak Co., First Tom Lyne, 9,000 ft | 2.82-3.92 | 5.15-6.99 | 140-210 | 16 | 61±14 | pd | 71-27 | thin shale breaks |
| *S. Cook,* De Witt Co., B sand, 10,850 ft | 7.35-14.71 | 5.1-22.4 | 350-790 | 20 | 588 | w | 168-74 | none |
| *S. Cook,* De Witt Co., C sand, 10,900 ft | 8.75-26.01 | 17.9-58.0 | 640-2,070 | 20 | 207 | w | 32-10 | thin shale breaks |
| *Yorktown,* De Witt Co., Migura, 11,000 ft | 3.71 | 9.8-10.5 | 280-300 | 14 | 576 | w | 203-191 | connection to south; $V_{aq}$ = 565-606 million bbl |
| *S. Yorktown,* De Witt Co., Migura, 10,800 ft | 1.96-2.87 | 4.2-5.0 | 150-180 | 14 | 82±14 | pd | 56-47 | thin shale breaks? |
| *Christmas,* De Witt Co., Migura, 10,800 ft | 2.35 | 4.0-8.0 | 100-250 | 14 | 49±1 | pd | 50-19 | poor control |
| *S. Peach Point,* Brazoria Co., Frio A, 11,250 ft | 0.61 | 0.72 | 19 | 15 | 33±3 | pd | 175 | connection to south |
| *Mobil-David L,* Nueces Co., Anderson, 11,100 ft | 1.22 | 4.25-4.75 | 180-200 | 24 | 185-290 | pd | 91-160 | none |

*Production estimates for water-drive reservoirs from Boardman (1980), using the method of Stuart (1970).*
% interconnection - *ratio of production estimate to geologic estimate of $V_{aq}$; a measure of that part of the sand connected with the wells.*
$V_{res}$ - *sand volume.*
$V_{aq}$ - *aquifer fluid volume.*
pd - *pressure depletion.*
w - *water.*

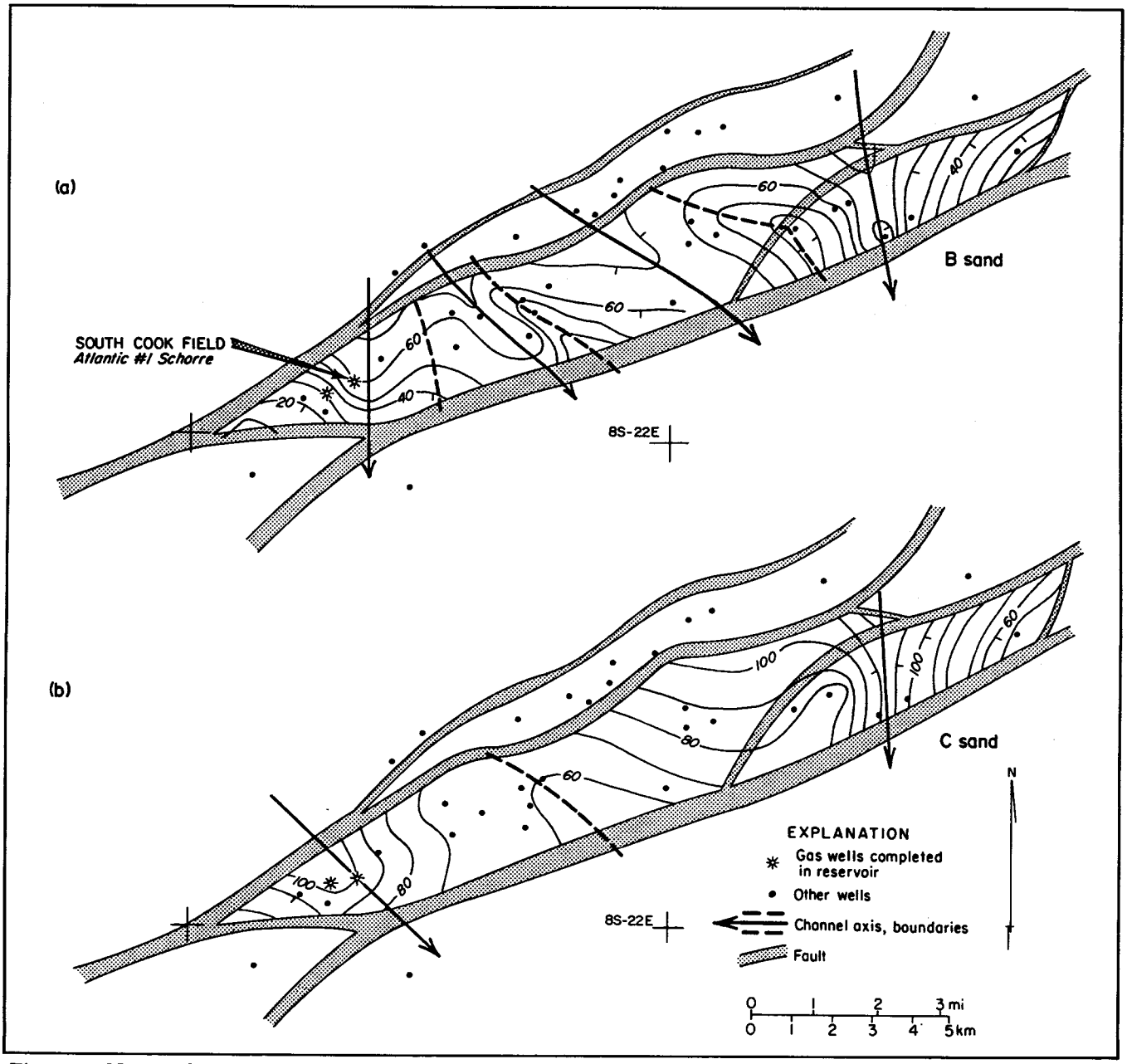


*Figure 7.* Net-sand map of B and C sands, South Cook field. Channel axes are shown. Modified from Bebout and others (1982).

## Reservoir Volume of the B Sand

Sand volumes of each channel (fig. 7) are 5.1, 4.8, 12.5, and 15.8 Bcf (from west to east). Estimated aquifer fluid volume of these channels (at 20-percent porosity) is 180 million, 170 million, 440 million, and 560 million bbl, respectively. The aquifer-fluid-volume estimate for gas production from the B sand in this water-drive reservoir is 588 million bbl, which is within the range of values of geologic estimates.

The production estimate, if correct, indicates that several of the B sand thicks are interconnected. The western channel, in which South Cook field is located, must be connected to at least one and probably two channels to the east. In the latter case, the ratio of production estimate to geologic estimate would be 75 percent.

## Reservoir Volume of the C Sand

Sand volumes measured for each channel (fig. 7) show that the western (South Cook) channel contains about 18 Bcf of sand, resulting in an aquifer fluid

volume of 638 million bbl. The eastern channel contains 40 Bcf of sand, resulting in an aquifer volume of 1,430 million bbl. The production estimate of aquifer volume for this water-drive reservoir is 207 million bbl. Production volume, then, is less than one-third of the geologic estimate for this sand, even if only the western channel is considered.

This discrepancy probably results from the thin shale break, noted previously, in the Atlantic No. 1 Schorre well. This break can be correlated throughout the area of the western channel. The three producing wells from this interval tap only the distributary-channel sand below the shale break. This lower sand pinches out within a short distance northeast of the field; its volume is about one-third the volume of western-channel sand (fig. 7). The production estimate, then, suggests that the upper and lower parts of the C sand are not connected.

## Summary

The B and C sands at South Cook field represent distributary-channel and related sands that prograded across a growth-faulted zone. The B sand apparently has good lateral continuity between channels, whereas the C sand apparently has poor lateral continuity and vertical continuity limited by a thin shale.

# *YORKTOWN AND SOUTH YORKTOWN FIELDS*

Yorktown and South Yorktown fields (fig. 5) are located southeast of Yorktown in De Witt County. Production in the fields (and from two other wells in the immediate vicinity) is from the 11,000-ft Migura sand of the lower Wilcox Group. Temperature in the Migura sand ranges from 245° to 260° F. Original shut-in pressures were 8,316 psi in South Yorktown field and 9,272 psi in Yorktown field, yielding pressure gradients of 0.75 and 0.83 psi/ft, respectively.

## Stratigraphy of the Migura Sand

The Migura sand lies about 700 ft below the top of the lower Wilcox Rockdale delta system of Fisher and McGowen (1967). The Migura interval is from 150 to 400 ft thick; sandstone content varies from more than 90 to less than 10 percent. Sand isolith contours (fig. 8) outline a dip-oriented sand having maximum thickness of more than 300 ft. Sand grades into a thick shale sequence to the southwest within 1.3 mi of the channel axis (fig. 9) and pinches out northeastward in an area of poor well control. To the northeast in South Cook field, the Migura interval is composed of shaly sand (fig. 9), which is part of a larger sequence of interbedded sand and shale. Updip, the Migura sand appears to become one of several upward-fining sequences. The sand has not been penetrated downdip of the Yorktown area.

Yorktown field is located on the main axis of the Migura channel. The sand in this area is 150 to 240 ft thick and contains three sub-sequences, as seen in Monsanto No. 1 Kulawik well (fig. 9). The interval has a high, sawtooth SP response, suggesting many thin intervals of less permeable sand or silt.

South Yorktown field is located on the northeastern edge of the Migura channel; sand thicknesses in Mosbacher *et al.* Nos. 1 and 2 C. F. Spies wells are 95 and 130 ft, respectively. The character of the sand is similar to that in the Yorktown field, increasing little in shale content.

## Structure of the Yorktown Area

The Yorktown area is a complex of strike-oriented normal faults (fig. 8); most faults are downthrown to the Gulf. Individual fault blocks are slightly tilted, and small rollover anticlines are developed. Most of the faulting occurred during lower Wilcox deposition, although upper Wilcox strata thicken over the southernmost faults.

The shape of the Yorktown fault compartment is fairly well determined. It is open to the southwest, although small cross faults may be present. The antithetic block mapped north of the field is displaced only slightly from the main block. The South Yorktown fault compartment, however, is poorly delineated. No wells have penetrated the Migura sand east and north of Mosbacher No. 1 Spies well. Shape of the eastern and northeastern margins of the fault block is therefore speculative, constrained by the known northern growth fault and the low elevation of the lower Wilcox horizon in Broseco (La Gloria) No. 1 Ferguson well (fig. 9). Consequently, minimum and maximum extents of the fault compartment were chosen in a northeastern direction. The compartment boundary west of the field is questionable; a small antithetic fault may lie just west of the field. Such a fault might be sufficient to break reservoir continuity westward.

## Reservoir Volume of Yorktown Field

The volume of the Yorktown reservoir was calculated by using a cutoff in the southwestern direction of 50 ft of net sand for the minimum case and 25 ft of net sand for the maximum case. Calculated sand volume is 9.8 Bcf for the minimum case and 10.5 Bcf for the maximum case; the antithetic block has a volume of 1.8 to 2.3 Bcf. In the De Witt fairway, porosity at 11,000 ft is typically about 14 percent (Bebout and others, 1982). Given this porosity, pore-water volumes are 245 million to 260 million bbl, plus about 35 million to 40 million bbl for the antithetic block. The estimate of aquifer fluid volume in this water-drive reservoir is 576 million bbl. Thus, if these geologic estimates are correct, more water

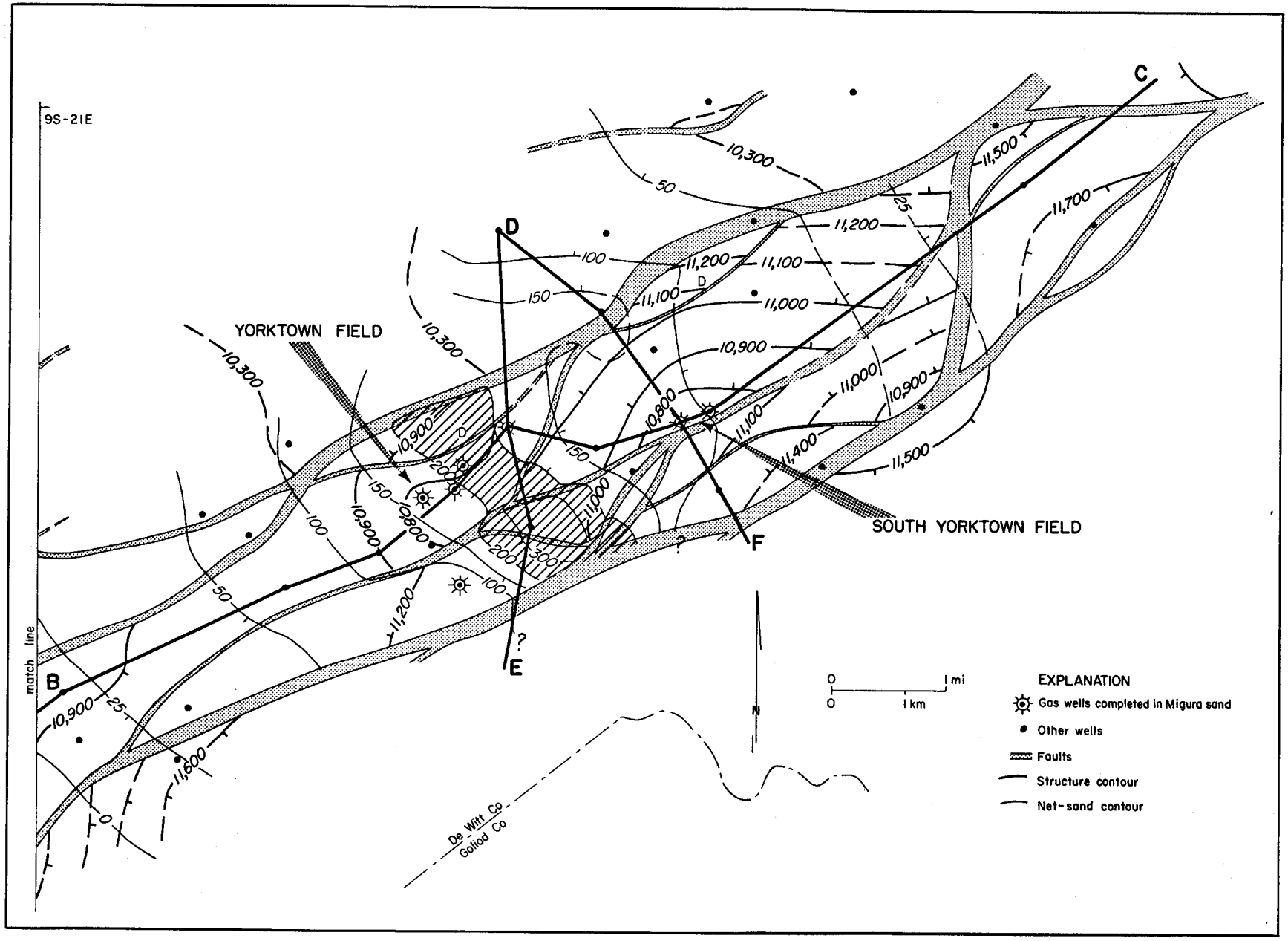


*Figure 8.* Structure and net-sand map of the Yorktown area. Heavy contours are structure on the Migura sand; light contours are net-sand isoliths of the Migura sand. Diagonal-line pattern indicates sand more than 200 ft thick. Faults downthrown to the southeast unless indicated. Match line is to figure 11.

drives this gas field than is contained in the Yorktown fault block.

This discrepancy may result from nonsealing faults (fig. 10a). Along the main axis of the Migura channel, sand thickness is 250 to 300 ft. The faults that bound Yorktown field on the south, however, have only 150 to 250 ft of throw. It is plausible, therefore, that the sand south of the Yorktown Y block is continuous with Yorktown field. Reservoir rock volumes of the two blocks mapped south of the field are 2.85 Bcf for the smaller A block and 8.4 Bcf for the larger B block. Aquifer fluid volumes of the A and B blocks at 14-percent porosity are 70 million and 210 million bbl, respectively. The production-volume estimate could then be matched (with the assumptions already outlined) if all of the previously mentioned blocks are connected along the Migura channel axis.

If the B block, which contains gas, is connected with the Yorktown Y block, both blocks should show similar pressure histories. The limited pressure data available support this hypothesis.

## Reservoir Volume of South Yorktown Field

The volume of the South Yorktown block was calculated for several cases: (1) For the minimum northeastern extent of the block, where sand is thinning to the northeast and an antithetic fault lies just west of the field, sand volume is 4.24 Bcf and aquifer fluid volume (at 14-percent porosity) is 151 million bbl. (2) For the maximum extent of the block, rock volume is 5.0 Bcf and aquifer fluid volume is 180 million bbl. (3) If there is no antithetic fault west of the field, these figures are 8.3 Bcf and 205 million bbl for the minimum case and 10.1 Bcf and 250 million bbl for the maximum case. The aquifer fluid volume estimated from production figures is 82 ± 14 million bbl for this pressure-depletion reservoir. All the geologically estimated volumes are much higher.

This discrepancy may be explained in several ways. Poor well control in this block may have allowed some faults to go unrecognized (or the thinning assumption may be too generous). Recalculation, accounting for this, lowers the estimate to 106 million bbl, which is close to the production estimate. A second possibility is that only part of the sand is currently being produced. Interconnection (assuming 14-percent porosity) is 80 percent for the minimum case. Perforations in the two producing wells are in the top third of the sand. As mentioned previously, there are many small silty breaks in the sand throughout the area. One or more of these breaks may be continuous throughout the block, thus sealing off part of the sand. Other possibilities are that porosity is markedly lower, or water saturation markedly higher, than the assumed values of 14 and 25 percent, respectively. The present data do not allow a choice among these possibilities.

Figure 10b shows that the thinner sand of the South Yorktown area is not continuous across the growth faults south of the field. Gas production from the well to the south, therefore, is from a separate reservoir; this is supported by pressure data.

## Summary

Yorktown and South Yorktown fields produce from the dip-oriented Migura sand. The Yorktown wells penetrate the channel axis, where more than 250 ft of sand apparently allows fluid flow among several fault blocks and production from a large reservoir volume. South Yorktown field lies on the northeastern side of the channel; production is restricted to the immediate fault block and may not be from the entire sand interval.

# *CHRISTMAS FIELD*

Christmas field is located 7.6 mi southwest of Yorktown in De Witt County (fig. 5). Production in the field is mainly from the 10,800-ft sand of the lower Wilcox Group, which is equivalent to the Migura sand of the Yorktown area. Temperature in the Migura sand is approximately 270° F. The original shut-in pressure for the field was 8,201 psi at Hanson *et al.* No. 1 F. L. Altman well, yielding a pressure gradient of 0.76 psi/ft.

## Stratigraphy of the Migura Sand

The Migura sand in the Christmas area (fig. 11) ranges in thickness from zero to 165 ft. The sand thins abruptly to the northeast; its southwestern limit is gradual and strongly strike oriented. Downdip to the southeast, sand percentage and net-sand thickness decrease rapidly; updip, sand is not correlatable. The Migura sands in the Christmas and Yorktown areas are separated by about 3 mi of silt and clay (fig. 11).

From well log patterns (fig. 12), the Migura sand in this area can be divided into three facies. In the northern and northeastern part of the field, a large, upward-fining sequence (seen in Cox *et al.* No. 1 Kleine well on fig. 12) suggests a thick channel sequence of sand and shale. To the southwest, the sand is divided into several parts by thin but correlatable shale breaks. Most of the sands in this facies have SP patterns typical of delta-front or crevasse-splay sands. The lower part of the upper sand in Hanson No. 1 Altman well shows an upward-fining sequence, possibly representing a thin channel deposit. The sands of this facies thin and grade into shale to the southwest. Separate from these sands in Nordheim field, fairly thick, blocky sands are found in the Getty Nos. 16 and 13 Nordheim wells (fig. 12).

The five wells of Christmas field penetrate the channel and delta-front/crevasse-splay facies of the Migura sand. One well, Cox No. 1 Kleine (fig. 12), produces from the base of the channel sequence. Three wells produce from the upper sand of the delta-front facies; one is perforated below a thin break, one is perforated above the break, and one straddles the break. The fifth well produces from a deeper sand.

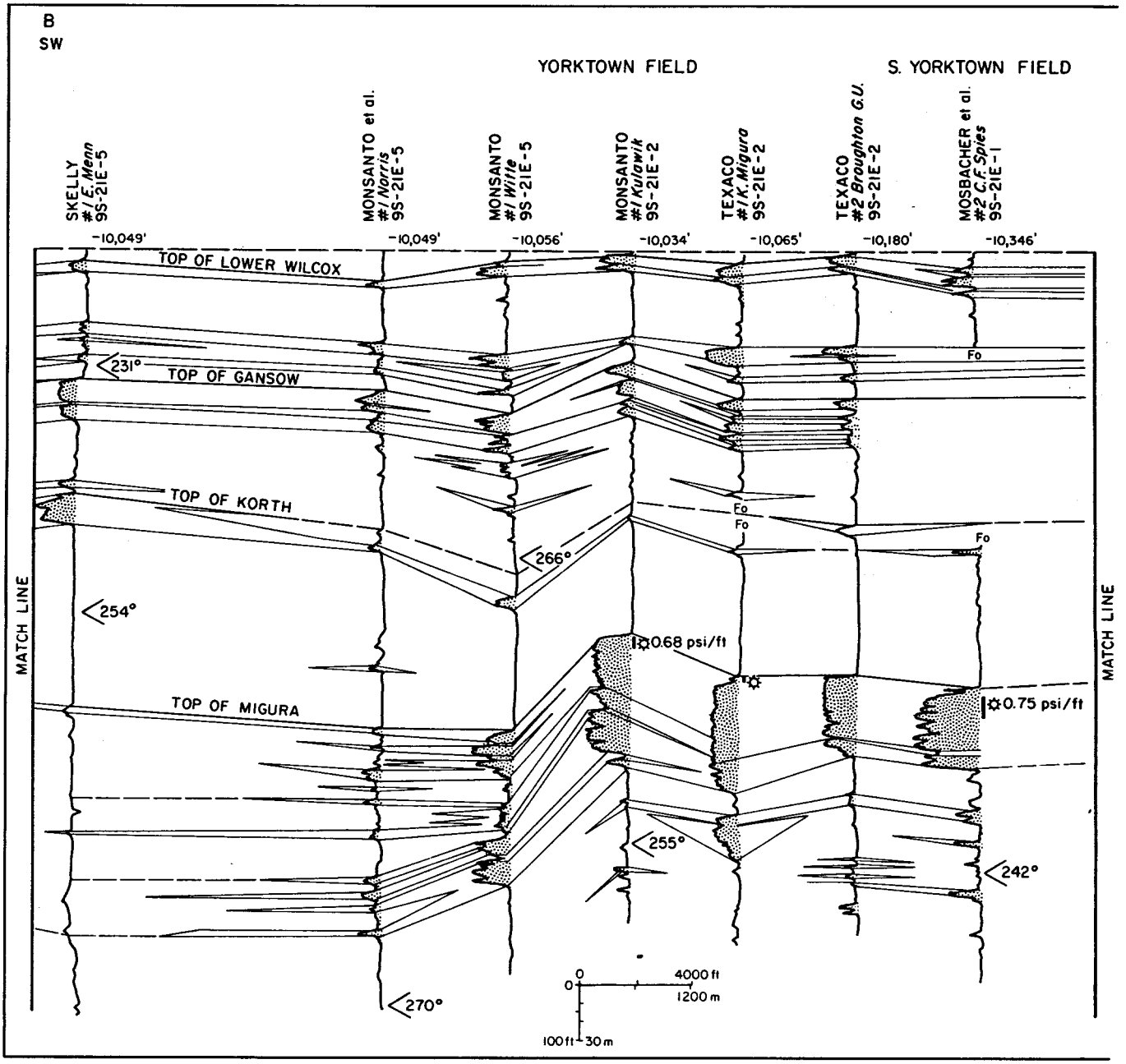


*Figure 9.* Stratigraphic section of lower Wilcox Group sands, Yorktown area. Datum is top of lower Wilcox Group (D4'). Match line, above left, is to figure 12. Letter intervals in South Cook field from Bebout and others (1982). Dot pattern

## Structure of the Christmas Area

Structure of the Christmas area is complex and not well determined (fig. 11). A network of normal faults divides the area into small compartments. Rapid facies changes in the Migura and overlying Korth intervals, together with intense faulting, make correlations tenuous, especially southwest and northwest of Christmas field.

The Christmas fault compartment is poorly defined. Its southeastern-bounding fault is found in four producing wells and is adequately located. The northeastern limit is not defined, but this does not affect volume calculation because sand is not present in this direction. The southwestern boundary is determined by the difference in elevation of the Migura sand to the southwest. Northwestern and northern boundaries are uncertain. A small fault crosses between four Christmas wells and the Hanson *et al.* No. 1 Buesing well, which lies northwest of the area mapped in figure 12. The large northwestern fault has been tentatively identified below the Migura sand in the Hanson No. 1 Buesing well; lack of deep well control in the upthrown block makes its location uncertain.

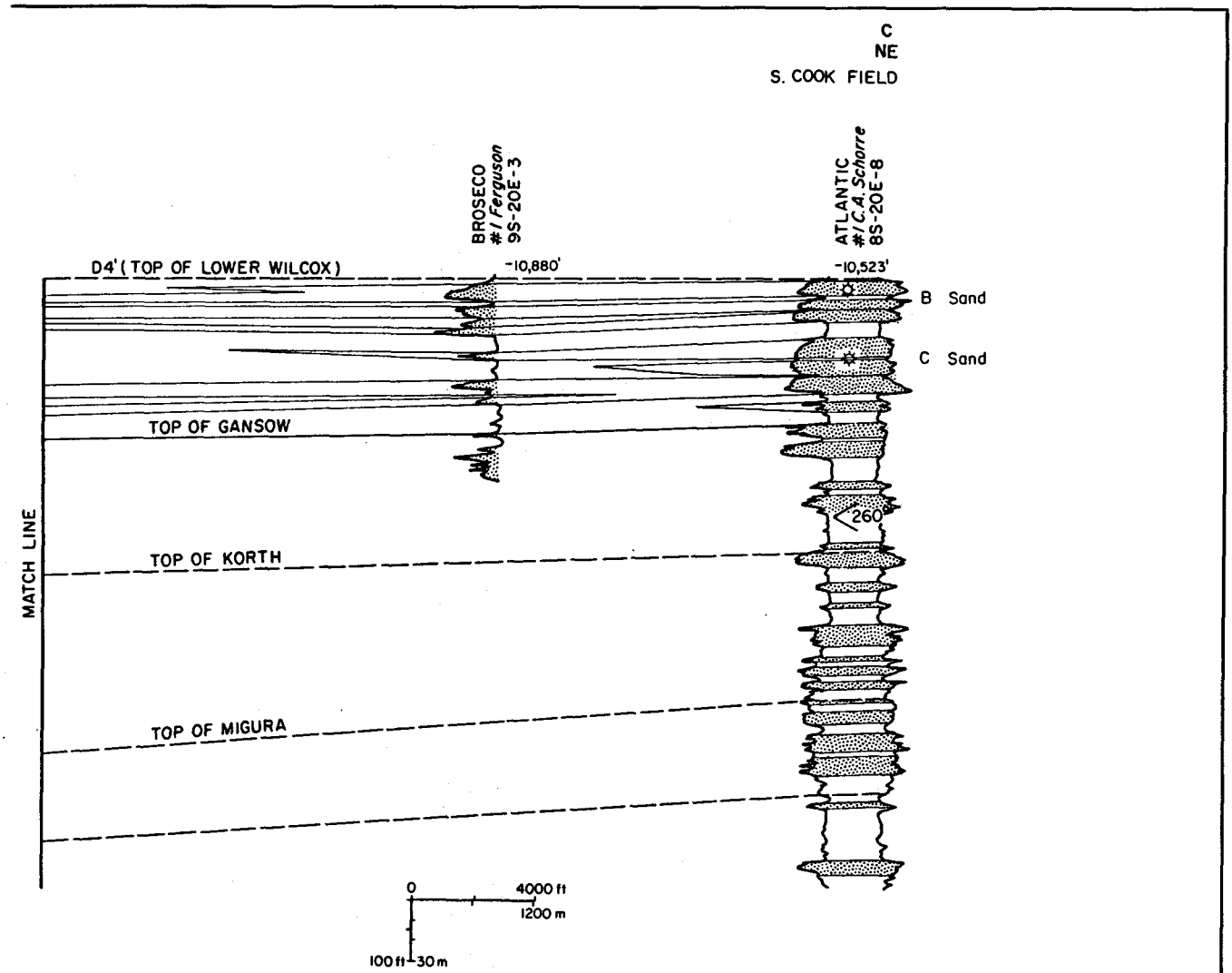


indicates sands in each well; producing zones, pressure gradients (psi/ft), and temperatures (°F) are given. All cross sections show spontaneous potential and resistivity logs unless indicated. Line of section shown in figure 8.

## Reservoir Volume of Christmas Field

The total volume of Migura sand in the Christmas fault compartment is calculated to be 6.3 Bcf; estimated uncertainty is 30 percent. Assuming a porosity of 14 percent (as used for Yorktown field), aquifer fluid volume is 160 million bbl. The volume estimate from production and pressure data for this pressure-depletion reservoir is 49 ± 1.2 million bbl. Overall percent interconnection (table 6), therefore, is 25 percent.

Several factors may account for this low degree of continuity. One is that Hanson No. 1 Buesing well does not produce from the Migura sand but has an identical pressure history. This suggests that the small faults between the Hanson No. 1 Buesing and the other wells are nonsealing. If so, the thinner sub-Migura sand should be used for calculations instead of the Migura itself; this would tend to lower the estimate of reservoir volume. Another factor is that Cox No. 1 Kleine well produces a small amount of gas from the base of the thick channel sequence (fig. 12), making its connection to the other wells doubtful. As mentioned previously, the

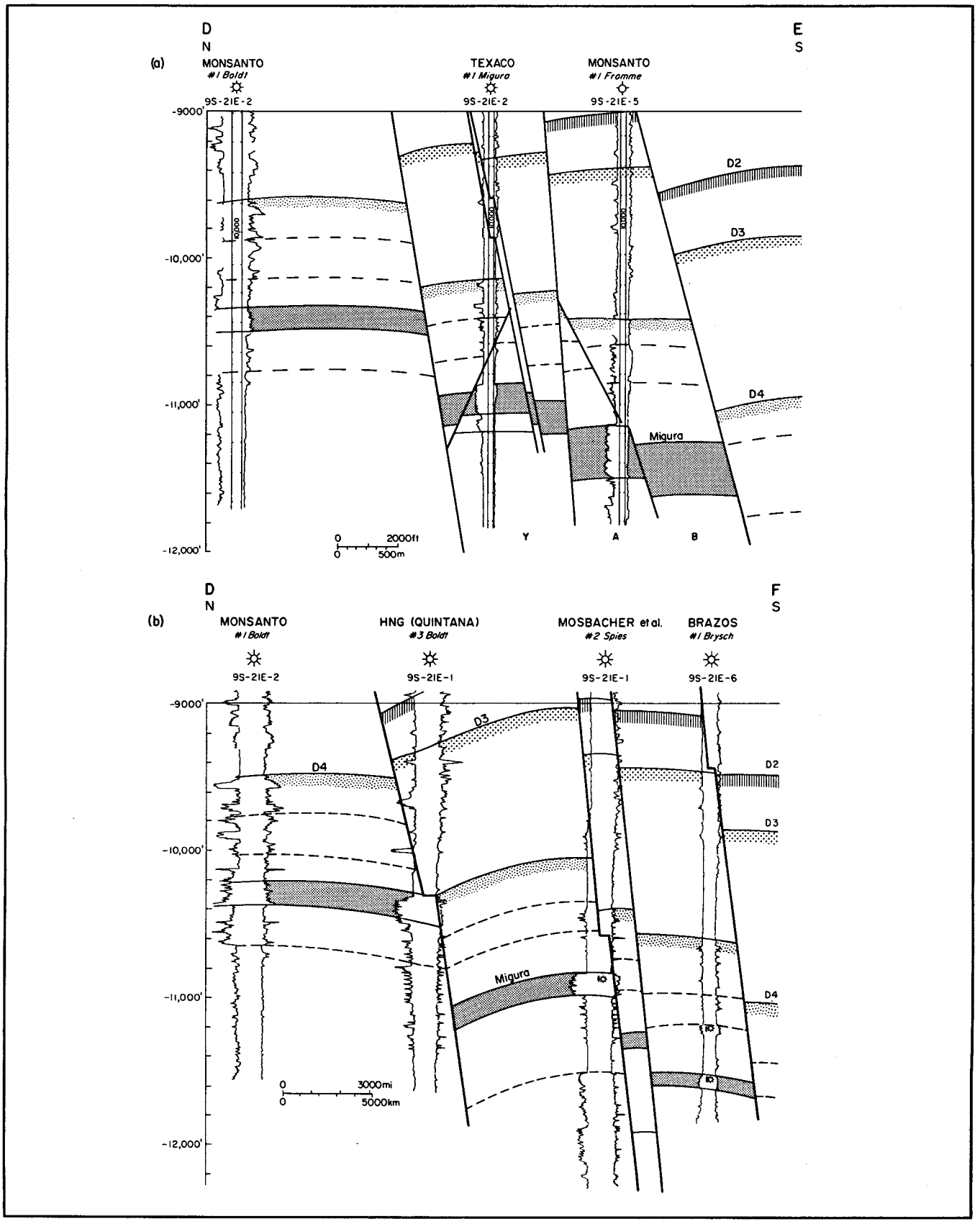


*Figure 10.* Structure sections of the Yorktown area through (a) Yorktown field, showing sand connections, and (b) South Yorktown field, showing sand isolation. Lines of section shown in figure 8.

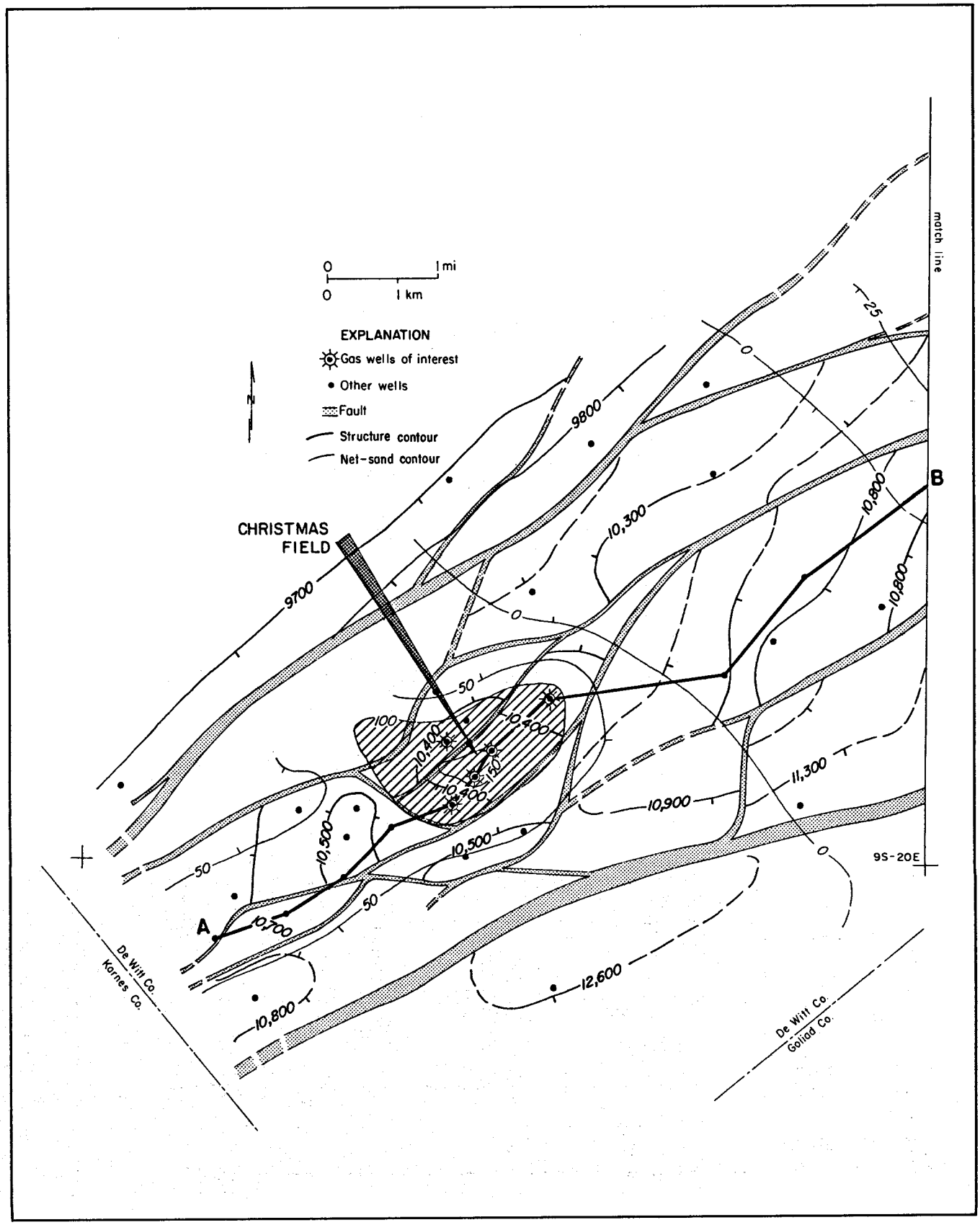


*Figure 11.* Structure and net-sand map of the Christmas area. Datum is Migura sand. Match line is to figure 8. Diagonal-line pattern indicates sand more than 100 ft thick. Faults downthrown to the southeast unless indicated.

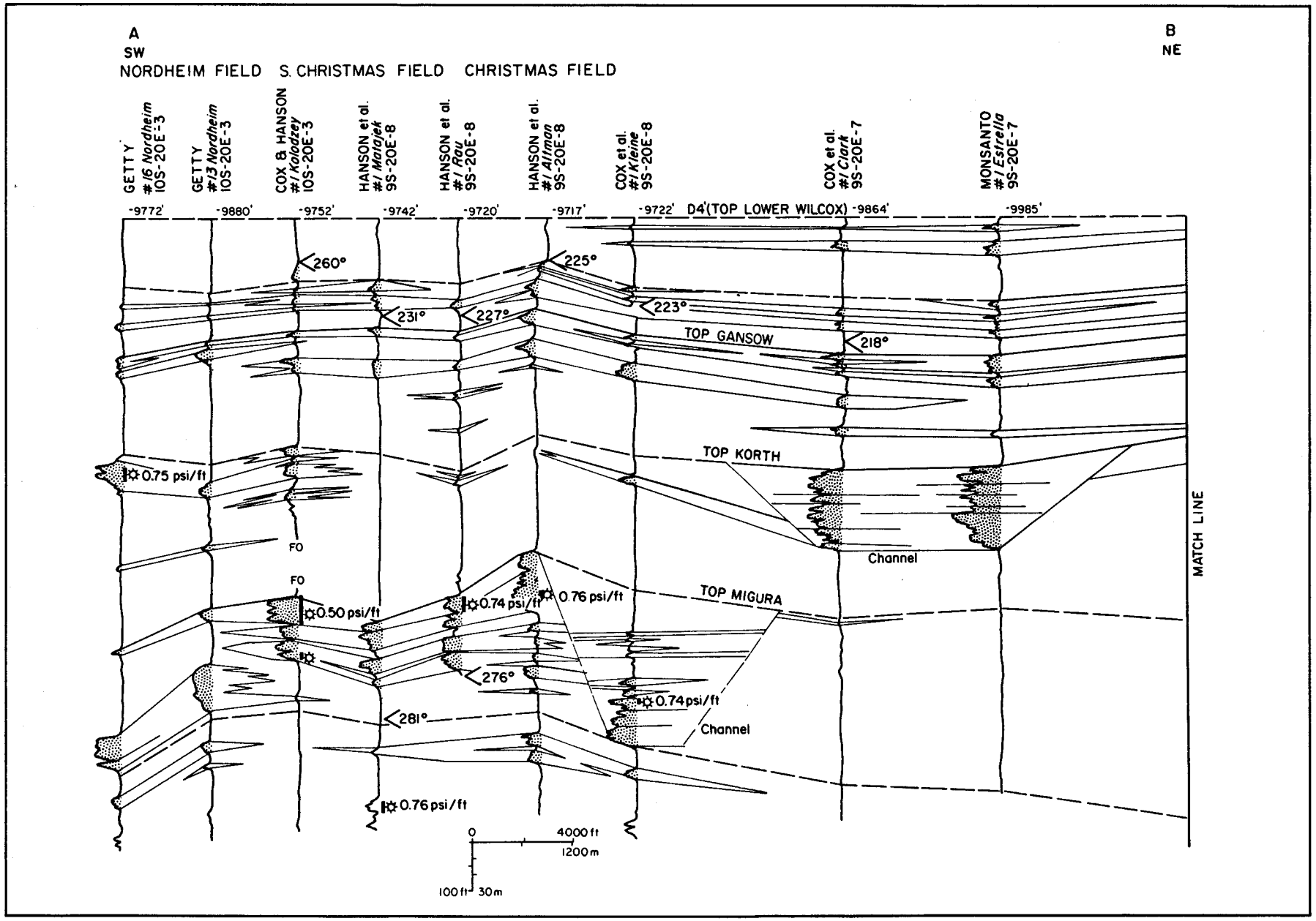


*Figure 12.* Stratigraphic section of lower Wilcox Group sands, Christmas area. Datum is top of lower Wilcox Group (D4'). Symbols as in figure 9; line of section shown in figure 11. Match line is to figure 9.

remaining three wells produce only from the upper sand of the delta-front facies. The sand probably is separated from the lower unit of the Migura, which reduces the reservoir volume considerably, and the thin shale break within the upper sand may further fragment the reservoir. Finally, the indeterminate size of the fault compartment may lead to an inflated geologic estimate. Some combination of these factors, or deviation from the porosity and saturation assumptions, may account for the difference between geologic and production estimates.

# *SOUTHEAST PETTUS FIELD*

Southeast Pettus field is located 2 mi southeast of Pettus in Bee County (fig. 5). Gas production in the field is from the Massive sands or First Massive sand of the upper Wilcox Group. Temperature in the First Massive sand averages about 230° F. The bottom-hole shut-in pressure for Hughes and Hughes No. 1 J. E. McKinney well in the field is 5,666 psi, yielding a pressure gradient of 0.64 psi/ft.

## Stratigraphy of the First Massive Sand

The First Massive sand lies within the Bee delta of the upper Wilcox Group, which is part of the Rosita delta system (Edwards, 1981). It occurs at the top of a sand-rich section of the Wilcox (the Massive sands) about 200 ft below the Mackhank sand, which is the uppermost unit of the Bee delta.

The area is transected by a large growth fault. Northwest of the fault, the Massive sands are thin and the First Massive sand is inseparable from lower sands. Downdip of the fault, sand reaches a maximum thickness of more than 100 ft immediately south of Southeast Pettus field (fig. 13) but thins to the east, south, and southwest. Sand percentage is highest in Southeast Pettus field; shale content increases downdip. Several shale breaks within the sand and in overlying sands can be correlated throughout much of the area (fig. 14).

On the basis of the net-sand map and the electric log, the First Massive sand is thought to be a lobe of the Bee delta. The area northwest of the growth fault represents a delta-plain facies. The blocky sands of the Southeast Pettus field area are either delta-plain to delta-front sands or sands reworked into barrier bars. Downdip of point B (fig. 13), upward-coarsening sequences are recognized in the First Massive sand interval, suggesting delta-front conditions. The relatively continuous shale breaks may indicate short-lived lobe abandonments, preserved from later reworking by rapid subsidence along the growth fault.

## Structure of the Pettus Area

The Pettus area (fig. 13) is marked by a uniform southeast dip to the northwest, broken only by minor faults and by a zone of closely spaced, syndepositional normal faults to the southeast. The major growth faults that occurred during deposition of the Massive sand are in a belt trending northwest to southeast through the Southeast Pettus field area. The more southeastern faults also affected deposition of the Massive sand but appear to have experienced their greatest movement during Mackhank time.

The fault compartment within which Southeast Pettus field is located is bounded by a major growth fault to the northwest and west. A fault of lesser displacement separates it from East Tuleta field to the south. This small fault joins to the east with a larger growth fault, which continues to the northeast beyond well control.

## Reservoir Volume of the First Massive Sand

Volume of the First Massive sand reservoir at Southeast Pettus field was calculated for two cases: a minimum area of the fault compartment, which includes only the producing area, and a maximum area (fig. 13). Calculations for these two cases yield reservoir areas of 2.0 and 4.3 $mi^2$, respectively. Assuming an average sand thickness of 80 ft and porosity of 16 percent, derived from the regional study in Live Oak fairway to the southwest (Bebout and others, 1982), sand volume ranges from 4.6 to 9.5 Bcf; aquifer fluid volume in this pressure-depletion reservoir is estimated at 130 million to 270 million bbl.

Production data, however, indicate an aquifer fluid volume of only 28 ± 2 million bbl, which is 10 to 23 percent of the geologically estimated volume. This discrepancy may be ascribed to the presence of thin, laterally continuous shale breaks. All the active wells in this field produce from the upper part of the First Massive sand. It is likely that the lower part of the sand is not in communication with the upper part within this small fault compartment. In support of this hypothesis, resistivity logs from Southeast Pettus field show two high-resistivity zones, indicating gas-filled sand within the First Massive. The lower gas zone is not being produced by the existing wells. A revised geologic calculation of sand volume yields an aquifer fluid volume of 60 to 120 million bbl. For unknown reasons, this figure is still too high.

# *SOUTH BRASLAU FIELD*

South Braslau field is located 3.8 mi southwest of the town of George West, Live Oak County (fig. 5). Four wells produce gas from the First Tom Lyne sand of the upper Wilcox Group. Reservoir temperature is approximately 240° F. The field had an original shut-in pressure of 6,652 psi, yielding a pressure gradient of 0.73 psi/ft.

## Stratigraphy of the First Tom Lyne Sand

The First Tom Lyne sand is located within the upper Wilcox Group between two larger sands, the Luling

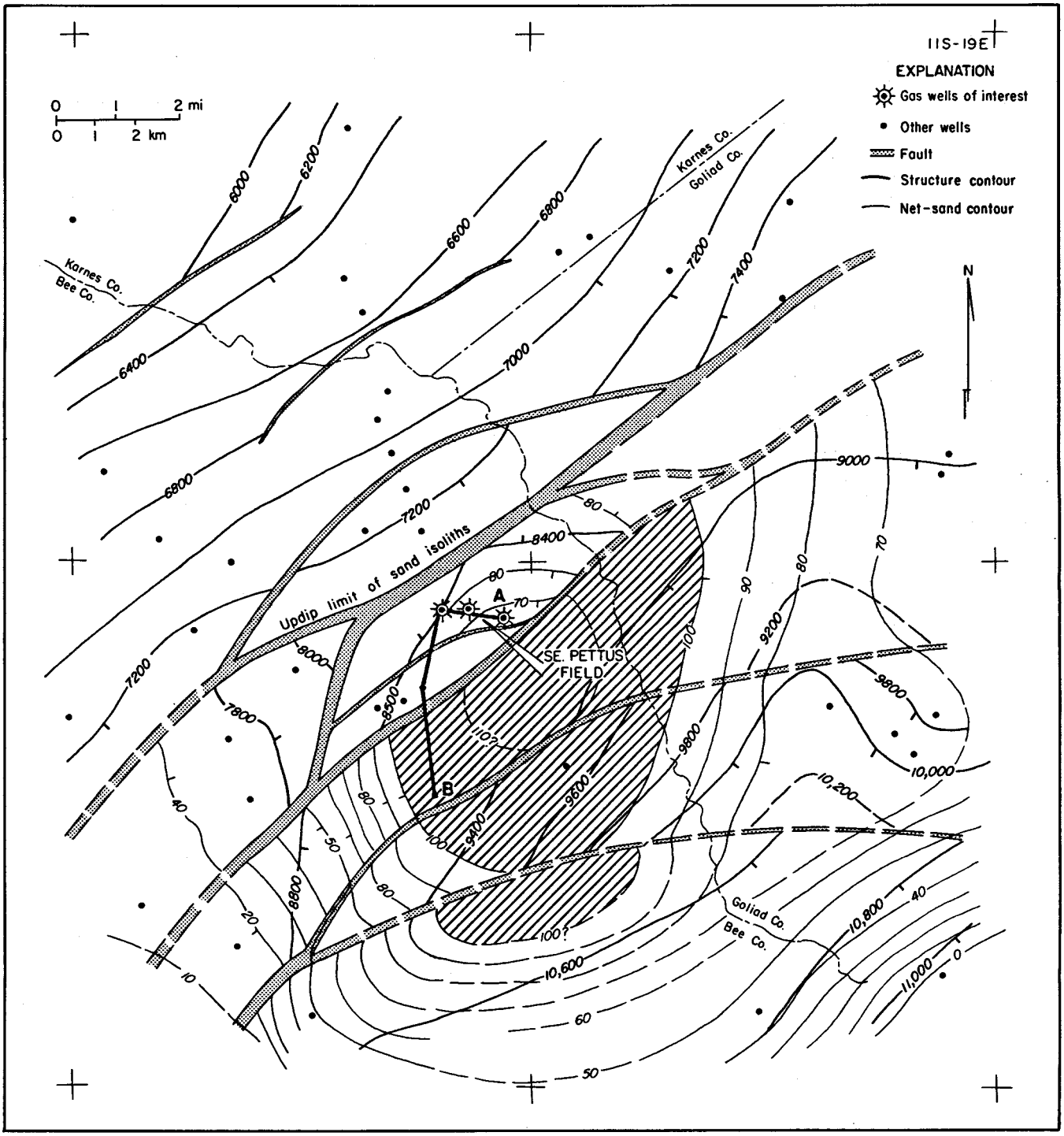


*Figure 13.* Structure and net-sand map of the Pettus area. Datum is First Massive sand. Diagonal-line pattern indicates sand more than 100 ft thick. Faults downthrown to the southeast unless indicated.

above and the Mackhank below. In the past, First Tom Lyne has been confused with the Mackhank sand in much of the area; recent work by Edwards (1981) has demonstrated that they are separate. The Luling and the overlying Slick sands compose the Live Oak delta of the Rosita delta system (Edwards, 1981), whereas the underlying Mackhank and Massive sands are part of the newly defined Bee delta (Weise and others, 1981). The First Tom Lyne sand, also a deltaic sand, lies between the two previously defined deltas.

The sand varies from less than 25 to more than 150 ft thick in the area (fig. 15) and is profoundly affected by

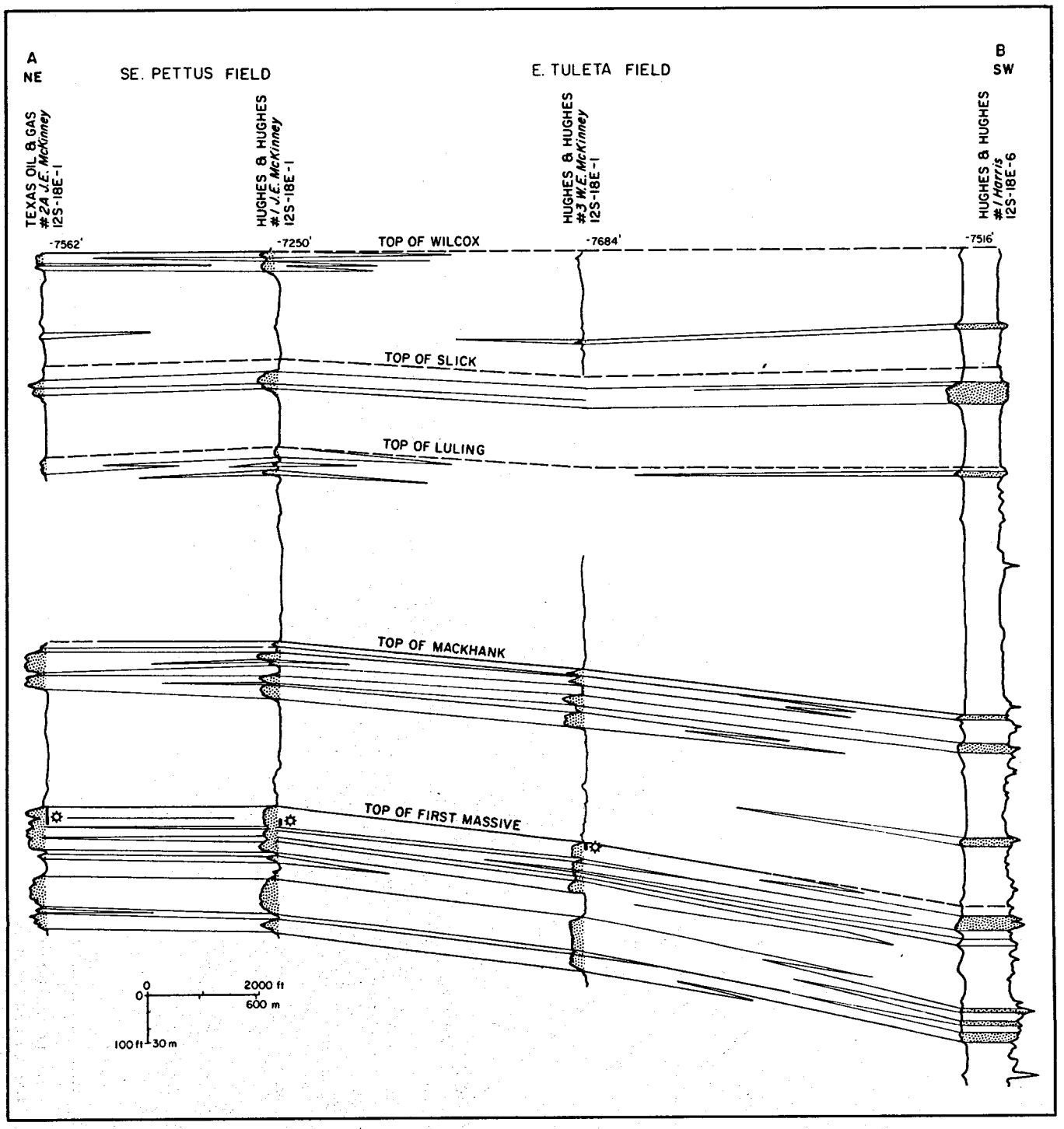


*Figure 14.* Stratigraphic section of upper Wilcox Group sands, Pettus area. Datum is top of Wilcox Group. Symbols as in figure 9; line of section shown in figure 13.

growth faulting. Updip of a large growth fault, the sand is not separable from the Mackhank, and both are less than 25 ft thick. Thickening occurs over two growth faults into the main sand depocenter southeast of the field. Sand thickness decreases rapidly to the east and somewhat less rapidly to the west. Overall shape of the sand isoliths suggests a high-constructive, lobate deltaic sand.

The First Tom Lyne is a composite deltaic sand (fig. 16). Basal upward-coarsening sequences are overlain by delta-plain and channel sands exhibiting blocky to upward-tapering SP patterns. Shale breaks

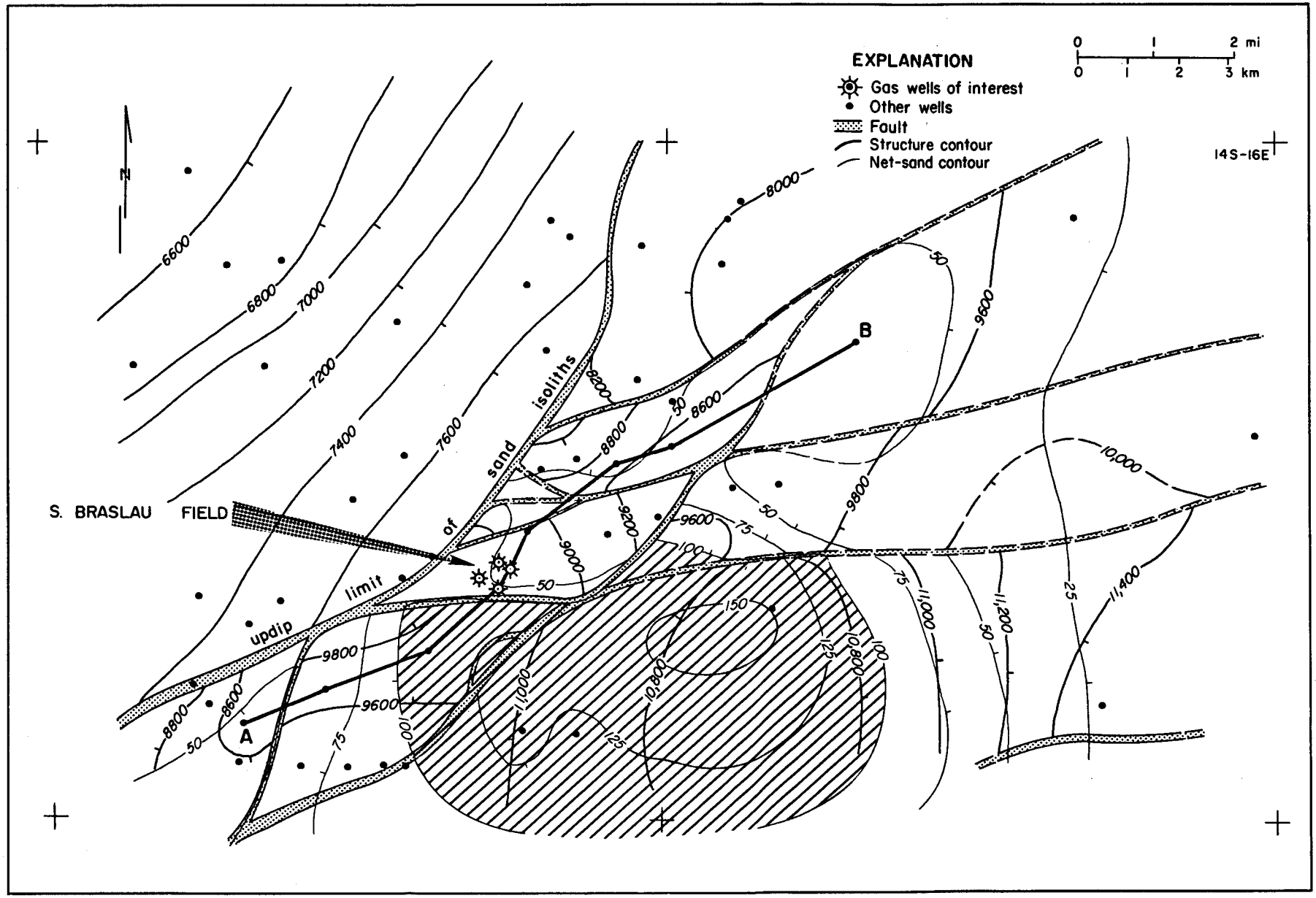


*Figure 15.* Structure and net-sand map of the Braslau area. Datum is First Tom Lyne sand. Diagonal-line pattern indicates sand more than 100 ft thick. Faults downthrown to the southeast unless indicated.

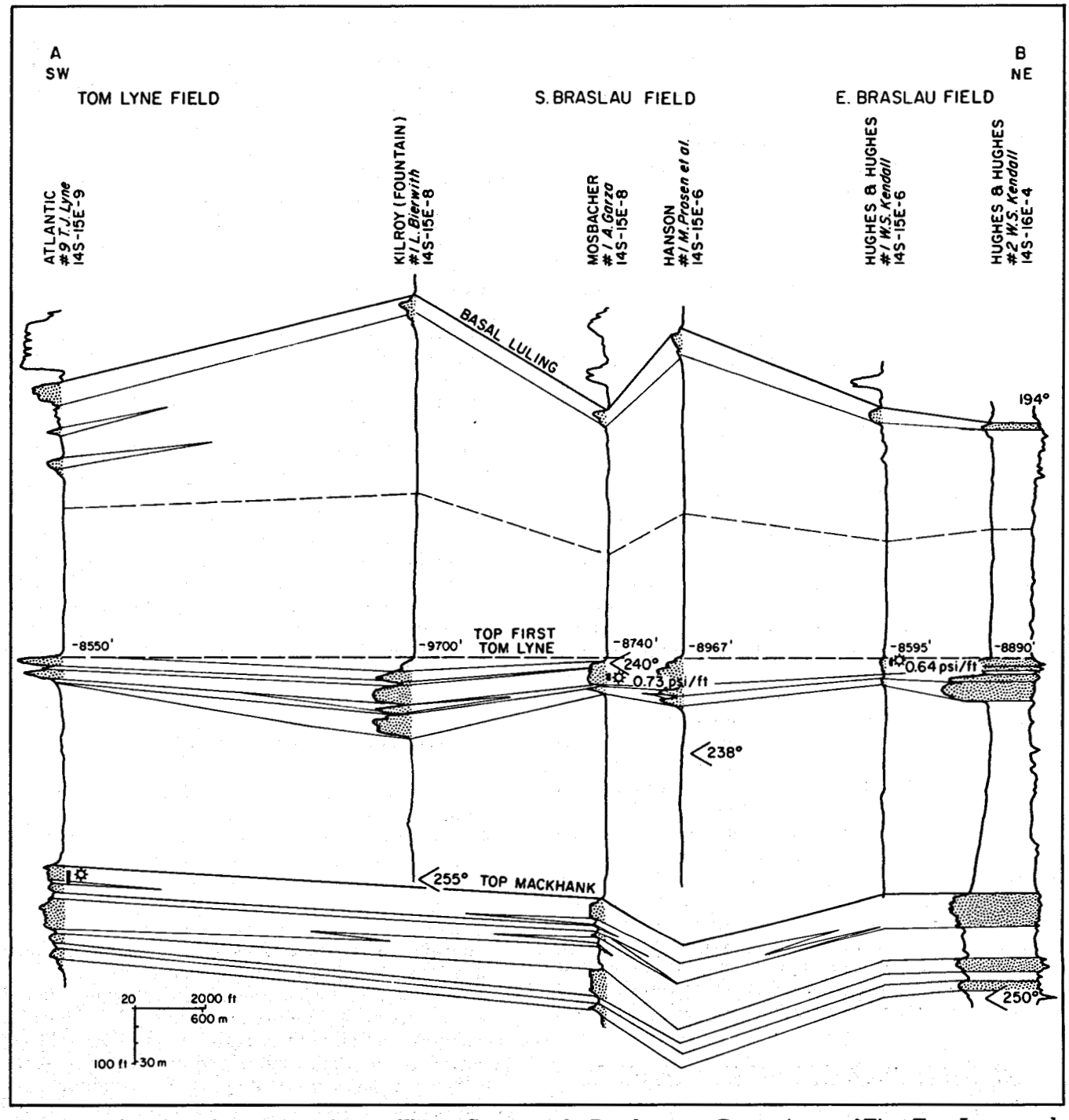


*Figure 16.* Stratigraphic section of upper Wilcox Group sands, Braslau area. Datum is top of First Tom Lyne sand. Symbols as in figure 9; line of section shown in figure 15.

are remarkably continuous in this area, extending more than 2.5 mi along strike. These may be delta-lobe-abandonment shales preserved from later erosion by rapid subsidence, similar to those in Southeast Pettus field. The shale breaks are thinnest in the South Braslau field area, but the lower delta-front sand is still separate from the rest of the sand sequence in all wells.

The depocenter of the First Tom Lyne sand lies between two depocenters of the immediately underlying Mackhank sand (Weise and others, 1981), and its main expansion faults are slightly southeastward of the Mackhank faults. The expansion faults and depocenters of the overlying Luling and Slick sands are still farther southeastward (Edwards, 1981).

## Structure of the South Braslau Area

South Braslau field lies within a complexly growth-faulted area (fig. 15). A belt of small fault compartments lies southeast of a gently dipping, unfaulted area having a thin Wilcox Group section. Southeast of the belt, fault-block size increases as well control decreases. Braslau, South Braslau, and Tom Lyne fields occupy successive fault compartments along the belt from northeast to southwest.

## Reservoir Volume of South Braslau Field

The South Braslau fault compartment (fig. 15) is bounded by major faults on all sides. A fault having 100 ft of throw is detected in Hanson *et al.* No. 1 M. Prossen well north of the field; it may or may not break reservoir continuity on the northwest. The eastern fault is poorly determined. For calculating aquifer fluid volume, the most westerly and most easterly locations of this fault yield minimum and maximum values, respectively.

Assuming that the entire net sand is produced in this compartment and that the small fault on the northwest does not break continuity, the area of the fault compartment is 2.8 to 3.9 $mi^2$, and sand volume in this compartment is 5.1 to 7.0 Bcf. At an estimated porosity of 16 percent (Bebout and others, 1982), aquifer fluid volume is about 140 million to 210 million bbl. Aquifer fluid volume estimated from production figures is 61 $\pm$ 14 million bbl. Hence, the production volume is only 22 to 54 percent of the geologic estimate.

If the small fault disrupts continuity, the area of the fault compartment is between 2.2 and 3.2 $mi^2$, the reservoir volume is 3.7 to 6.0 Bcf, and the aquifer fluid volume at 16-percent porosity is 105 $\pm$ 17 million bbl, yielding an apparent interconnectedness of 27 to 71 percent. This low degree of interconnection is probably caused by thin shale breaks. As noted above, shale breaks are remarkably continuous in the sand, and the lower delta-front sand is separated from the rest of the sand by 5 to 10 ft of shale. If this lower sand is not connected with the producing upper sand, the two volume estimates are in close agreement. However, porosity could be much lower and water saturation higher than assumed.

# *SOUTH PEACH POINT FIELD*

South Peach Point field is located 7 mi west-northwest of Freeport in Brazoria County (fig. 5). Two wells produce gas from the Frio A sand, and one well produces gas from the underlying Frio A′ sand. Reservoir temperature is approximately 250° F. The field had an original shut-in pressure of 9,572 psi, yielding a pressure gradient of 0.85 psi/ft.

## Stratigraphy of the Frio A Sand

The Frio A sand of the Peach Point area lies in the *Nodosaria blanpiedi* zone of the subsurface Frio. At Peach Point, three named sands are found in this interval: the A, A′, and B sands. The A sand ranges in thickness from zero to more than 60 ft (fig. 17). The sand is thickest and contains fewest breaks northwest of Clemens Dome, where it shows blocky SP patterns and suggests upward-coarsening sequences. In the Peach Point fields, sands are less regular and have many silty breaks (fig. 18); both upward-coarsening and upward-fining sequences are observed. Southeast and west of Peach Point, upward-fining sequences dominate and the sand is thinner. Sand isoliths (fig. 17) show that the thicker sand intervals are roughly dip oriented; a sand-free area occurs northeast of the Peach Point fields.

This complex thickness pattern can be interpreted as a delta-margin sequence. Channel deposits form a thick, upward-fining, sandy sequence through the Clemens Dome fields and a thinner sequence through Peach Point. Delta-front sands of irregular thickness occur at the ends and margins of these channels in the area southeast of Peach Point and in the Allen Dome area. Similar sand-development patterns characterize the other sands of the interval in this area.

The Peach Point area lies about 25 mi south of the main middle Frio sand depocenter (fig. 18 of Bebout and others, 1978). Regional mapping suggests that this area was at the seaward margin of the Houston delta system (Galloway and others, 1982) and that the sands represent the maximum progradation of that delta system.

## Structure of the Peach Point Area

The complex structure of the Peach Point area is primarily the result of salt tectonics. The Peach Point fields lie atop a ridge trending east to west (fig. 17), which is presumably salt cored at depth. At the west end of the ridge is Clemens Dome, a piercement salt dome. Bryan Mound salt dome is at the east end, southeast of a sag in the ridge. A large salt-withdrawal basin lies north of the ridge and another salt-withdrawal basin, in which Allen Dome is uplifted, lies south of the ridge.

Faulting is complex and of several types. Radial fractures separate fields around Clemens Dome and also occur at Allen Dome. Axial grabens dominate the Peach Point ridge (fig. 19). In the salt-withdrawal basin to the northeast, two growth-fault systems having numerous antithetic faults have been recognized on regional seismic data. These growth faults interfere with the Peach Point ridge, giving rise to complex, large-scale displacements of up to 1,000 ft. The extent of faulting in the Allen Dome withdrawal basin is unknown because of lack of well control and seismic data.

The productive blocks at Peach Point and South Peach Point fields are profiled in figure 19. Peach Point field lies in a north-dipping section on the north side of the ridge. South Peach Point lies in the axial graben of the ridge (for the A sand production) and on the south side of the ridge (for the A′ sand production). The A and A′ sands are juxtaposed along the south fault of the graben (fig. 19).

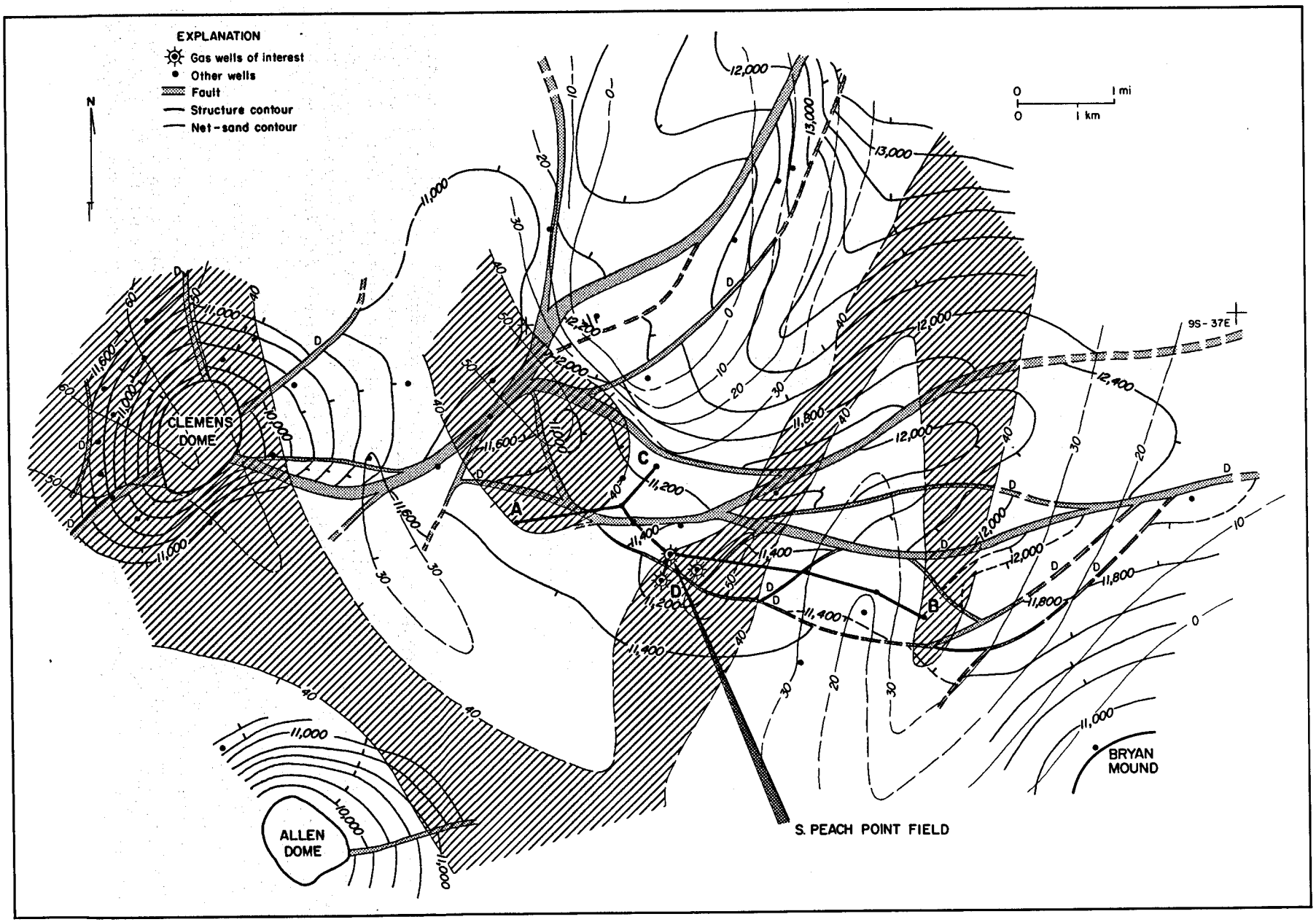


*Figure 17.* Structure and net-sand map of the Peach Point area. Datum is Frio A sand. Diagonal-line pattern indicates sand more than 40 ft thick. Faults downthrown to the south unless indicated.

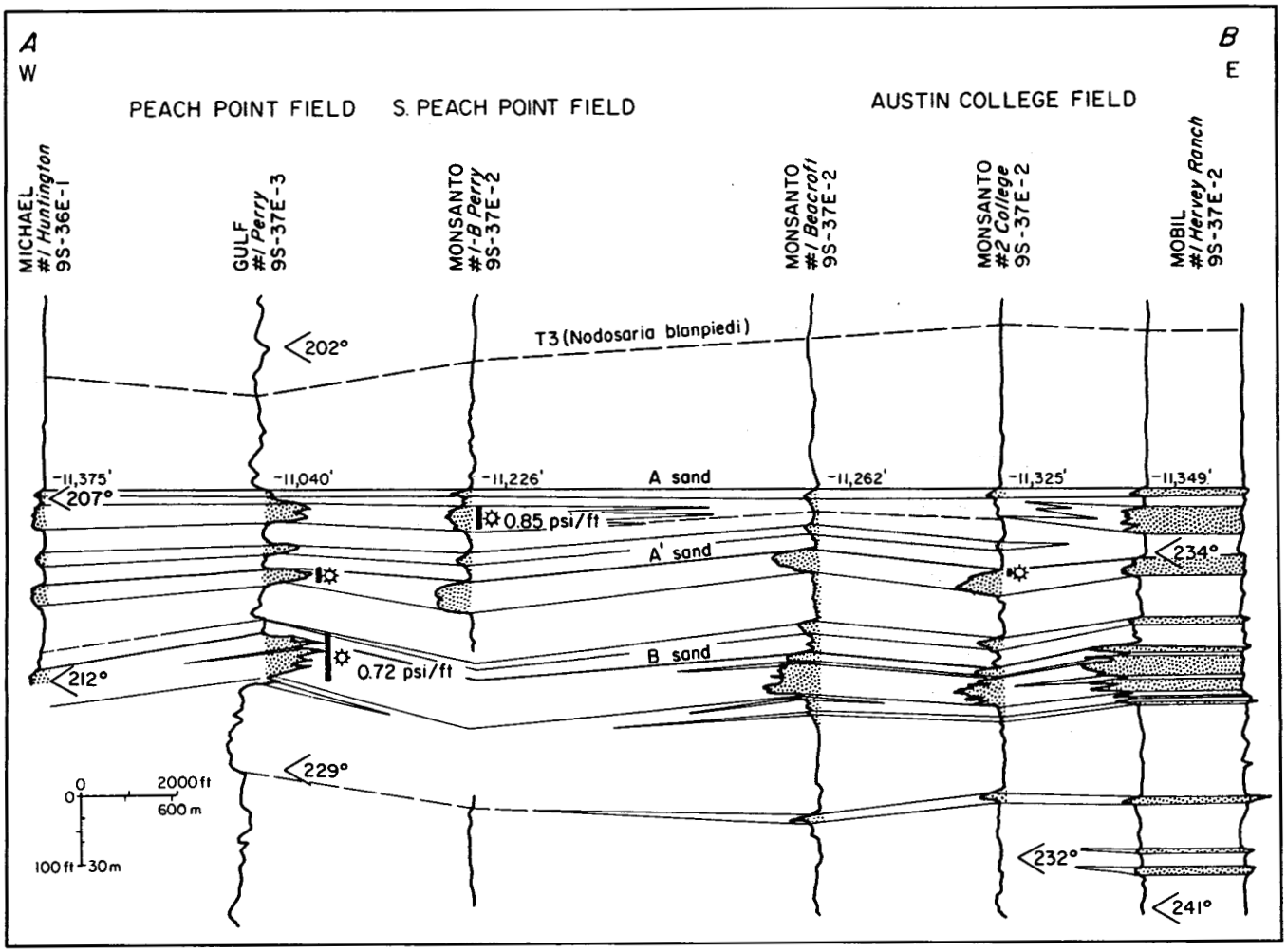


*Figure 18.* Stratigraphic section of sub-*Nodosaria blanpiedi* sands of the Frio Formation, Peach Point area. Datum is top of A sand. Note reversed spontaneous potential in one well. Symbols as in figure 9; line of section shown in figure 17.

## Reservoir Volume of South Peach Point Field

The South Peach Point fault compartment (fig. 17) is bounded by minor faults on the south and east and by a larger fault on the north. Assuming that the entire net sand is produced in this compartment, sand volume is 0.72 Bcf; the fault compartment area is 0.61 $mi^2$. Assuming a reasonable porosity of 15 percent (from Brazoria fairway, Bebout and others, 1982), aquifer fluid volume is 19.2 million bbl; at a high porosity of 20 percent, the volume is 25.5 million bbl. Reservoir volume from pressure-decline data is 33 ± 3 million bbl. Thus, the calculated aquifer fluid volume is too small for the observed production at reasonable porosities.

As shown on the structure section (fig. 19), the A′ sand to the south is juxtaposed with the producing A sand. The southern A′ sand block is a likely candidate for providing the extra volume. If the two sands are connected, (1) the fault is nonsealing and (2) the observed volume must be recalculated to include production from the third well, yielding 46 ± 6 million bbl. This connection is supported by the pressure history of the A′ well. The extent of the A′ fault compartment is unknown; therefore, no volumes can be calculated. To match the observed and calculated values, a fault-block area equal to 70 percent of the known fault compartment is needed.

## *MOBIL-DAVID L FIELD*

Mobil-David L field lies southwest of Corpus Christi in Nueces County (fig. 5). Deep production in the area comes from the Anderson sand of the Frio Formation, approximately 11,000 ft below sea level. The field includes several fault compartments; one of these, the L compartment, contains the reservoir of interest. In the L reservoir, the initial shut-in pressure was 9,507 psi, yielding a pressure gradient of 0.84 psi/ft. Reservoir temperature is estimated at 266° F (Duggan, 1972).

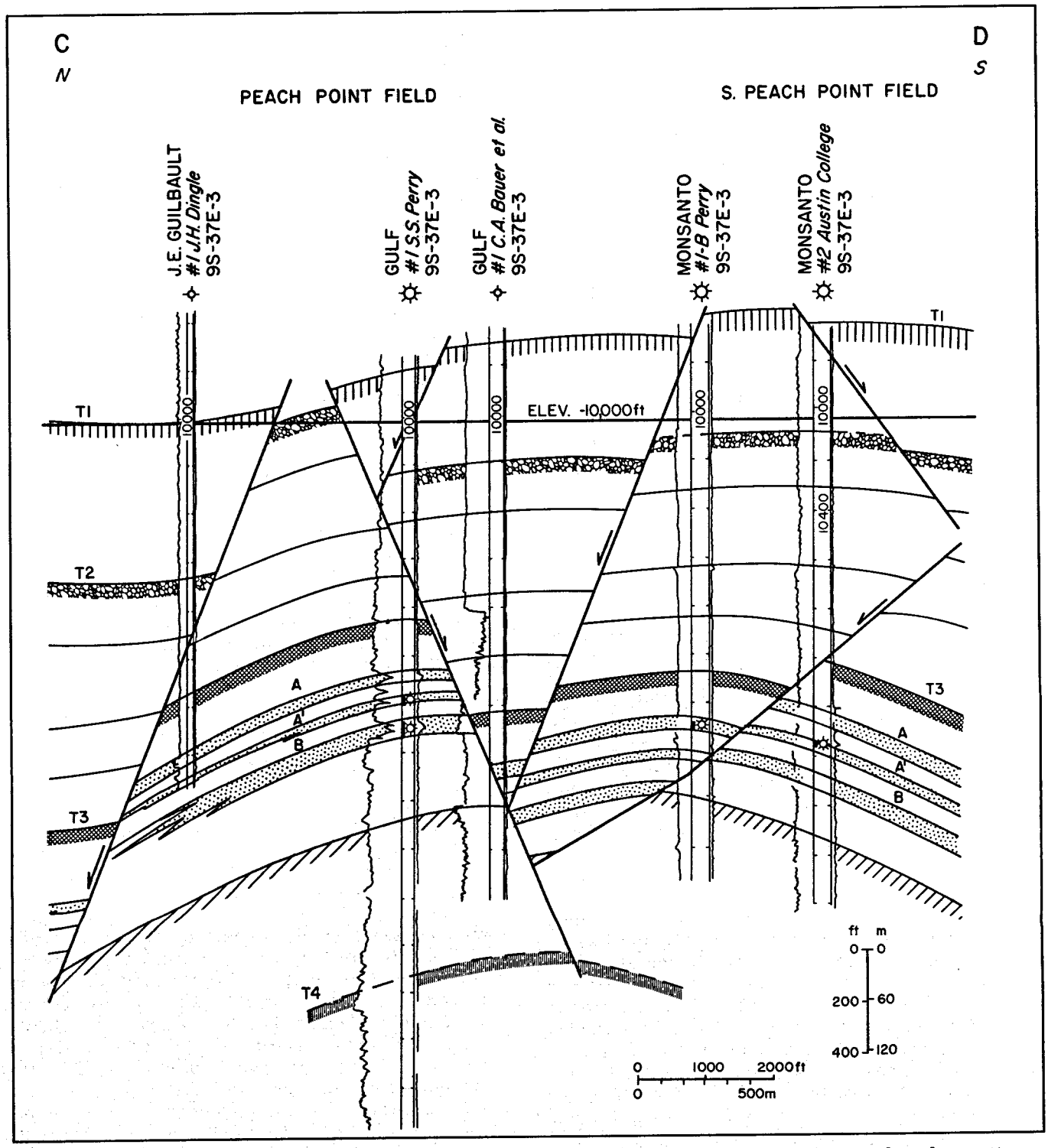


*Figure 19.* Structure section of the Peach Point area. Dot pattern indicates Frio Formation sands; other patterns emphasize stratigraphic horizons. Line of section shown in figure 17.

## Stratigraphy of the Anderson Sand

The Anderson sand is one of several lower Frio sands in the Corpus Christi area. It occurs within the *Anomalina bilateralis* zone at the CC 11 marker of Weise and others (1981), their deepest correlation marker. In the area of interest, the Anderson sand lies more than 1,000 ft below the CC 10 (Harvey sand) marker.

In the Corpus Christi fairway, the Anderson sand is recognized in a belt between two major growth faults that form the western edges of the Nueces Bay and Corpus Channel fault blocks. In this area, there are two major sand thicks. The northern one, in San Patricio County, ranges up to 100 ft thick, averaging 50 to 60 ft. The southern one is larger and ranges up to 160 ft thick; this depocenter contains the Mobil-David field and the Ross (Coastal States) No. 1 Pauline Kraft well. Net-sand isopachs outline a combination of dip and strike trends; strike trends are dominant toward the Gulf.

In the Mobil-David area, sand thickness is controlled by many small growth faults (fig. 20). Mobil-David field produces gas from a thick, blocky Anderson sand (fig. 21). The sand becomes thinner and broken by shale partings to the southwest. Northeast toward Ross No. 1 Kraft well, it becomes slightly less blocky in its SP response but thickens into a downfaulted block. North of Ross No. 1 Kraft well, the sands contain more shale and exhibit upward-coarsening sequences. Westward, thickness variations are pronounced; eastward, sand thickness and quality deteriorate toward a large growth fault.

## Structure of the Mobil-David Area

Structure of the Anderson sand (fig. 20) is complex, although little of that complexity occurs at shallower depths. In Mobil-David field, many growth faults having displacements of 100 to 200 ft divide the Anderson sand into small fault compartments, such as the L compartment described by Duggan (1972). These small faults are not clearly distinguishable on a seismic profile that crosses the field. A similar structure occurs north of Ross No. 1 Kraft well. In both of these areas, the Anderson sand lies at 11,000 to 11,500 ft.

In contrast, a block between these two fractured areas is depressed more than 1,500 ft. Five wells provide control within this downthrown block, two of them penetrating the Anderson sand. The depression is filled by a thick sequence of Anderson sand and post-Anderson shale and silt. Whereas many faults are revealed by the Mobil-David wells, few minor growth faults can be found in the interval above the Anderson sand; apparently, this downfaulted block has been spared the extreme fragmentation that occurred over the structural highs to the north and south. This dome and basin structure, reminiscent of salt-tectonic features (but here probably shale-controlled), was filled in mostly by the top of the lower Frio.

## Reservoir Volume of the Anderson Sand

The Anderson sand in the L fault compartment ranges from 80 to more than 100 ft thick. Shale breaks in the interval are minor and sand quality appears good. The fault compartment has an area of about 1.2 $mi^2$ and contains 4.25 to 4.75 Bcf of sand. Assuming a porosity of 24 percent (Duggan, 1972), the aquifer fluid volume is 180 million to 200 million bbl.

Production data on the Anderson L reservoir are given by Duggan (1972). Although a simple pressure-depletion drive was expected, the BHP/z-versus-production curve shows a negative deflection. Duggan attributed this to pressure maintenance by the dewatering of adjacent shales. The gas-in-place estimate from early data was 112 Bcf, but approximately 70 Bcf was expected from volume recalculation. More recent data (to October 1980) show cumulative production to be approaching a maximum of 55 Bcf.

Data presented by Duggan (1972) suggest that the aquifer fluid volume derived from production data ranges from 185 million to 290 million bbl, the lower figure being calculated from the revised gas-in-place estimate. These figures agree with the geologic estimate, the lower figure more closely. The actual near-ultimate gas production of 55 Bcf, then, indicates a percent interconnection of 75 to 80 percent.

The concave-down production curve for Mobil-David L field has not been noted in the other production curves used for this study. Ramagost and Farshad (1981) considered this deviation to be common in geopressured gas reservoirs and to be caused by rock and water compressibility. However, revising the production-volume calculations as they proposed will reduce the volume estimates, which in most cases would only increase the gap between production estimates and geologic estimates of aquifer fluid volume.

# *COMPARISONS AND CONCLUSIONS*

Comparisons of geologic and production estimates of aquifer fluid volumes for nine Texas Gulf Coast reservoirs (table 6 and fig. 22) show that in general, geologic estimates tend to be higher than production estimates in small pressure-depletion reservoirs (except where nonsealing faults are present). This tendency is due in part to thin (2 to 7 ft) shale breaks within the sand sequence, which seal off parts of the sand body within the small fault compartments. The larger reservoirs (aquifer fluid volume >100 million bbl) generally show a closer agreement between geologic and production estimates, although problems caused by shale breaks and nonsealing faults may still exist.

Nonsealing faults have been inferred in two or three cases. In Yorktown field, a small fault cuts a thick (300 ft) sand. The same sand is juxtaposed on both sides of the nonsealing fault. At South Peach Point field, two thin sands are juxtaposed across a small (100 ft) nonsealing fault. Christmas field may contain a nonsealing fault similar in magnitude and geometry to the one at South Peach Point field. All other faults in the fields studied are apparently sealing, including all the faults that have large displacement and those that juxtapose sand and shale.

In evaluating geopressured reservoirs, continuity of the sand should be taken into account. Given adequate

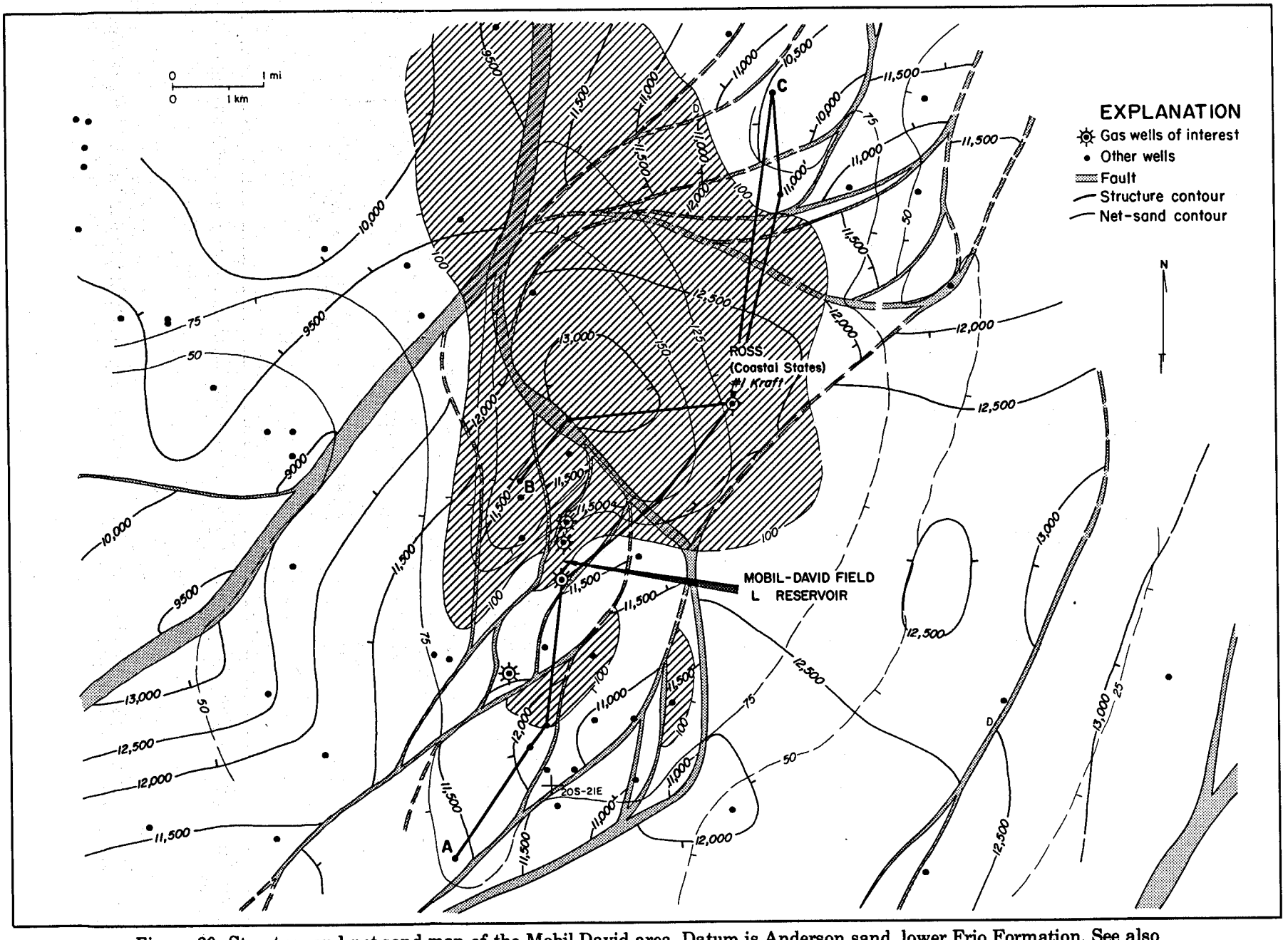


*Figure 20.* Structure and net-sand map of the Mobil-David area. Datum is Anderson sand, lower Frio Formation. See also figure 27. Diagonal-line pattern indicates sand more than 100 ft thick. Faults downthrown to the southeast unless indicated.

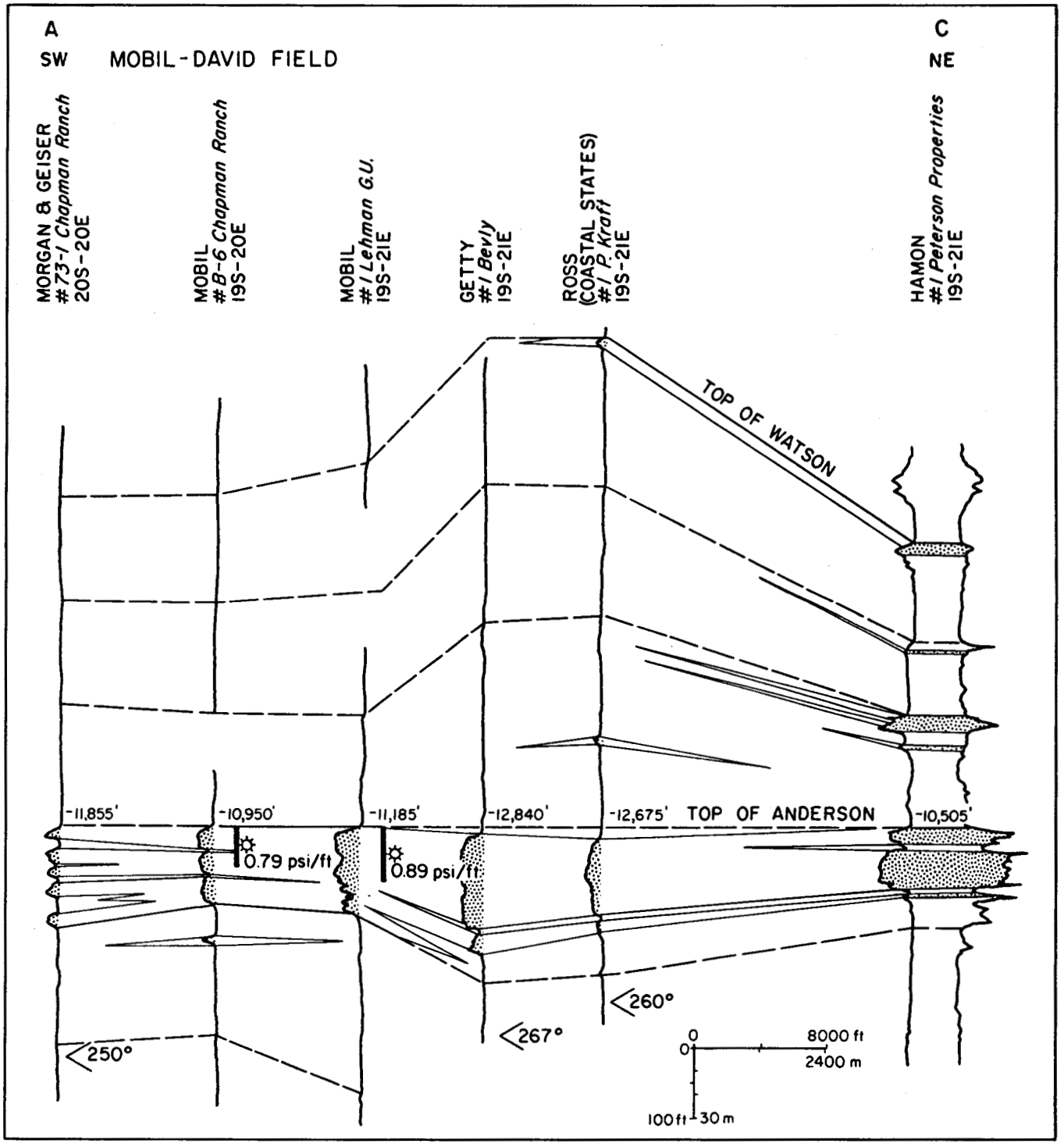


*Figure 21.* Stratigraphic section of lower Frio Formation sands, Mobil-David area. Datum is top of Anderson sand. Symbols as in figure 9; line of section shown in figure 20.

well control, it should be possible to recognize potentially nonsealing faults by their small displacement and by the juxtaposition of sands. If well control is not present, this recognition will be very difficult because these small faults will generally not show up on seismic sections. Faults having small displacement can also be sealing, as in the Mobil-David L field. Such faults could seriously impair a prospective geopressured geothermal aquifer, but this problem is partially alleviated in areas of thick and numerous sands.

Thin, continuous shale breaks can be correlated within a fault block if there is sufficient well control.

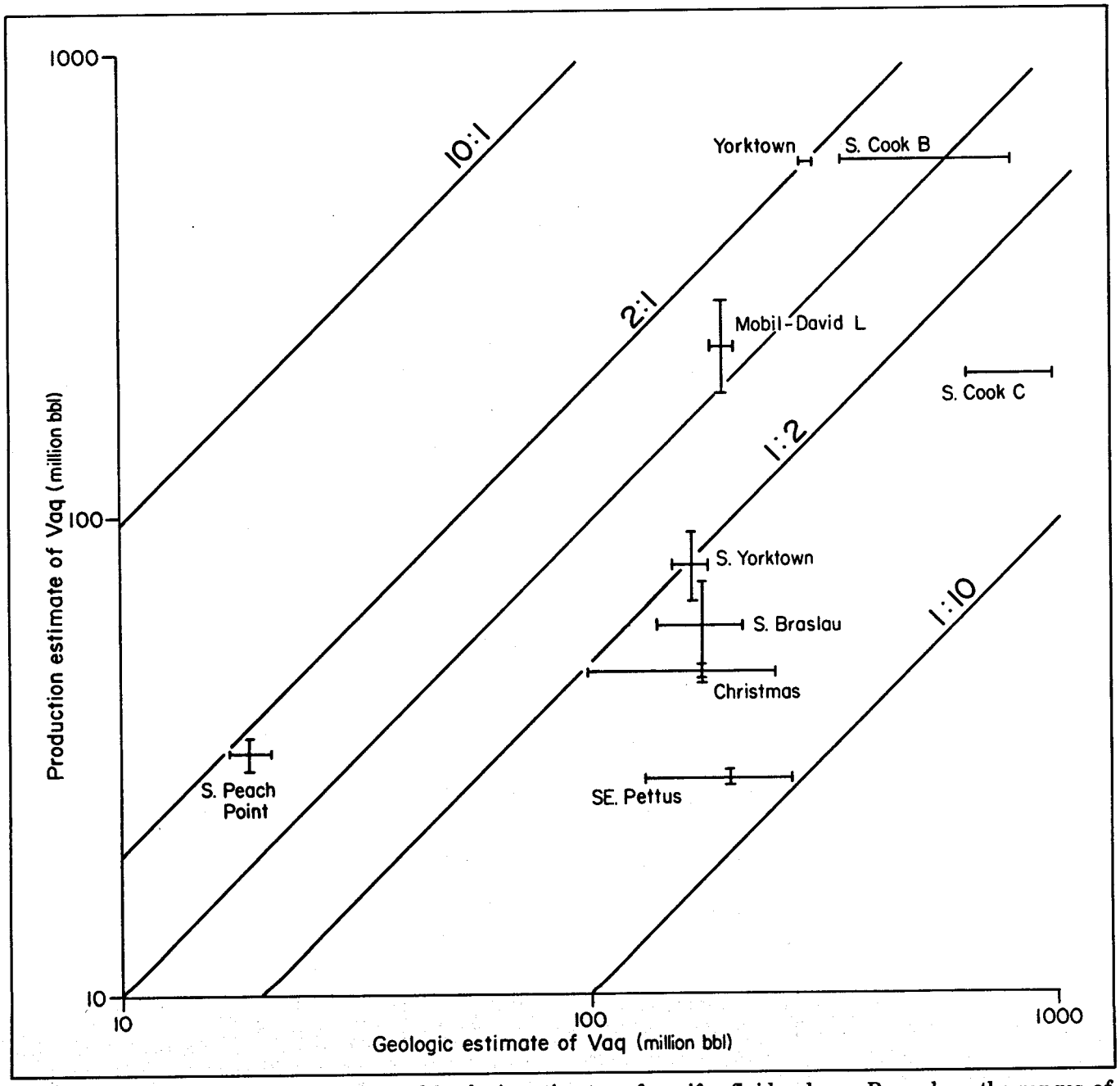


*Figure 22.* Comparison of production and geologic estimates of aquifer fluid volume. Bars show the ranges of estimated volumes.

These permeability barriers are generally subtle and are not usually considered in sand correlation, but they do affect potential production of the reservoir. Stratigraphic horizons at specific locations within the growth-fault systems may display a distinctive style of sedimentation. In particular, the Southeast Pettus and South Braslau areas, in a part of the upper Wilcox growth-fault trend that exhibits high expansion across closely spaced growth faults, show similar continuous shale breaks in different sand units. Thus, knowledge of sedimentation styles could help in evaluating reservoirs in areas of poor well control.

## GEOLOGIC SETTING AND RESERVOIR CHARACTERISTICS, WELLS OF OPPORTUNITY

Three deep wells in the Texas Gulf Coast (fig. 5, table 7) have been tested for solution gas and geothermal resources by Eaton Operating Co. under contract

*TABLE 7. Reservoir area and volume of Texas Gulf Coast wells of opportunity.*

| NAME, AREA, COUNTY, SAND, DEPTH | PRIMARY GEOLOGIC ESTIMATES AREA ($mi^2$) | $V_{res}$ (Bcf) | $V_{aq}$ (million bbl) | POROSITY (%) | DRIVE ESTIMATES | COMMENTS |
|---|---|---|---|---|---|---|
| *Riddle No. 2 Saldana,* Martinez Wilcox area, Zapata Co., First Hinnant, 9,120 ft | 3.6 | 7.0 | 200 | 16 | w(?) | compartment to N. poorly determined; possible shale breaks |
| *Ross No. 1 Kraft,* Mobil-David area, Nueces Co., Anderson, 12,675 ft | 4.77-8.34 | 17.9-28.6 | 640-1,220 | 20-24 | np | poor compartment control on N., NW. |
| *Lear No. 1 Koelemay,* Doyle area, Jefferson Co., Leger, 11,590 ft | 2.5+ | 7 | 250 | 20 | w | very poor compartment control |

$V_{res}$ - *sand volume.*
$V_{aq}$ - *aquifer fluid volume.*
w - *water.*
np - *no production.*

to the U.S. Department of Energy. To provide detailed geologic contexts for these wells of opportunity, the structure and stratigraphy of the areas adjoining them have been studied by the methods previously outlined for geologic estimation of aquifer volumes.

## *RIDDLE NO. 2 SALDANA WELL*

Riddle No. 2 Saldana well lies in Martinez field in eastern Zapata County. The test reservoir, the First Hinnant sand in the upper Wilcox Group, is also the main reservoir of Northeast Thompsonville field (Jim Hogg and Webb Counties) 10 mi to the northeast.

Martinez field is located on a high-relief domal structure cut by three southeast-down normal faults that were active during Wilcox deposition (fig. 23). First Hinnant gas production occurs from two small gas caps, one in the western fault block, the other in the eastern. Riddle No. 2 Saldana well tested the central fault block but yielded salt water and some free gas; the gas cap in that block, if any, is small. In the test well, the First Hinnant sand had a shut-in pressure of 6,627 psi (gradient of 0.68 psi/ft) and a temperature of 300° F. Reservoir properties were determined by Eaton Operating Co.: Average porosity (from the sonic log) is 16 percent, average permeability is 7 md, and measured water salinity is 13,000 ppm. Porosity is fairly uniform throughout the sand, whereas permeability shows two upward-decreasing cycles (fig. 24).

### Stratigraphy of the First Hinnant Sand

The First Hinnant sand occurs within the uppermost Wilcox Group interval, about 200 ft below the regional top of the Wilcox. In Martinez field, First Hinnant is the uppermost Wilcox sand and occurs within a dominantly shale sequence. The sand is more than 600 ft above the top of the Zapata delta complex (Edwards, 1981) and correlates stratigraphically with the Live Oak delta complex in McMullen and Live Oak Counties 75 mi to the northeast.

The productive sand in the two fields is more than 50 ft thick. Blocky SP and resistivity responses and minor shale breaks can be correlated within each field. Despite lack of well control between the two fields, the correlation is good (fig. 25). To the north and south, the sand merges into a mixed sand and shale sequence having a subdued SP response. To the south, this transition occurs over about 1.5 mi; to the north, it is much sharper (less than 4,000 ft), occurring just north of Atlantic No. 1 Bruni well (fig. 25).

The sand thins to both the east and the west (fig. 26). Within 2.5 mi to the east, it grades into silt. The sand thins markedly and migrates upsection to the northwest, where it overlies several upward-coarsening sequences that increase in sand content westward. These lower sands are interpreted as deltaic sequences having a western source.

The First Hinnant sand has been studied previously in Northeast Thompsonville field, where it was interpreted as a barrier-bar deposit by Wood (1962) and Young (1966); Berg and Tedford (1977) proposed a deep-sea fan origin. The sand exhibits a well-defined N. 30° E. trend of maximum sand thickness, having abrupt thinning to the southeast and gradual thinning to the west (fig. 23). This geometry is consistent with a barrier-bar origin for the First Hinnant sand but conflicts with the dip-oriented fan model of Berg and Tedford (1977). The upward-coarsening sequences to the west represent small late-stage deltas, which in part formed as bayhead

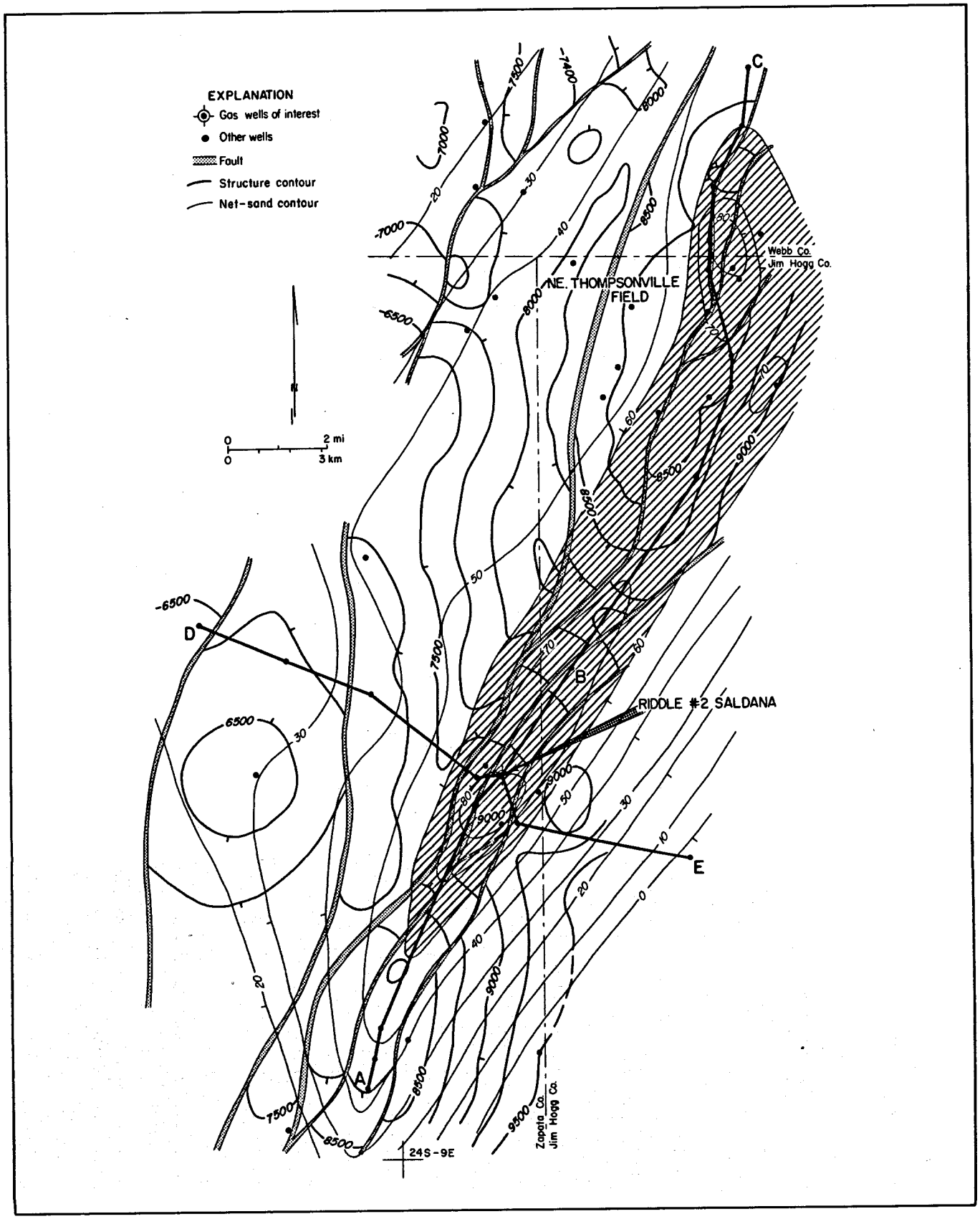


*Figure 23.* Structure and net-sand map of the Riddle No. 2 Saldana area. Datum is top of First Hinnant sand, upper Wilcox Group. Diagonal-line pattern indicates sand more than 60 ft thick. Faults downthrown to the southeast unless indicated. Faults from Geomap.

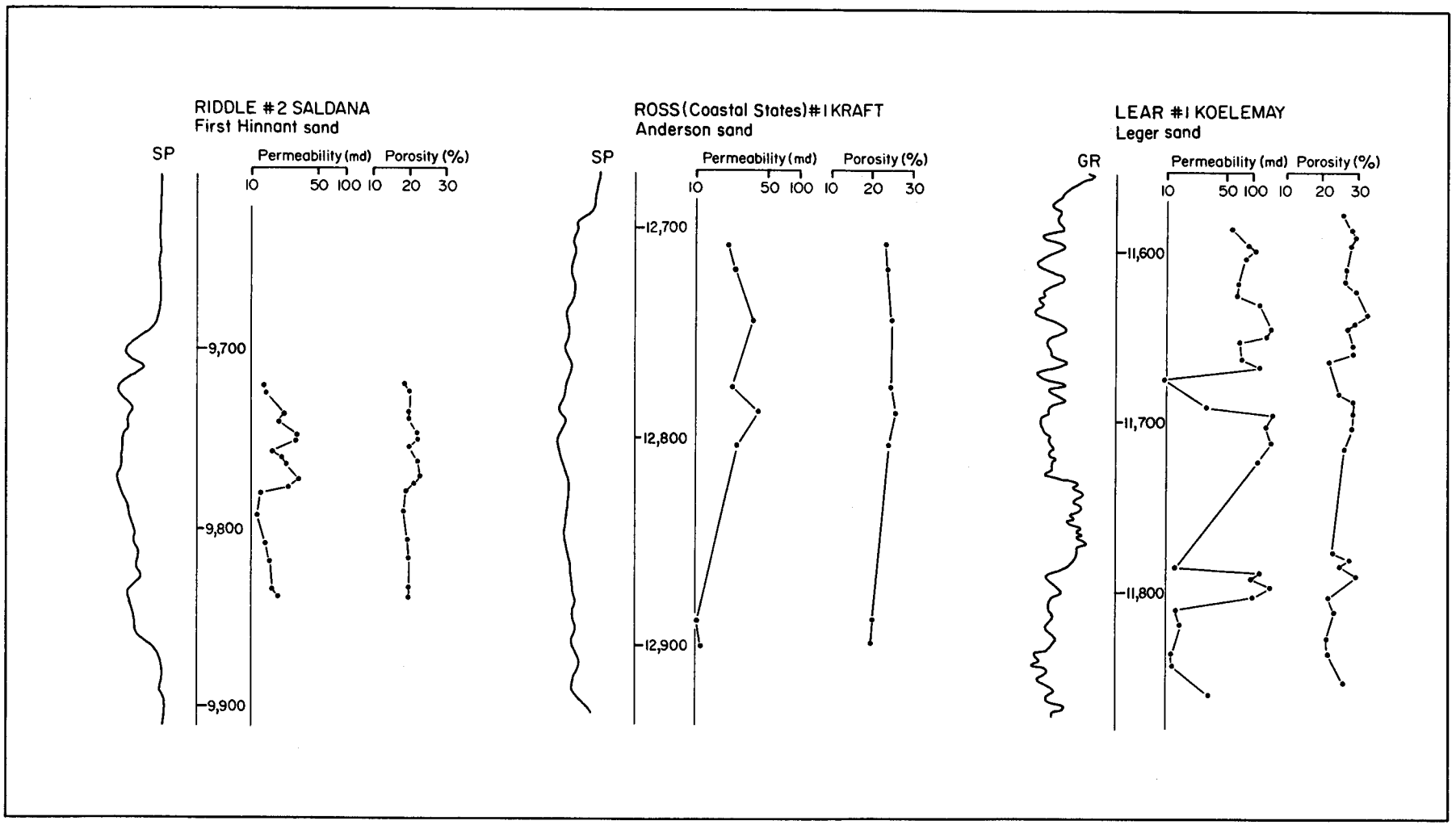


*Figure 24.* Porosity and permeability variations and spontaneous potential of three reservoirs tested by the well-of-opportunity program. See figure 5 for locations.

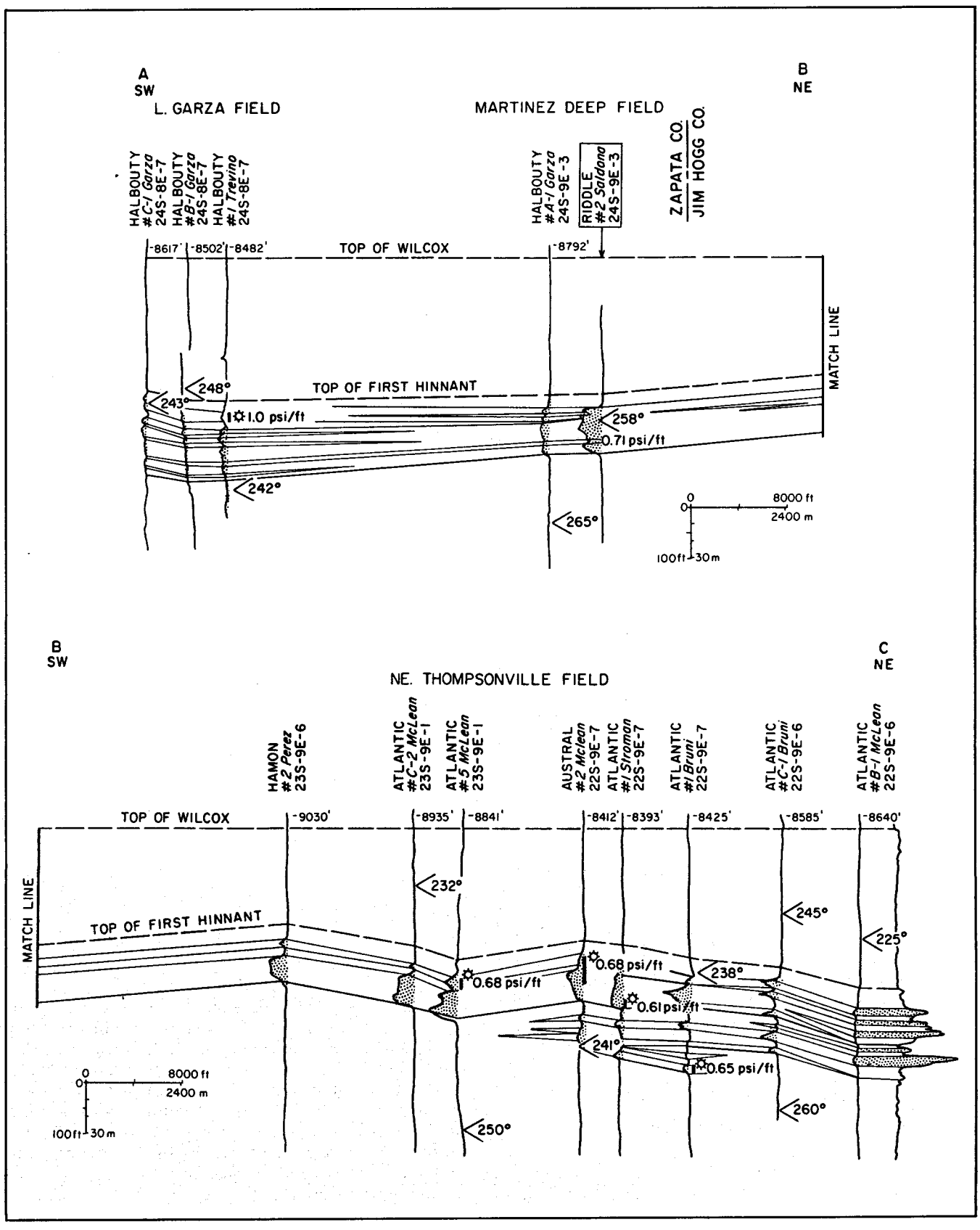


*Figure 25.* Stratigraphic section of First Hinnant sand, Riddle No. 2 Saldana and Northeast Thompsonville areas. Datum is top of Wilcox Group. Symbols as in figure 9; line of section shown in figure 23.

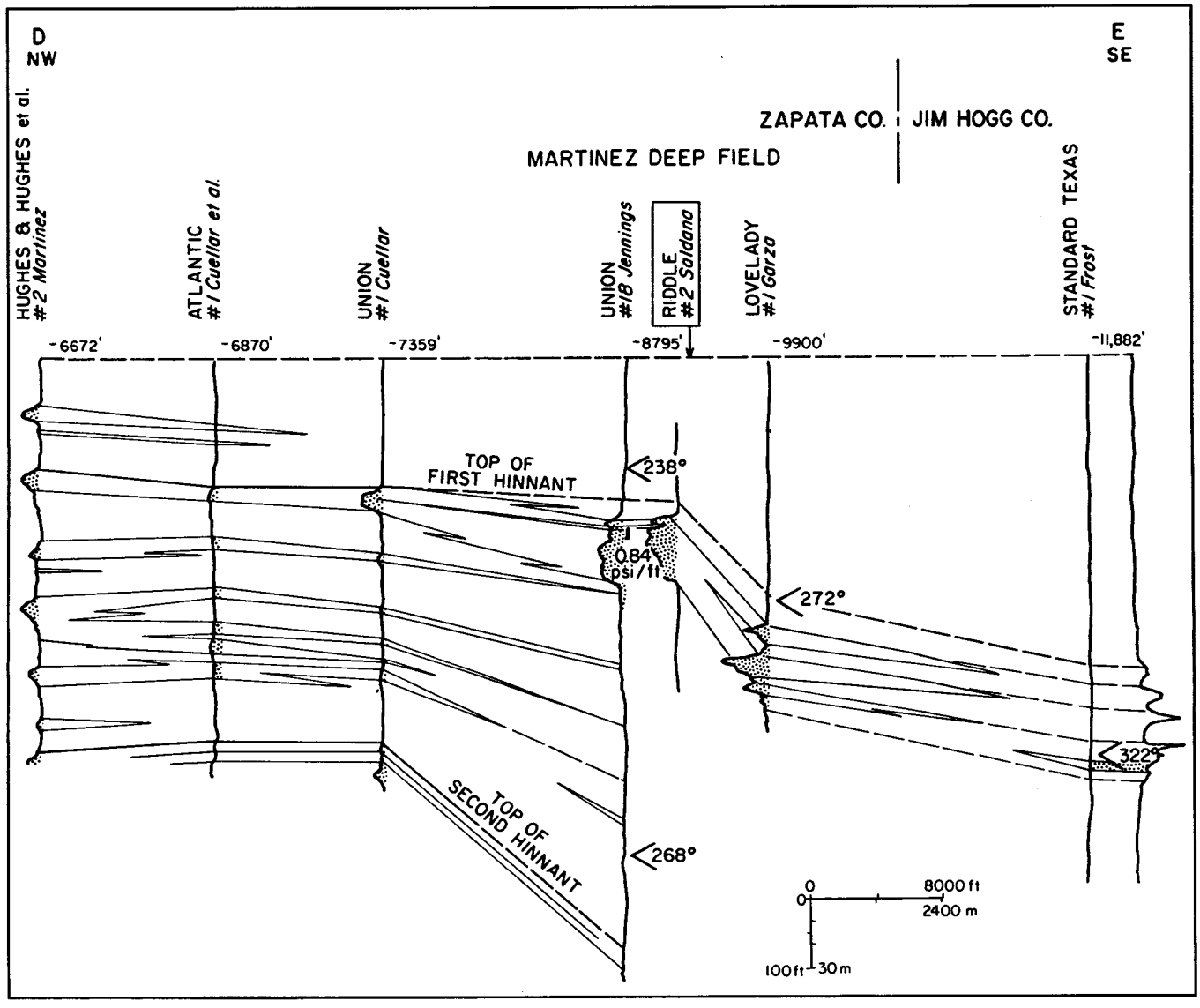


*Figure 26.* Stratigraphic section through Riddle No. 2 Saldana well of uppermost Wilcox Group sands. Datum is top of Wilcox Group. Symbols as in figure 9; line of section shown in figure 23.

deltas behind the bar. The source of bar sand is uncertain, but it may be the Live Oak delta to the northeast.

## Reservoir Volume of the First Hinnant Sand

Four continuous shale breaks may disrupt continuity within the reservoir sand in Martinez Deep field (figs. 24, 25, and 26). However, a well immediately east of the well of opportunity was originally completed in 1965 below the major shale break and had a shut-in pressure of 8,882 psi; in 1974, it was recompleted above the shale break and had a shut-in pressure of only 5,558 psi. The marked difference in pressure suggests that the two sands were connected within the small eastern block despite the large shale break (no other well produces from the compartment at this interval).

Reservoir volume is difficult to estimate because of the lack of control for 2 mi to the north and south. A conservative estimate of compartment size, with a northern boundary just east of the Jim Hogg county line and a southern boundary near Martinez field, is about 3.6 $mi^2$. Estimating an average sand thickness of 70 ft, rock volume is 7 Bcf. Measured porosity averages 16 percent, yielding a pore-water volume with an estimated range of 100 million to 800 million bbl. This volume is similar to that observed in smaller water-drive geopressured reservoirs, such as the South Cook field reservoirs.

The First Hinnant sand exhibits good reservoir continuity (especially along strike) and poor to excellent reservoir quality (parts of Northeast Thompsonville field range up to 22-percent porosity and 140-md permeability). The reservoir has a high pressure gradient (0.7 to 0.8 psi/ft) and moderate temperatures (240° to 260° F).

## *ROSS (COASTAL STATES) NO. 1 PAULINE KRAFT WELL*

Ross (Coastal States) No. 1 Pauline Kraft well lies on the northeastern fringe of Mobil-David field in Nueces County (figs. 5 and 20). The well lies within the Corpus Christi fairway of Weise and others (1981) and is immediately south of the Nueces Bay prospect. The reservoir of interest is the Anderson sand of the lower Frio (fig. 27). The Anderson sand in Ross No. 1 Kraft well has a bottom-hole pressure of 10,986 psi at 12,805 ft, yielding a pressure gradient of 0.86 psi/ft. Corrected bottom-hole temperature is estimated to be 290° F.

### Structure of the Mobil-David Area

Structure of the Mobil-David area has been previously described in relation to the Mobil-David L reservoir. Structural mapping indicates two domes, one of which localizes Mobil-David field, separated by a downdropped block. A northeast to southwest structure section (fig. 27) shows that this transverse dome-and-trough structure is largely concealed by the time of CC 9 deposition but has more than 1,500 ft of relief at the CC 11 marker (the Anderson sand).

Ross No. 1 Kraft well lies within the downdropped block (fig. 20). The southwestern-bounding fault of this block is precisely located; its northwestern boundary probably occurs near the large fault to the northwest. The northern boundary is poorly known but must lie on the southwestern flank of the dome to the north. The southeastern-bounding fault probably cuts Ross No. 1 Kraft well and also can be inferred from a minor growth fault seen in a regional seismic line and in regional study. This fault compartment is estimated to have a minimum area of 4.8 $mi^2$ and a probable maximum area of 8.4 $mi^2$.

### Reservoir Volume of the Anderson Sand

Within the fault compartment, the Anderson sand ranges from less than 10 to more than 150 ft thick (fig. 20). It is generally continuous, having only minor shale breaks (fig. 24). Planimetry of the net-sand map over the minimum and maximum fault-compartment sizes yields a sand volume of 17.9 to 28.6 Bcf. Porosity ranges from 20 to 24 percent, on the basis of sidewall cores in Ross No. 1 Kraft well and estimates given for Mobil-David field by Duggan (1972). At 20-percent porosity, the aquifer fluid volumes of the minimum and maximum cases are 640 million and 1,020 million bbl; at 24 percent, they are 700 million and 1,200 million bbl. The aquifer fluid volume is larger than those of the water-drive geopressured gas reservoirs in Texas but smaller than those of several in Louisiana calculated by Boardman (1980). If permeabilities were higher, this reservoir might support 14,000 bbl/d for 10 years at 5-percent recovery, using 20-percent porosity and the larger fault-compartment size.

The Ross No. 1 Kraft well of opportunity was completed in a thick sand in an unusually large fault compartment; however, insignificant quantities of fluids were produced during the short-term test because of very low permeabilities. Sidewall cores indicate that permeabilities are highest in the central part of the sand and lowest at the top and bottom of the sand (fig. 24). Low permeabilities that preclude large volumes of water production are common in many South Texas reservoirs (Loucks and others, 1981).

## *LEAR NO. 1 KOELEMAY WELL*

Lear No. 1 Koelemay well was drilled as a wildcat in the Doyle area of northwestern Jefferson County (fig. 5). The test reservoir is the Leger sand of the Yegua Formation at 11,590 ft below sea level (fig. 28). The sands of this area lie within a geopressure trend that has been referred to as Vicksburg (Loucks, 1979), although there are no sands in the Vicksburg interval in the immediate area. The Leger sand is geopressured in most of the area considered. In Lear No. 1 Koelemay well, bottom-hole pressure was measured as 9,441 psi at 11,669 ft, yielding a gradient of 0.81 psi/ft. Measured bottom-hole temperature is 257° F. Porosity and permeability trends within the sand are complex, but they increase irregularly upward (fig. 24).

### Stratigraphy of the Leger Sand

The Leger sand occurs about 700 ft below the top of the Yegua (Cockfield) Formation in the study area, as correlated by paleontologic information from Texaco No. 1 K. B. B. Doyle well and regional cross sections (Dodge and Posey, 1981). It is one of several lenticular, shaly sands that occur in the shale-dominated Yegua section south and east of Sour Lake (fig. 29). Correlations in this sequence are generally unreliable, but the Leger sand is fairly persistent. Electric log patterns of many of these sands suggest a deltaic origin; the sands were probably deposited as delta-front sands in a high-constructive delta.

The Leger sand shows two depocenters in the study area (fig. 28). The main depocenter of interest is south-southeast of Sour Lake Dome; in this area, the sand is more than 100 ft thick on the downthrown side of several growth faults. Immediately updip, this sand is only 15 to 40 ft thick, but it thickens northward to 80 ft. The second depocenter, west of Sour Lake, is slightly younger. Its dip-oriented sand reaches a thickness of 95 ft in

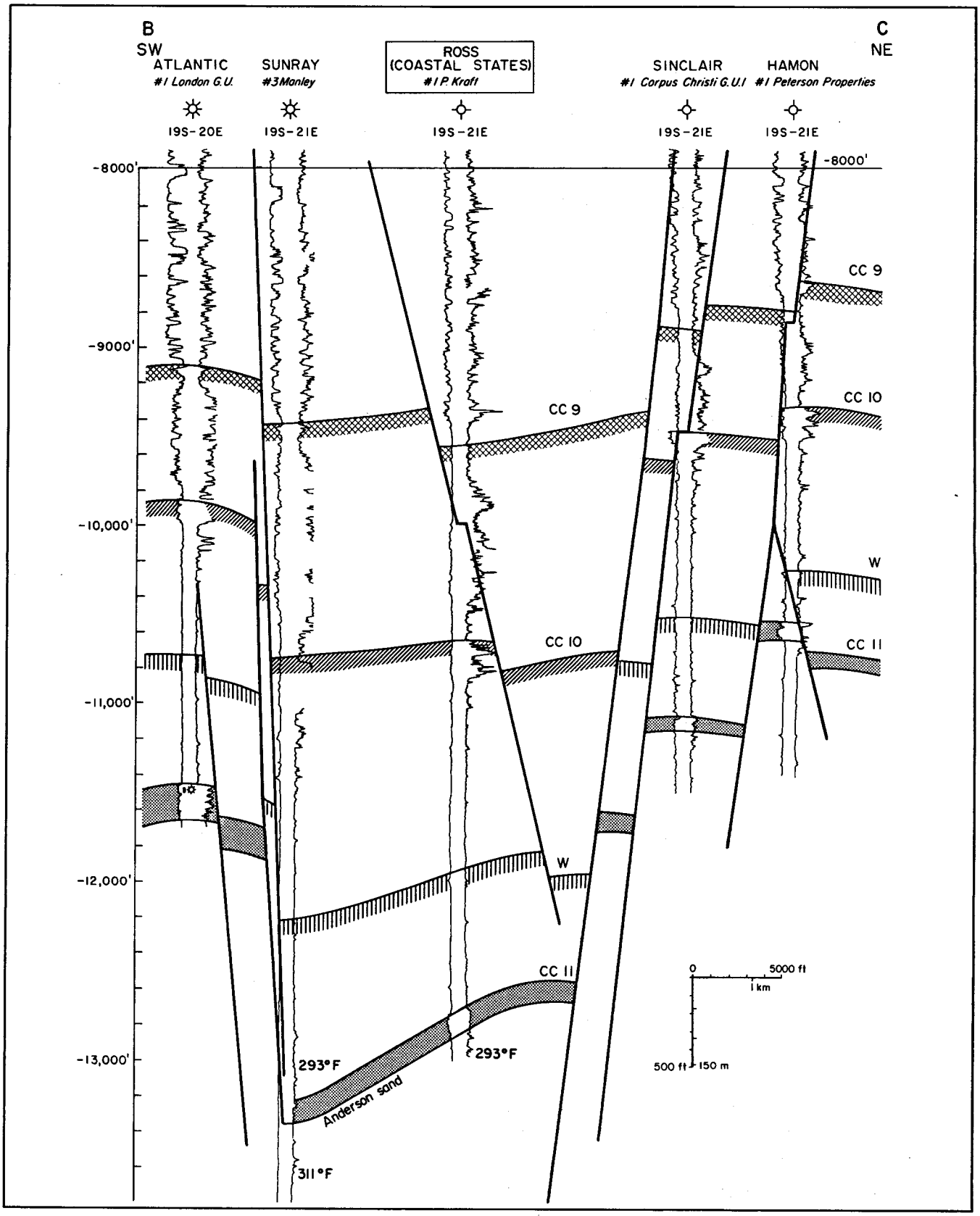


*Figure 27.* Structure section through Ross (Coastal States) No. 1 Pauline Kraft well, Mobil-David area. Anderson sand (lower Frio Formation) is at CC 11 (dot pattern); other patterns highlight stratigraphic markers. Line of section shown in figure 20.

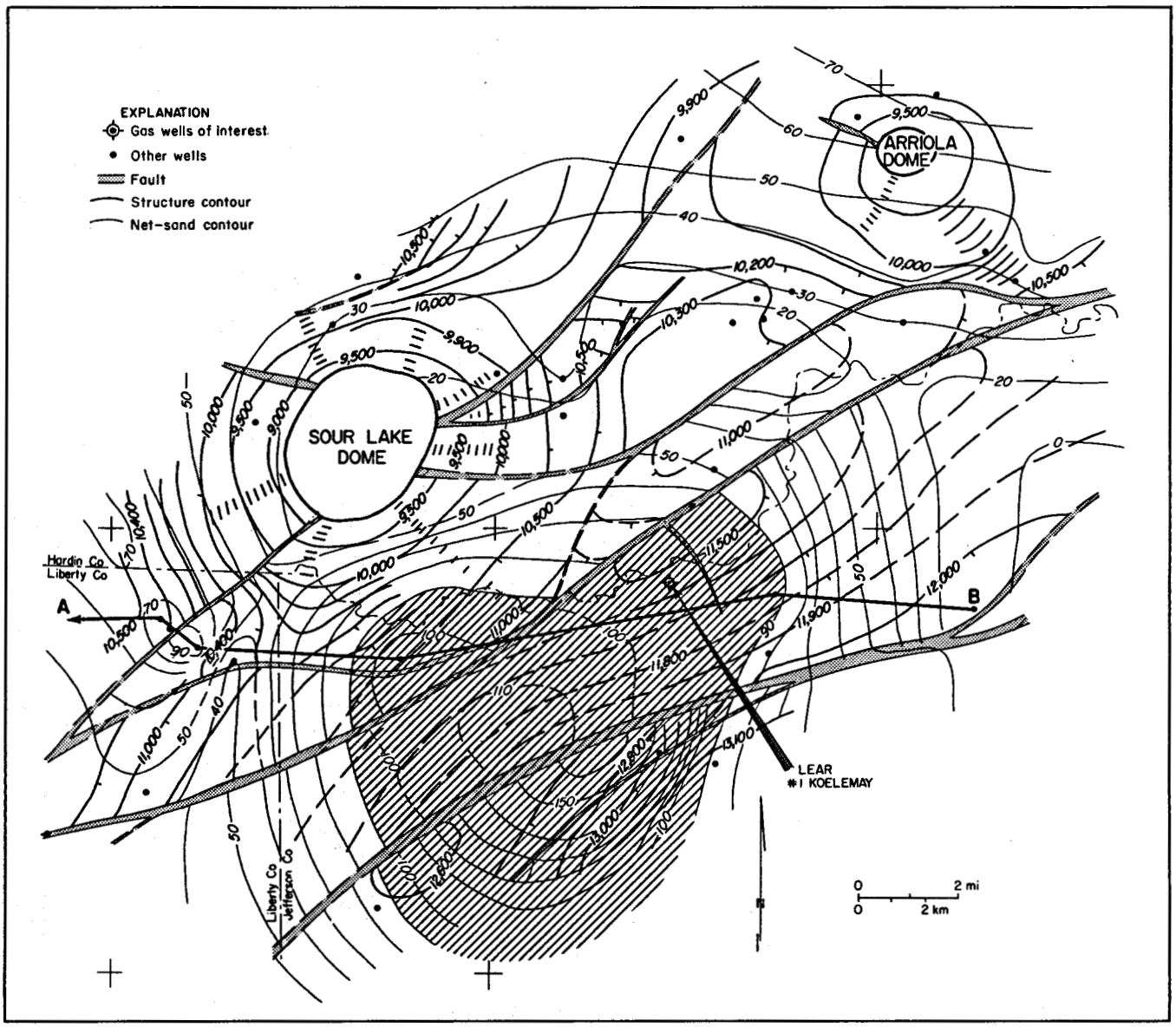


*Figure 28.* Structure and net-sand map of the Lear No. 1 Koelemay area. Datum is top of Leger sand, Yegua Formation. Diagonal-line pattern indicates sand more than 90 ft thick. Faults downthrown to the south unless indicated.

Hathaway field, Liberty County. It cannot be assumed that sands in these two depocenters are connected.

The stratigraphic section (fig. 29) suggests a recurrent pattern of sedimentation in this area. The depocenter contains an upward-coarsening sequence of shales to sands, presumably a delta-front sequence. Southwest of this depocenter are thinner, cleaner sands that have blockier SP responses. These may represent barrier or offshore-bar sands reworked along strike from the delta front by longshore currents.

## Structure of the Leger Sand

Because well control at depth is sparse in the Leger sand area, most of the major structures are not precisely located. Structure in the area consists of growth faults that separate gently gulfward-tilting fault blocks, which are locally pierced by salt domes (fig. 28). Expansion across the faults suggests Yegua and Jackson movement on all faults (with greatest Jackson expansion on the southernmost fault), Vicksburg movement on the southern faults, and slight Frio movement on the most seaward fault. The long history of growth across these faults may be related to low sedimentation rates in the shale-dominated Yegua-Jackson-Vicksburg sequence. Three salt domes occur in the area: Hull (west of area mapped on fig. 28), Sour Lake, and Arriola; the Yegua sands are uplifted to shallow depths around each salt stock. This uplifting has not relieved the geopressured condition of the Leger sand in the basin between Sour

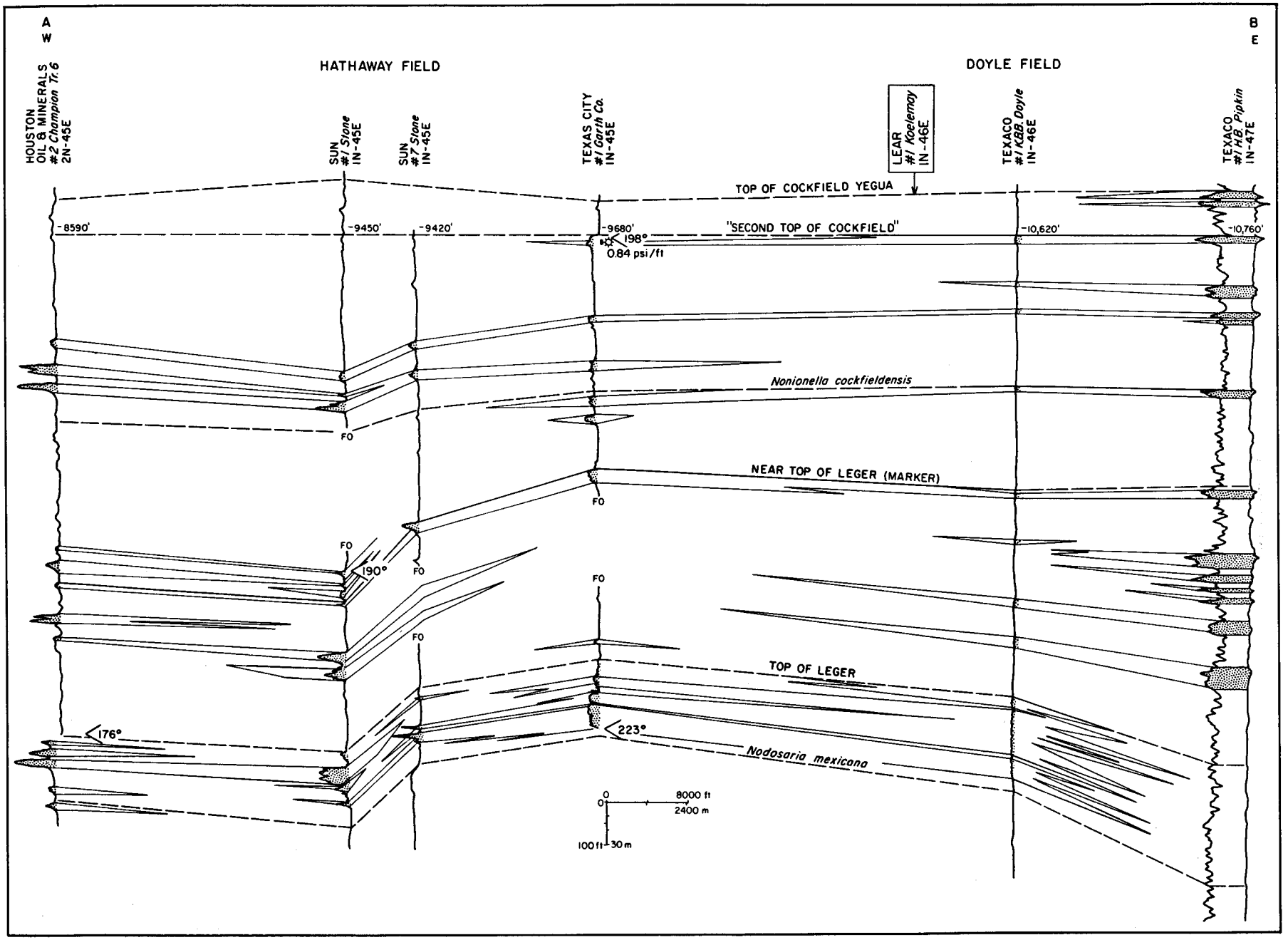


*Figure 29.* Stratigraphic section of Yegua Formation sands, Lear No. 1 Koelemay area. Datum is "Second Top of Cockfield" of industry usage. Symbols as in figure 9; line of section shown in figure 28.

Lake and Arriola Domes, where East Sour Lake field has a pressure gradient of 0.65 psi/ft.

## Reservoir Volume of the Leger Sand

The sparsity of deep well control makes it impossible to estimate a meaningful compartment area or reservoir volume of the Leger sand without seismic data. At least 2 to 3 $mi^2$ of reservoir area might be expected, having a gross sand thickness of roughly 100 ft. This would yield a sand volume of 7 Bcf and, at 20-percent porosity, a pore volume of 250 million bbl. This is, however, only an order-of-magnitude estimate.

Continuity of this reservoir is difficult to estimate. No major shale breaks appear to be continuous through the area; however, minor shaly intervals are abundant in most wells and may interfere with vertical continuity. The fault on the northern boundary of the area is marginally sealing. The Leger sand in the Doyle area shows marginal geopressure conditions in an area of poor well control. The Lear No. 1 Koelemay test does, however, appear to be typical of the Yegua geopressured reservoirs in this area.

# *CONCLUSIONS, WELL-OF-OPPORTUNITY STUDY*

Reservoir volumes were estimated for three wells of opportunity that penetrated (1) a Wilcox barrier sand, (2) a Yegua distal delta-front sand, and (3) a thick Frio delta-front or composite sand (table 7). Two wells are located in South Texas and one in southeast Texas. All of the aquifers tested are similar in volume and in the ratio of fault-block area to water-drive gas reservoirs. Two of the aquifers (at Riddle No. 2 Saldana well and Lear No. 1 Koelemay well) have fluid volumes similar to Yorktown field in De Witt County. The Frio aquifer tested in Ross No. 1 Kraft well is similar in volume to the Wilcox reservoirs of South Cook field. For comparison, sands in Blessing field of Matagorda County (Winker and others, in press) are larger, having aquifer fluid volumes of 1,700 million to 2,900 million bbl.

The greatest obstacle to determining aquifer fluid volume of the wells of opportunity is poor delineation of fault-compartment geometry. In all of these cases, seismic data are essential for correct evaluation of fault-compartment area and, therefore, reservoir volume. The uncertainty of fault-compartment geometry contrasts with the case histories for producing reservoirs, in which lack of compartment control affected only a few cases. This difference is partly inherent in the data base; the case histories are of developed fields having production histories, whereas the wells of opportunity were wildcat holes in which structure is less well determined.

# INTERNAL PROPERTIES OF SANDSTONES

Reservoirs within a fault-bounded sandstone represent the smallest subdivision discussed in this report; however, variations in rock properties within reservoirs greatly influence production behavior and recovery efficiency. These variations are macroscopic heterogeneities in the tripartite classification (megascopic, macroscopic, microscopic) of Alpay (1972).

The basic constructional elements of sand bodies (laminae, beds) can exhibit large variations in grain size over a space of inches. These textural differences may be enhanced during diagenesis and result in major reductions in transmissivity after sandstone consolidation. Chemical precipitates that coat grains and fill pores further restrict fluid flow. The small-scale inhomogeneities of reservoirs are controlled by degree of cementation, size and shape of grains (texture), sorting and packing (texture), and stratification. Predicting fluid flow through a reservoir by using sandstone facies models requires that original variations in pore properties be preserved in rocks. If vestiges of those trends are preserved, they may be important to well completion and production strategies.

# *POROSITY AND PERMEABILITY OF MODERN SANDS*

Most modern Gulf Coast sands are typically fine grained to very fine grained because of their source and multicycle origin. Such fine-grained sands generally have higher porosities but lower permeabilities than do coarse-grained sands from comparable environments. In fact, some modern point-bar and beach sands from the Gulf Coast have original permeabilities that are 5 to 10 times lower than those of equivalent sand types found elsewhere (Pryor, 1973).

Pryor (1973) studied inhomogeneities associated with grain sorting and directional properties of modern sand bodies, including several Gulf Coast beaches and a Mississippi River point-bar deposit. He found that river sands have greater permeability variations than beach sands and that both sand types have well-organized directional permeabilities. The directions of greatest permeability are parallel to the length of river bars and perpendicular to the long axis of beaches. Permeabilities of modern river and beach sands range from a few millidarcys to tens of darcys, depending on grain size and sorting. This range of more than 4 orders of magnitude decreases as the sediments compact and are buried, but ranges of 3 orders of magnitude (0.1 to 100 md) are common in consolidated sandstones, even at great depths.

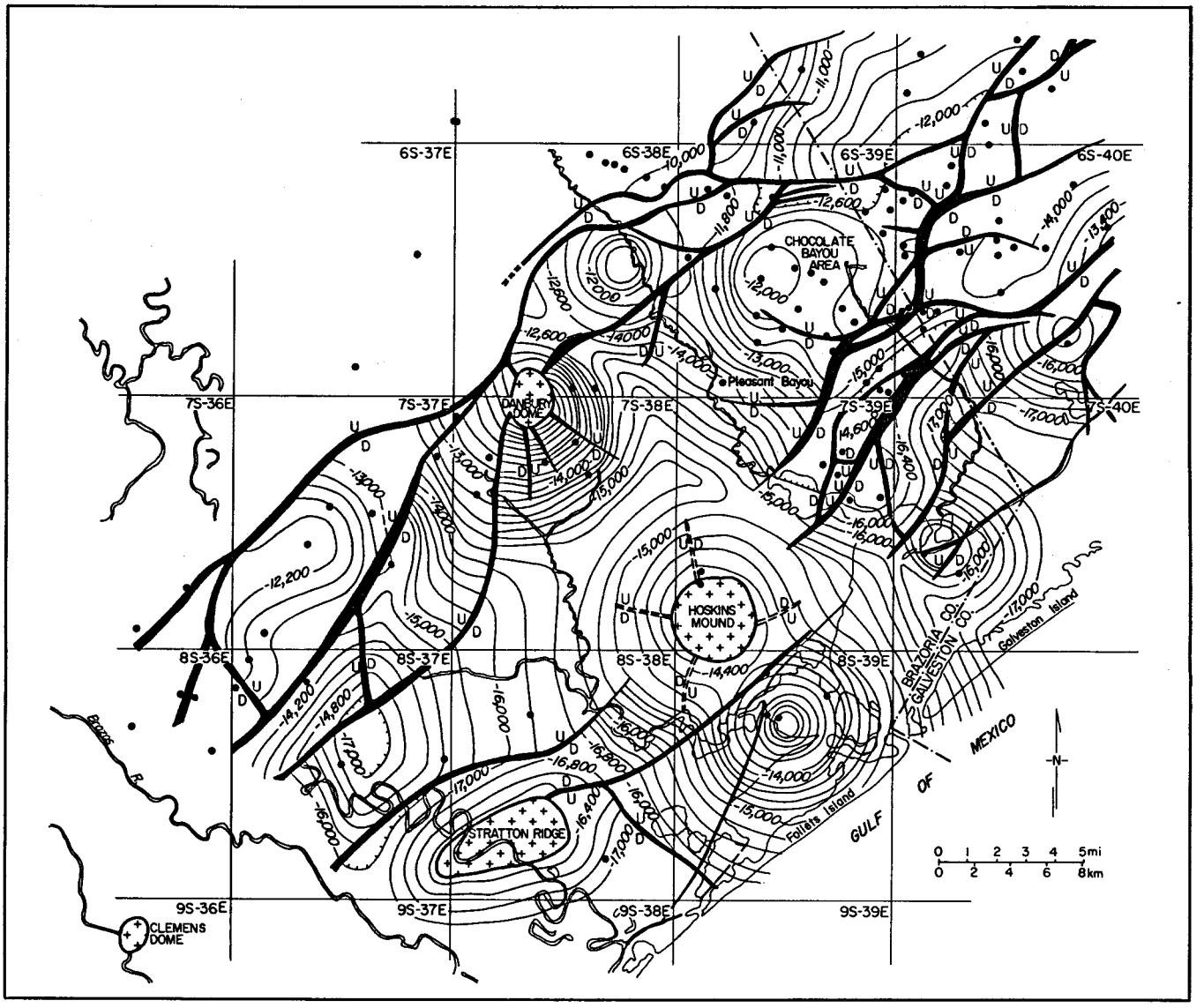


*Figure 30.* Location of the General Crude Oil-Department of Energy Pleasant Bayou Nos. 1 and 2 geopressured geothermal test wells and structure at the T5 marker (*Anomalina bilateralis*). The wells, which were drilled 500 ft apart, are on the flanks of the Chocolate Bayou domal structure in a salt-withdrawal basin associated with Danbury Dome. Northeast-trending growth faults are of Frio age. Modified from Bebout and others (1980).

## *DETAILED INVESTIGATION OF VERTICAL CHANGES IN POROSITY AND PERMEABILITY*

Cored intervals from the GCO-DOE (General Crude Oil-Department of Energy) Pleasant Bayou Nos. 1 and 2 wells were selected for detailed analysis of vertical variation in porosity and permeability because of the excellent condition of the core and because the geology of the area (fig. 30) is well documented (Bebout and others, 1978, 1980; Winker and others, in press). All of the cored intervals examined occur between the T2 and T6 correlation units (*Cibicides hazzardi* through *Anomalina bilateralis* zones) of the Oligocene Frio Formation. A variety of depositional environments, ranging from distributary-channel and associated subaerial levees to shallow marine storm-related deposits on the shoreface toe, are represented. More than 300 ft of core was examined and described. Selected intervals of the core are presented in figures 32 through 35; symbols used in these figures are explained in figure 31.

Diagenesis is an important modifier of initial porosities and permeabilities in ancient sandstones. The diagenetic history of the Frio Formation in the Chocolate Bayou/Danbury Dome area has been described in detail (Bebout and others, 1978; Loucks and others, 1981; Milliken and others, 1981). Lithic arkoses

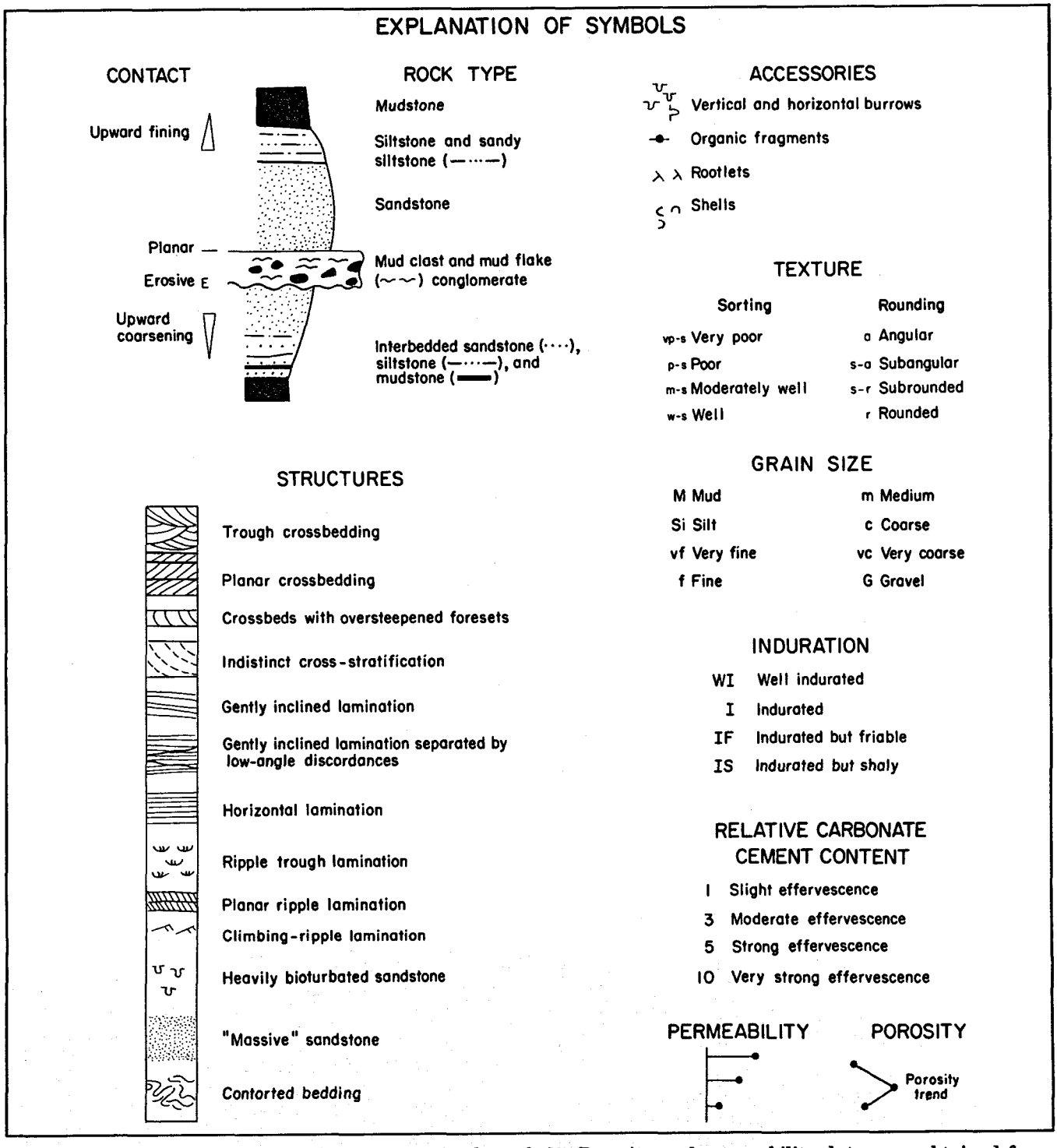


*Figure 31.* Explanation of symbols in figures 32 through 35. Porosity and permeability data were obtained from laboratory whole-core analyses.

and feldspathic volcanic arenites of the Frio Formation underwent early near-surface leaching of feldspars, accompanied by replacement and cementation by calcite. Compaction of the sediments and subsequent generation of clay coats and feldspar overgrowths were followed by precipitation of varying quantities of quartz overgrowths and minor sparry calcite. This early phase of passive diagenesis took place to a depth of approximately 8,500 ft (Milliken and others, 1981) and reduced porosity to less than 15 percent (Bebout and others, 1978). Below 8,500 ft in the geopressured zone, leaching of feldspars, volcanic rock fragments, and

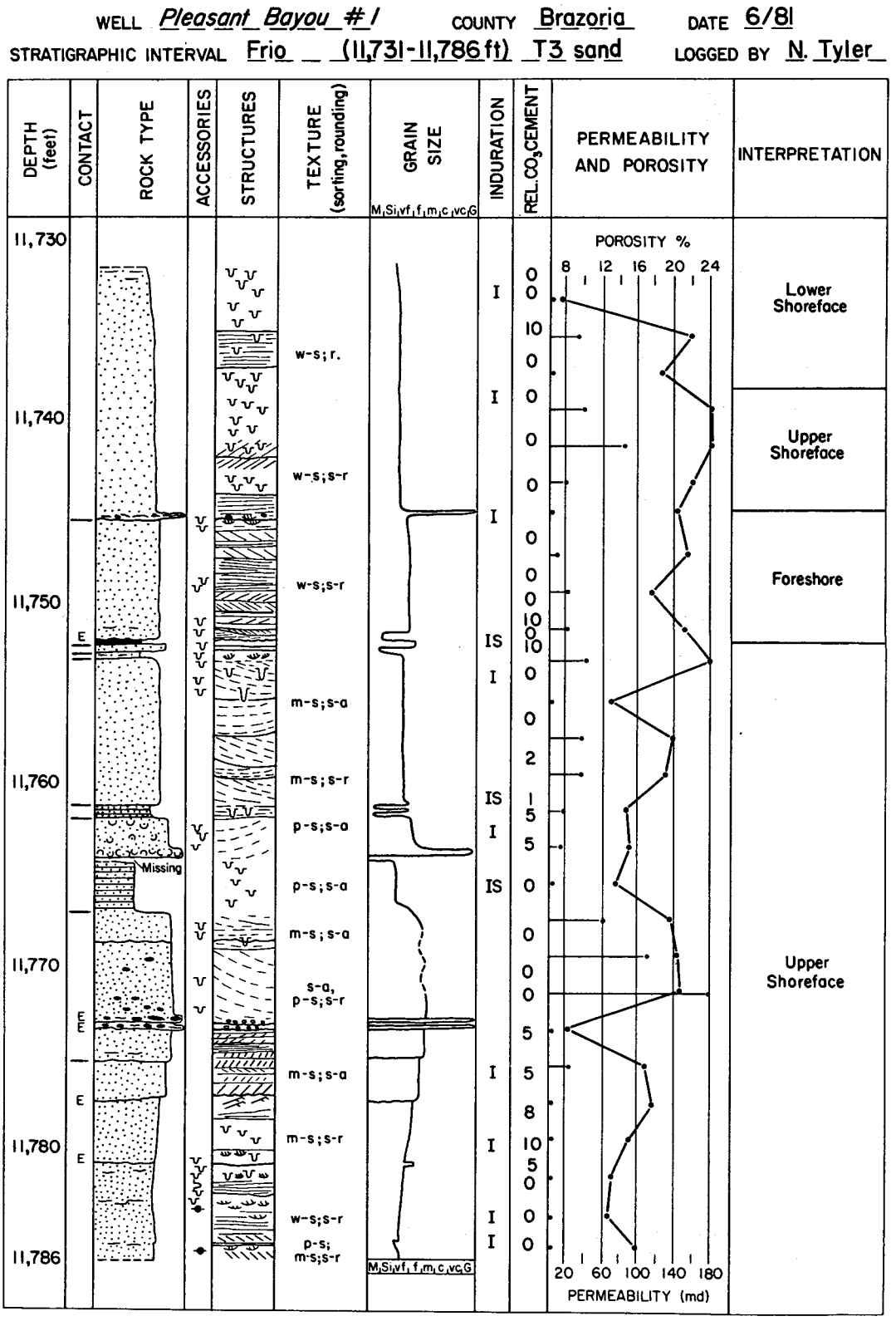


*Figure 32.* Detailed core description, pore properties, and interpretation of the upper part of the Frio T3 correlation unit. Vertical changes represent a composite of several trends, the highest porosities and permeabilities being associated with large-scale crossbedding and the coarsest grain size present. Vertical porosity trends and permeability data (indicated by horizontal bars) were obtained from laboratory whole-core analyses. See figure 31 for explanation of symbols.

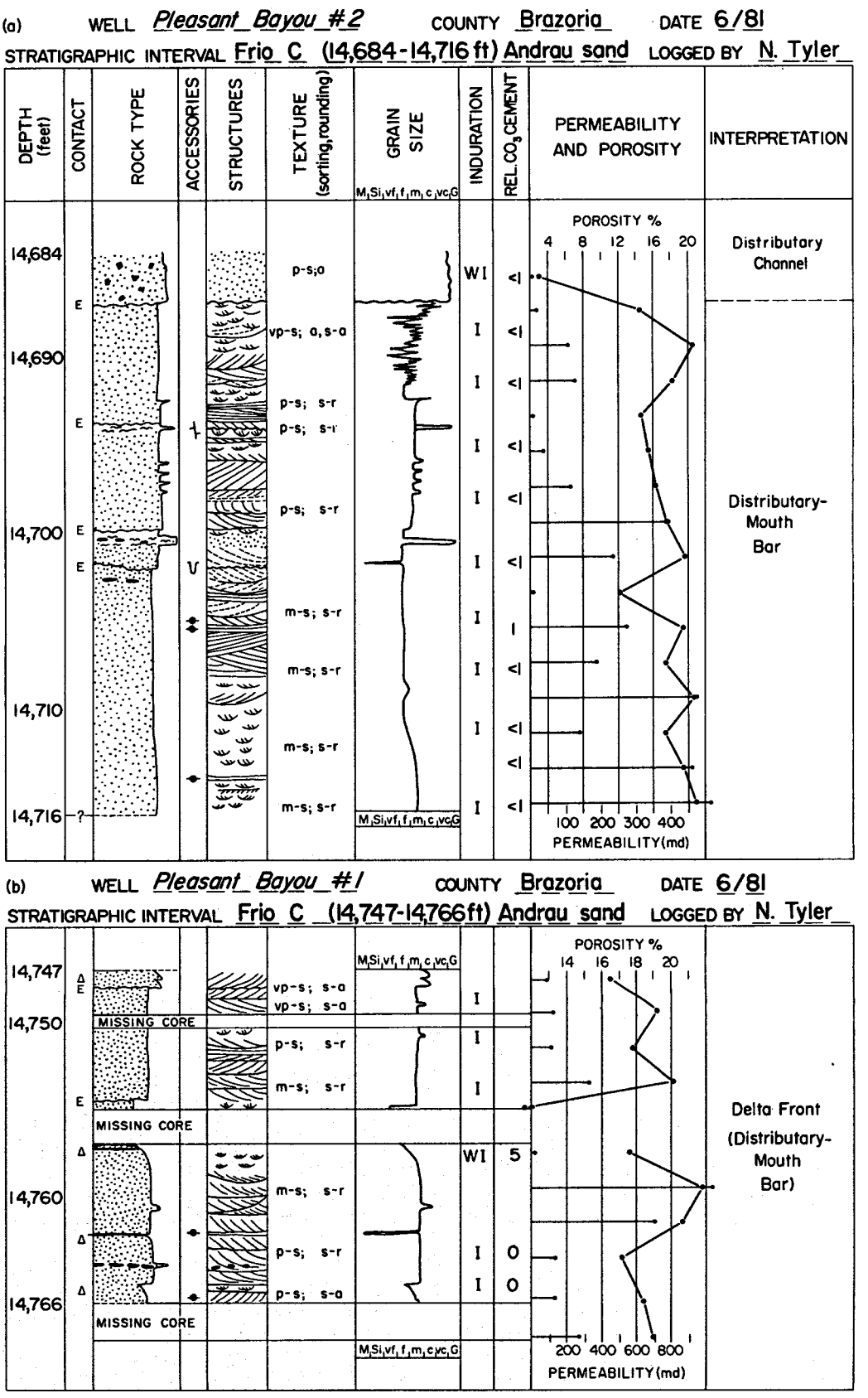


*Figure 33.* Detailed core description, pore properties, and interpretation of the geopressured geothermal production interval (Andrau, or C, sand). Vertical changes generally show an upward decrease in porosity and permeability for both sections. See figure 31 for explanation of symbols.

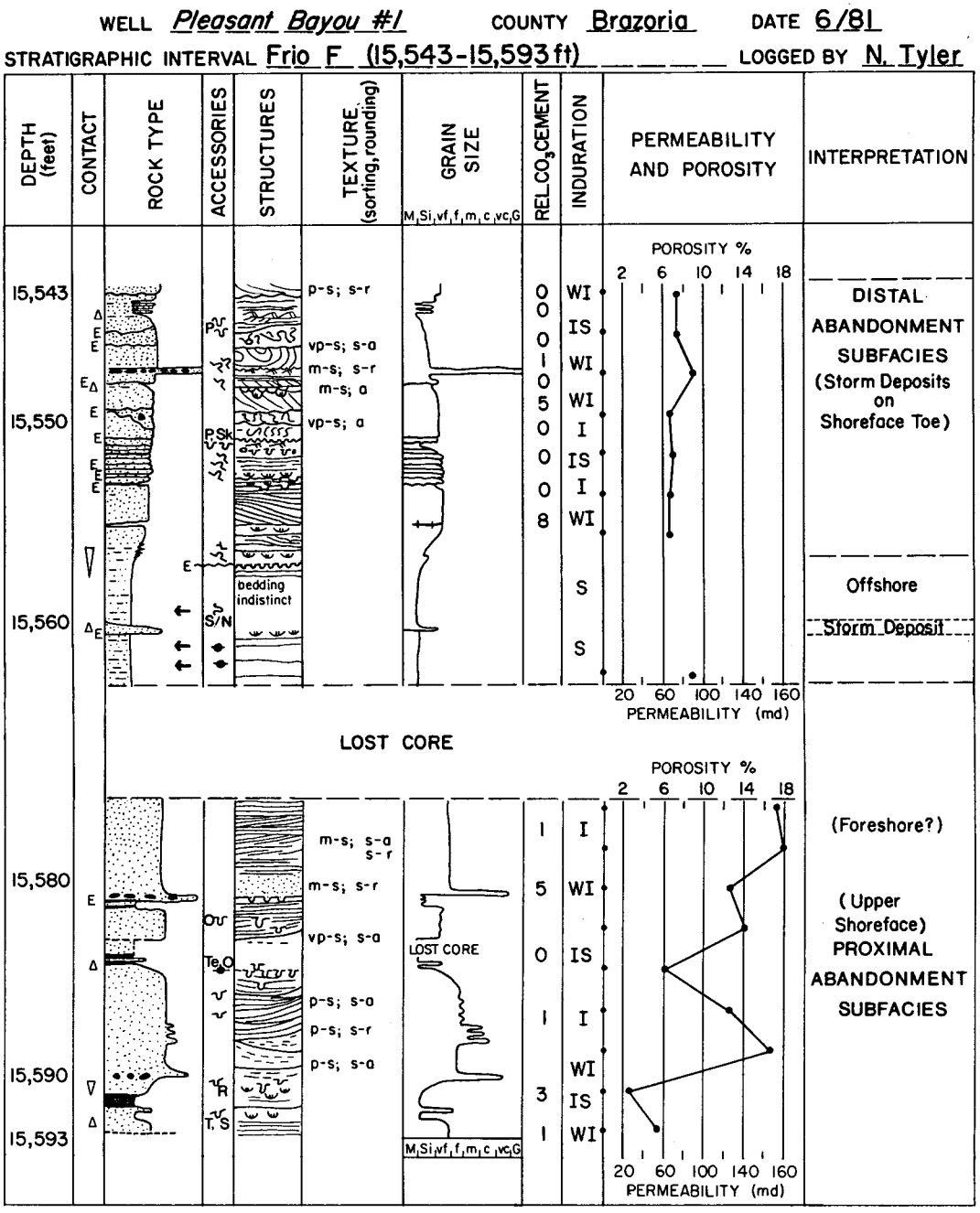


*Figure 34.* Detailed core description, pore properties, and interpretation of the upper part of the Frio F correlation interval (T5 unit). The sand exhibits uniformly low porosity and permeability. Contorted beds in this sand have lower porosities than the interbedded undeformed beds (15,543 to 15,556 ft). Trace fossils recognized: O - *Ophiomorpha,* P - *Planolites,* Sk - *Skolithos,* S/N - *Scalarituba/Nereites,* Te - *Teichichnus,* R - *Rhizocorallium,* S - *Scoyenia,* and T - *Thalassinoides.* Arrows indicate positions of micropaleontological samples. See figure 31 for explanation of symbols.

early calcite cement created secondary porosity, but this was somewhat reduced in the deep subsurface by precipitation of kaolinite and iron-rich calcite cement.

The primary objective of this analysis is to "look through" the diagenetic overprint to examine the influence of variations in grain size, primary sedimentary structures, bioturbation, and texture (rounding and sorting of grains) on porosity and permeability trends in the geopressured Frio Formation. In the GCO-DOE Pleasant Bayou cores, porosity and horizontal permeability vary in direct relation to changes in these parameters. Usually, change in one parameter is accompanied by change in one or more of the remaining variables. For example, a decrease in grain size is accompanied by an increase in bioturbation (fig. 32, 11,732 to 11,740 ft); consequently, considering

WELL *Pleasant Bayou #2* COUNTY Brazoria DATE 6/81

STRATIGRAPHIC INTERVAL Frio (15,615-15,674 ft) LOGGED BY N. Tyler

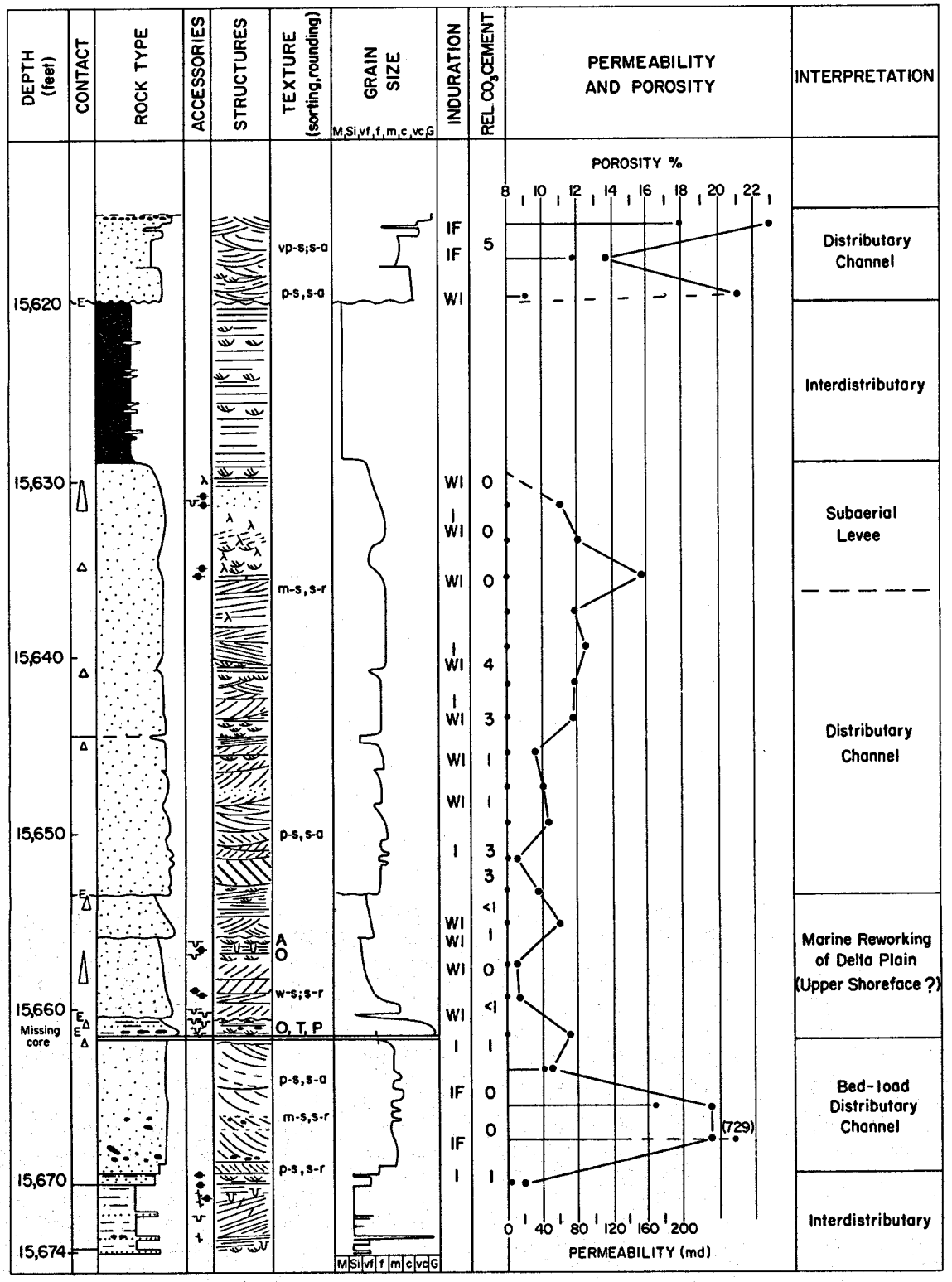


*Figure 35.* Detailed core description, pore properties, and interpretation of the lower part of the Frio F correlation interval (T5 unit). This composite sandstone shows a central decrease in porosity. Large-scale crossbeds (15,670 to 15,661 ft and 15,620 to 15,616 ft) have higher porosities and permeabilities than do small-scale crossbeds (15,653 to 15,640 ft). Trace fossils in the marine-reworked interval: A - *Arenicolites,* O - *Ophiomorpha,* T - *Thalassinoides,* and P - *Planolites.* See figure 31 for explanation of symbols.

each of these parameters separately would place artificial constraints on the analysis. Likewise, grain size and sedimentary structures should be discussed jointly because changes in one are commonly accompanied by changes in the other and because these two parameters exert the most influence on porosity and permeability.

## Variations in Grain Size and Primary Sedimentary Structures

In the GCO-DOE Pleasant Bayou cores, a decrease in grain size is accompanied by a decrease in porosity and permeability (fig. 32, 11,732 to 11,741 ft; fig. 33b, 14,757.5 to 14,759 ft; fig. 35, 15,629 to 15,632 ft). This decrease is most marked where a decrease in grain size involves a change in lithology from sandstone to siltstone or mudstone (fig. 32, 11,765 to 11,772 ft); permeability decreases from an average of 100 to less than 1 md and porosity from 20 to 13.5 percent. However, even very subtle changes in grain size, unassociated with changes in sedimentary structures, result in dramatic changes in permeability. For example, in an interval of ripple cross-laminations (fig. 33a, 14,713 to 14,716 ft), a gradual decrease in grain size from medium-grained to fine-grained sand is accompanied by a threefold decrease in permeability from 475 to 140 md. The coincident decrease in porosity is less dramatic, from 20 to 17.5 percent. The reverse also holds true; an increase in grain size (fig. 32, 11,775 to 11,785 ft) results in a porosity increase from 13 to 17 percent.

Changes in grain size are generally accompanied by changes in primary sedimentary structures. A progressive increase in grain size from the base of the T3 cored interval (fig. 32) corresponds to a vertical gradation in the scale of structures from horizontal laminations and scattered rippled zones, through climbing ripples, to small-scale planar crossbeds, and finally to a large-scale trough crossbed in the coarsest grain size present (11,771 to 11,785 ft). The highest permeabilities encountered in this interval occur in the medium-grained sandstone of the large-scale trough crossbed (fig. 32, average 118 md at 11,772 ft).

Some of the sandstone intervals described do not exhibit a change in grain size but are characterized by variations in the scale and types of the primary sedimentary structures. These variations in bed thickness and configuration at constant grain size result from changes in either water depth or current velocity, or both (Simons and others, 1965; Southard, 1971). Porosity and permeability appear to be influenced by the scale and type of sedimentary structures. Generally, the larger the scale of the sedimentary structure, the higher the relative porosity and permeability, all else being equal. Large-scale crossbedded sandstones (fig. 36a, right core slab) have higher porosity and permeability values than do small-scale crossbedded sandstones (fig. 36a, left core slab; fig. 36b), which in turn have higher values than do rippled sandstones (fig. 36c). Horizontal (fig. 36c) and gently inclined laminated sandstones have variable permeabilities, which probably result from fluids moving along bedding planes rather than between the sand grains (interstratal versus intrastratal flow). Nonbiogenic structures also affect porosities and permeabilities. In an interval consisting of interbedded undeformed and contorted upward-fining cycles, the undeformed beds have porosities significantly higher (2 to 3 percent) than those of the adjacent contorted beds (figs. 34 and 37a), which are similar in grain size.

## Bioturbation and Texture

The effects of bioturbation on permeability and, to a lesser extent, on porosity in the GCO-DOE Pleasant Bayou cores are well defined. Permeabilities in intensely bioturbated zones are reduced markedly more than those in adjacent slightly bioturbated horizons. This is partly because burrowing and feeding trails of trace fossils disrupt and destroy bedding, thereby inhibiting fluid movement along bedding planes. Porosity and permeability reductions also are caused by the mixing of finer grained detritus into the sand by the organisms. An example of the effects of bioturbation on reservoir quality is illustrated in figure 32 (11,732 to 11,743 ft). Three zones of intensely bioturbated, very fine grained sand are interbedded with weakly to moderately bioturbated sands in which sedimentary structures are still recognizable. In the bioturbated zones, primary sedimentary structures are obliterated by burrowing of organisms, their activities now recorded by the trace fossil *Ophiomorpha* (fig. 37b). Permeability in the weakly bioturbated zones (11,735 to 11,741 ft) is significantly higher than in the adjacent intensely bioturbated sands. Permeabilities decrease from an average of 50 to less than 30 md, and two of the zones have permeabilities of less than 1 md.

The response of porosity to bioturbation is varied. Porosity of one sample in the bioturbated interval of 11,737 to 11,741 ft (fig. 32) was similar to that in adjacent weakly bioturbated sandstones, whereas the other sample had a porosity that is 5 percent lower. Where bioturbation is accompanied by a decrease in grain size, porosities decrease markedly (from 23 to 7.5 percent; 11,735 to 11,732 ft). The probable cause of this decrease is introduction by the organisms of finer grained, muddy detritus from the overlying deposits into the sandstones.

The influence of textural variations on porosity and permeability in the GCO-DOE Pleasant Bayou cores is largely masked by the overriding effects of diagenesis. However, the importance of textural controls on reservoir quality is indicated in the core described in figure 33b (14,760 to 14,766 ft). Here, changes in sorting from poor to moderate and in grain shape from subangular to subrounded are accompanied by an increase in permeability (from 125 to an average of 850 md) within sandstones of constant grain size and a similar scale of sedimentary structures. Likewise, a decrease in sorting and rounding results in a decrease in permeability and porosity (fig. 33b, 14,750 to 14,754 ft).

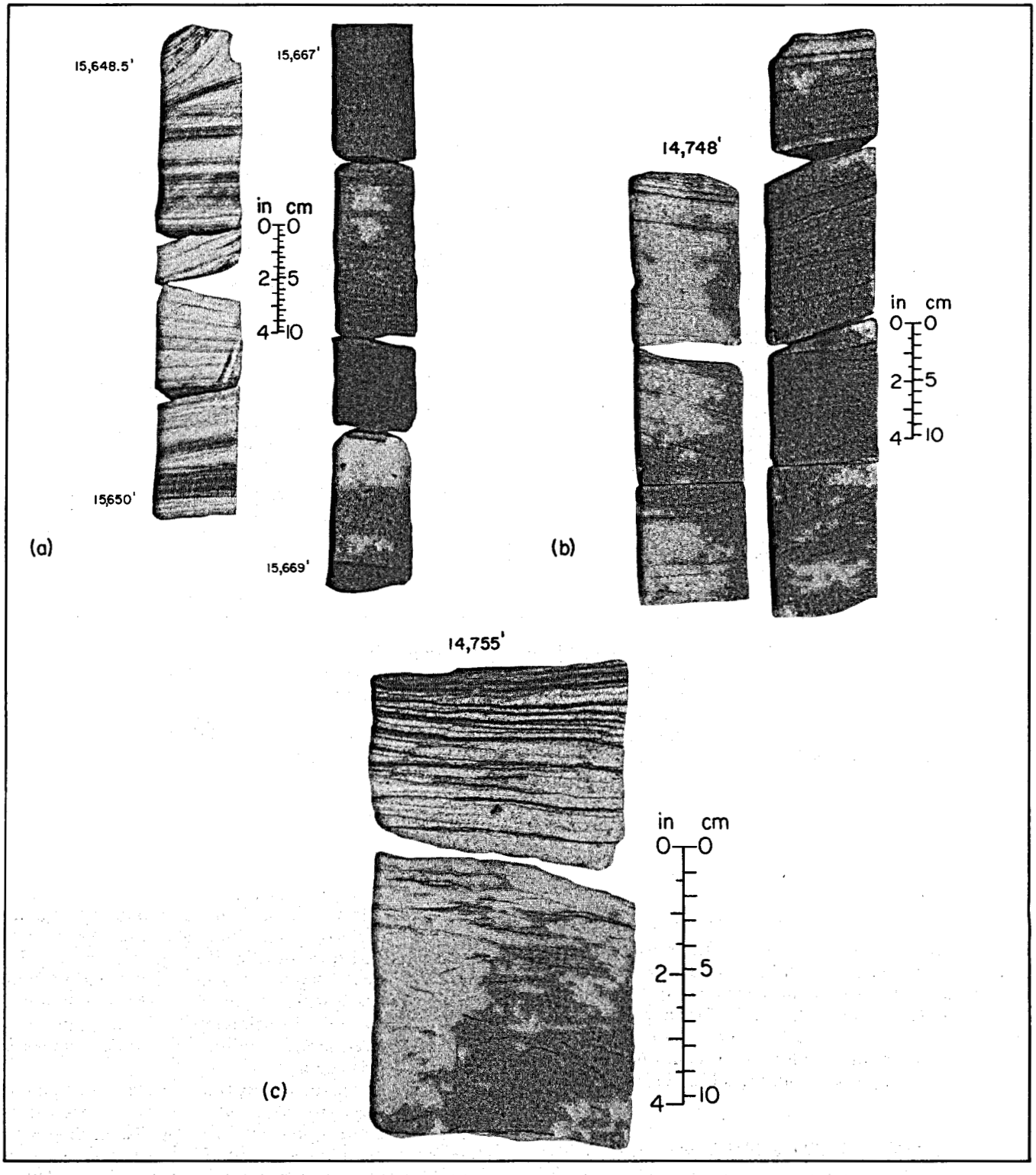


*Figure 36.* (a) Large-scale cross-stratification in permeable (729 md), porous (19 percent) sandstone (right slab) interpreted as a bed-load distributary-channel deposit (Frio F correlation interval, fig. 35). Intermediate- to small-scale crossbeds (left slab), which were also deposited within bed-load channels in this interval, have negligible permeabilities (<1 md) and significantly lower porosities (10 to 12 percent) than do sandstones having large-scale cross-stratification. (b) Intermediate- to small-scale crossbedded sandstone of the geopressured geothermal production interval (fig. 33b). Porosity (16.5 percent) and permeability (100 md) are less than those of large-scale crossbedded sandstone. (c) Ripple-laminated sandstone overlain by horizontally bedded sandstone with thin mud drapes. Ripple-laminated sandstone has the lowest permeability in the production interval and relatively low porosity (fig. 33b).

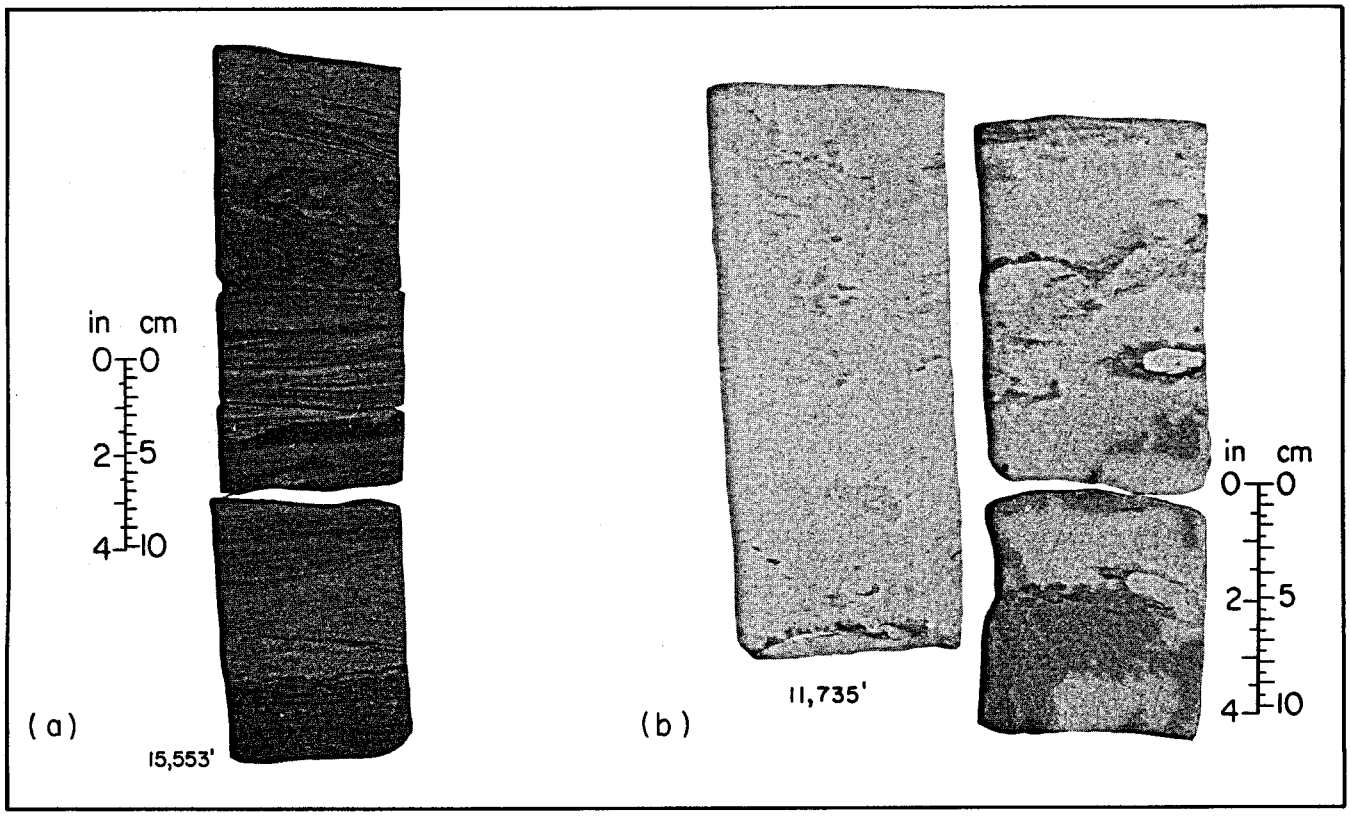


*Figure 37.* (a) Interlaminated very fine grained sandstone and siltstone interpreted as shallow marine storm-related sequences. Undeformed units have higher porosities (2 to 3 percent) than do adjacent contorted deposits (fig. 34). (b) Highly bioturbated sandstone (trace fossil *Ophiomorpha*) in which porosities and permeabilities have been substantially reduced by destruction of primary sedimentary structures and introduction of fine-grained detritus. In these lower shoreface deposits, porosities in unbioturbated sandstones were reduced from 23 to 7.5 percent, and permeability was reduced from 60 to 1 md (fig. 32) by the burrowing of marine organisms.

## Induration

Induration, which refers to the hardness and cohesion of sandstones, can be an indicator of porosity and permeability. Well-indurated sandstones in the Frio Formation (figs. 33a, 33b, and 35) have negligible permeabilities. On the other end of the spectrum, indurated but friable sandstones are characterized by comparatively high permeabilities (fig. 35).

# *POROSITY AND PERMEABILITY AS A FUNCTION OF DEPOSITIONAL ENVIRONMENT*

Interpretations of the depositional environments of the sandstones intersected by the GCO-DOE Pleasant Bayou cores were based on sandstone geometries (Bebout and others, 1978, 1980) and on the vertical arrangement of grain size and primary sedimentary structures. Bioturbation and micropaleontological evidence were also taken into account. The overall depositional setting of the Frio Formation in the Chocolate Bayou/Danbury Dome area is thought to be a high-constructive deltaic system in which individual depositional sequences exhibit lobate net-sand patterns. Various subenvironments within this deltaic system are indicated in the cores.

Porosity and permeability trends within these subenvironments are directly related to grain size, sedimentary structures, and bioturbation. Thus, the lower shoreface, which is composed of bioturbated, very fine grained, horizontally laminated sandstone, has lower porosities and permeabilities than do the sparsely bioturbated, crossbedded, very fine grained to fine-grained sandstones of the upper shoreface (figs. 32 and 34). Similarly, the medium-grained, crossbedded sandstones of distributary-mouth bars (figs. 33a and 33b) and sand-filled distributary channels have higher porosities and permeabilities than do associated subenvironments (fig. 35).

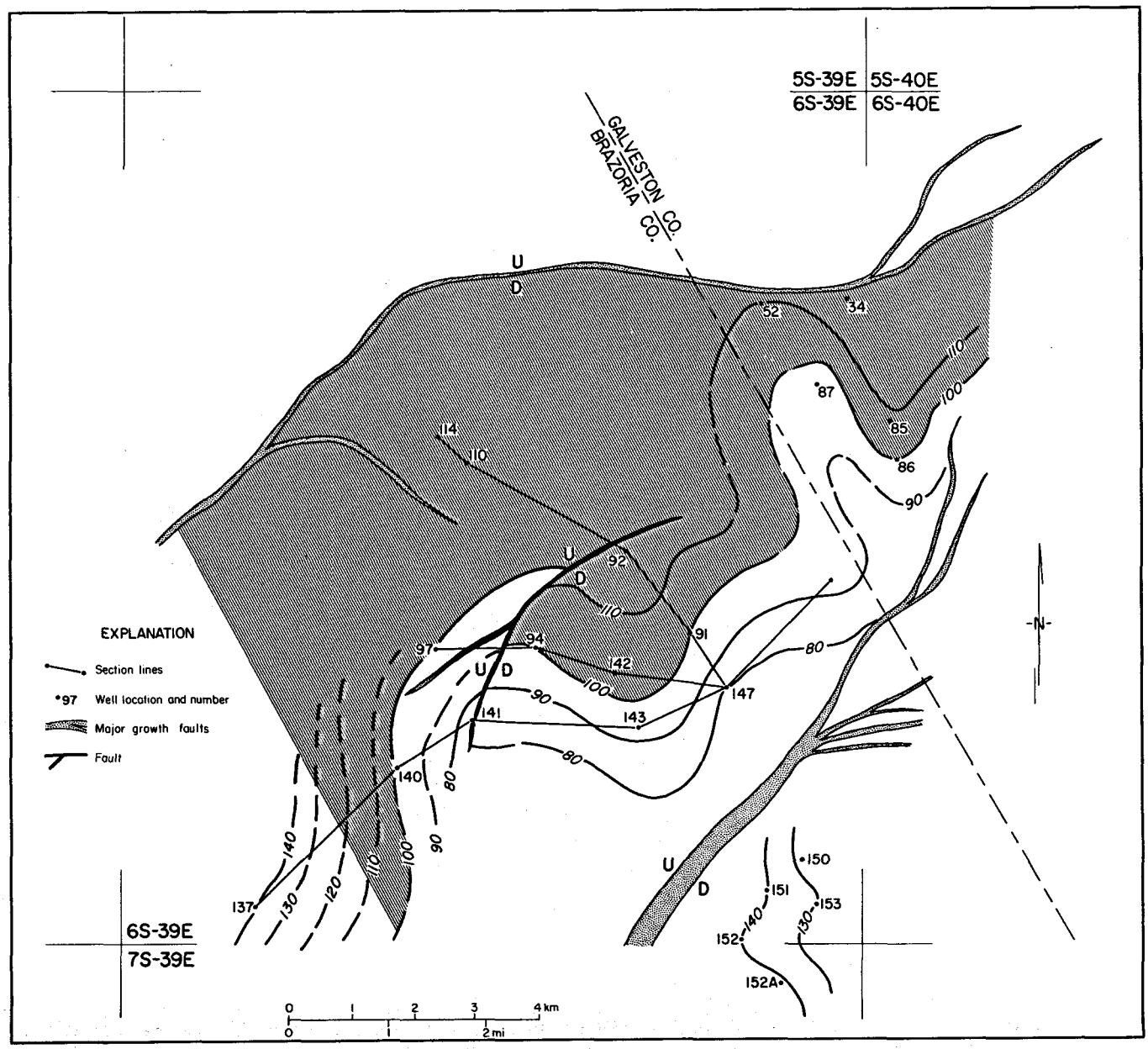


*Figure 38.* Net-sand map of the sub-T5 Andrau sand (the geopressured geothermal production interval) and location of wells in figure 39 (fence diagram). Sandstone patterns suggest a high-constructive, lobate deltaic origin of the Andrau sand.

Because of the dynamic nature of the deltaic-marine interface, there often is a rapid alternation of subenvironments within the deltaic-shallow marine system. For example, marine reworking of delta-plain sediments following lobe abandonment by switching of fluvial activity elsewhere on the delta plain results in nearshore marine deposits of varying thickness interbedded within a predominantly subaerial sequence (fig. 35, 15,660 ft). This vertical alternation of subenvironments can substantially influence reservoir behavior. Hartman and Paynter (1979) illustrated the separation of hydrocarbon reservoirs by superposition of various deltaic sandstone facies.

## *FACIES CONTROL ON RESERVOIR CONTINUITY*

Sandstone reservoirs are rarely the uniform, laterally persistent sheet sands that they are often thought to be. Sandstone geometries differ markedly as a result of deposition under widely divergent conditions; for example, thick, laterally persistent sheet sands deposited as distributary-mouth bars in the delta-front setting of a constructive lobate delta, such as the Andrau (C) sand (figs. 38 and 39), constitute more attractive targets for exploration than do the thin,

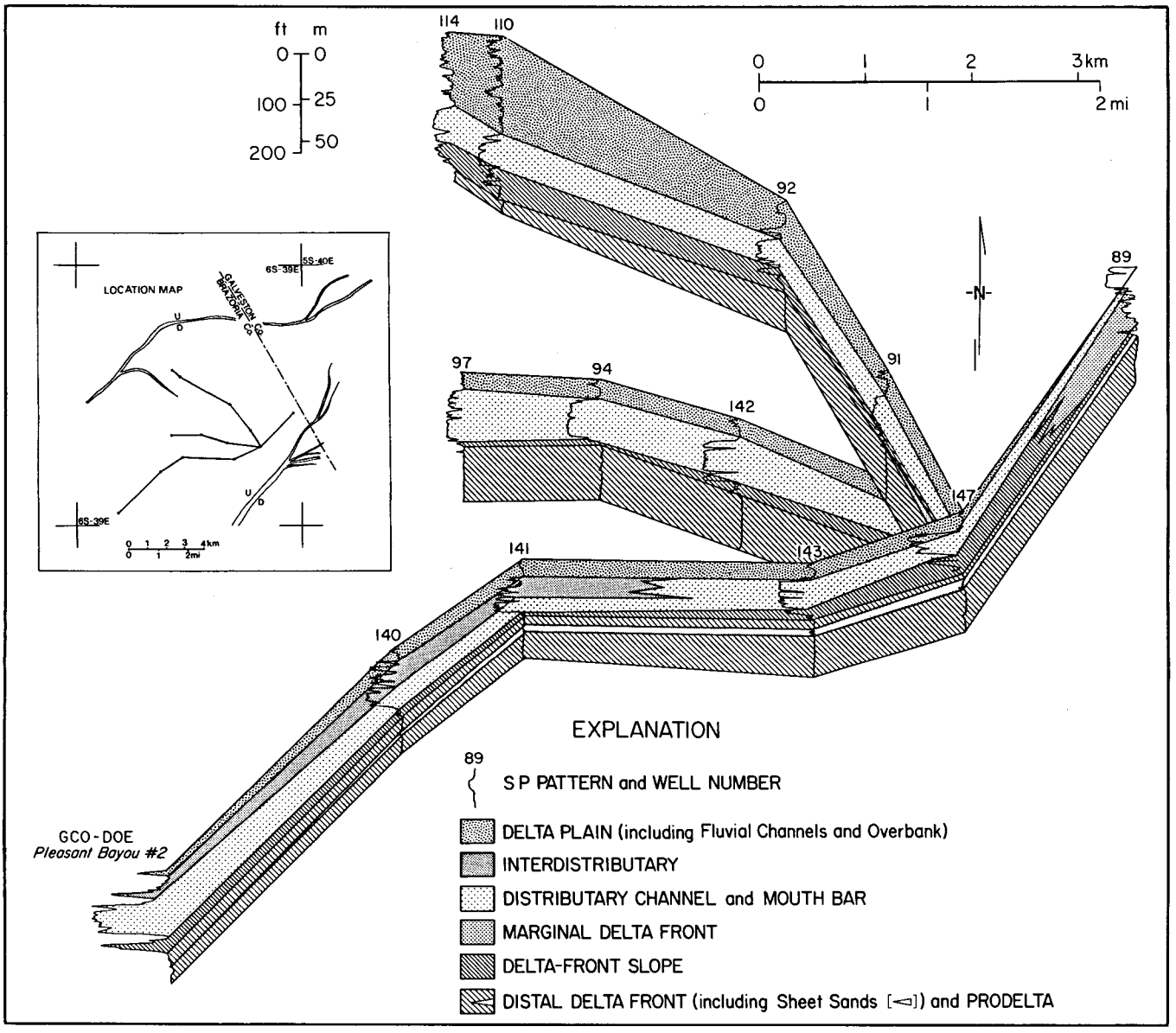


*Figure 39.* Fence diagram showing the continuity of depositional units in the geopressured geothermal production interval. Delta-front sheet sands and distributary-mouth-bar and channel deposits are laterally persistent and constitute a more attractive target for exploration than the thin, impersistent sands of the delta plain and delta margin.

impersistent, fluvial sandstones of the delta plain. Similarly, thin, shaly sandstones of the reworked delta margin have a lower production potential than do continuous sand stringers (possibly deposited under storm-related conditions) of the distal delta front.

In addition to the influence of depositional geometry on reservoir continuity, vertical and lateral superposition of subenvironments creates heterogeneity in hydrocarbon and geothermal reservoirs. Thinly interbedded interdistributary mudstones and sandstones deposited upon laterally extensive distributary-channel and delta-front sandstones (fig. 39) inhibit vertical permeabilities in the potential reservoir, making positioning of wells and perforated intervals critical. Similarly, laterally continuous floodplain mudstones interbedded within fluvial sandstones of a high-constructive, lobate delta (fig. 40) increase the heterogeneity and reduce the continuity of a potential production interval (fig. 41). Distributary-mouth-bar sands in this lobate delta thicken and become more laterally persistent in a basinward direction but are not as extensive as sands in the previous example (fig. 39). This is possibly a result of positioning the cross sections in the proximal reaches of the delta and not in the region of maximum marine reworking of fluvial sediments. Marine reworking of the delta-front sands winnows the

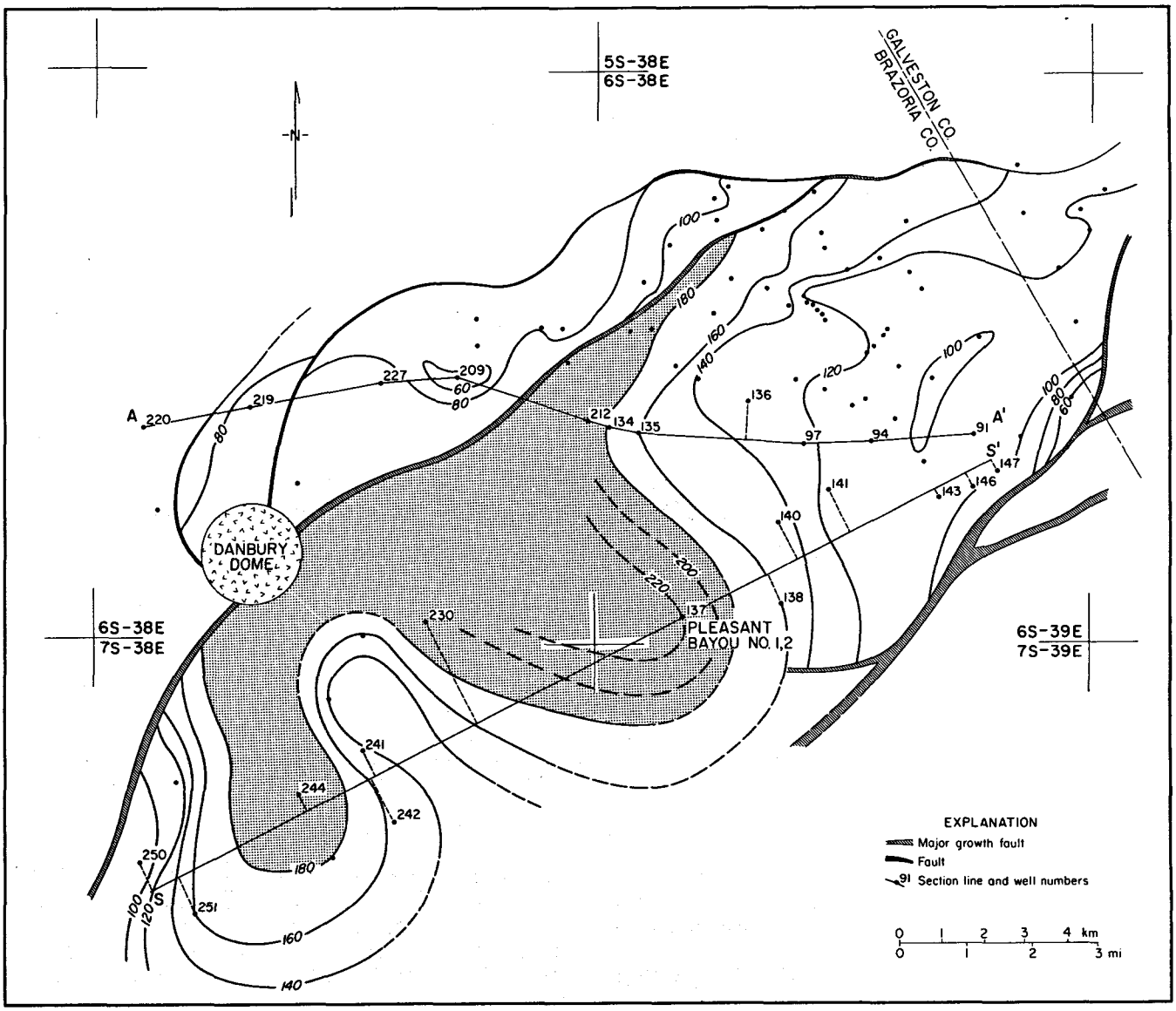


*Figure 40.* Lobate net-sand pattern of the T3 correlation interval and location of cross sections in figure 41.

finer fraction, creating clean, laterally persistent sheet sands in which inhomogeneities are minor. On a smaller scale, distributary-mouth-bar sands have been shown to have the coarsest grain size and to contain large primary sedimentary structures (fig. 33); as such, they compose the most favorable reservoir in the constructive-deltaic setting.

## Vertical Patterns of Pore Properties

Porosity and permeability values reported for modern sands (Pryor, 1973; Fulton, 1975) and outcrops (Hutchinson and others, 1961; Polasek and Hutchinson, 1967) and by whole-core analyses (figs. 24, 32 through 35) provide a wealth of data for interpreting vertical changes in pore properties. Earlier researchers relied on nonuniform variants and statistical (Monte Carlo) techniques to describe and represent permeability in reservoir models because variations were thought to be random (Warren and others, 1961). Polasek and Hutchinson (1967) measured permeabilities of seven vertical outcrop sections in the Cretaceous Almond sandstone and concluded that differences were random. However, reexamination of their data reveals definite permeability trends dipping across the outcrop at 1 degree (apparent structural dip?) and having cycles of higher and lower permeability about 15 to 20 ft thick. Reevaluation of pore properties in this report using depositional models aids prediction of variability, which previously was considered unpredictable.

Porosity and permeability are not directly related; however, vertical trends of porosity and permeability within sandstones are remarkably consistent and form repetitive patterns. Of the six patterns documented (fig. 42), five are systematic — (1) upward increase,

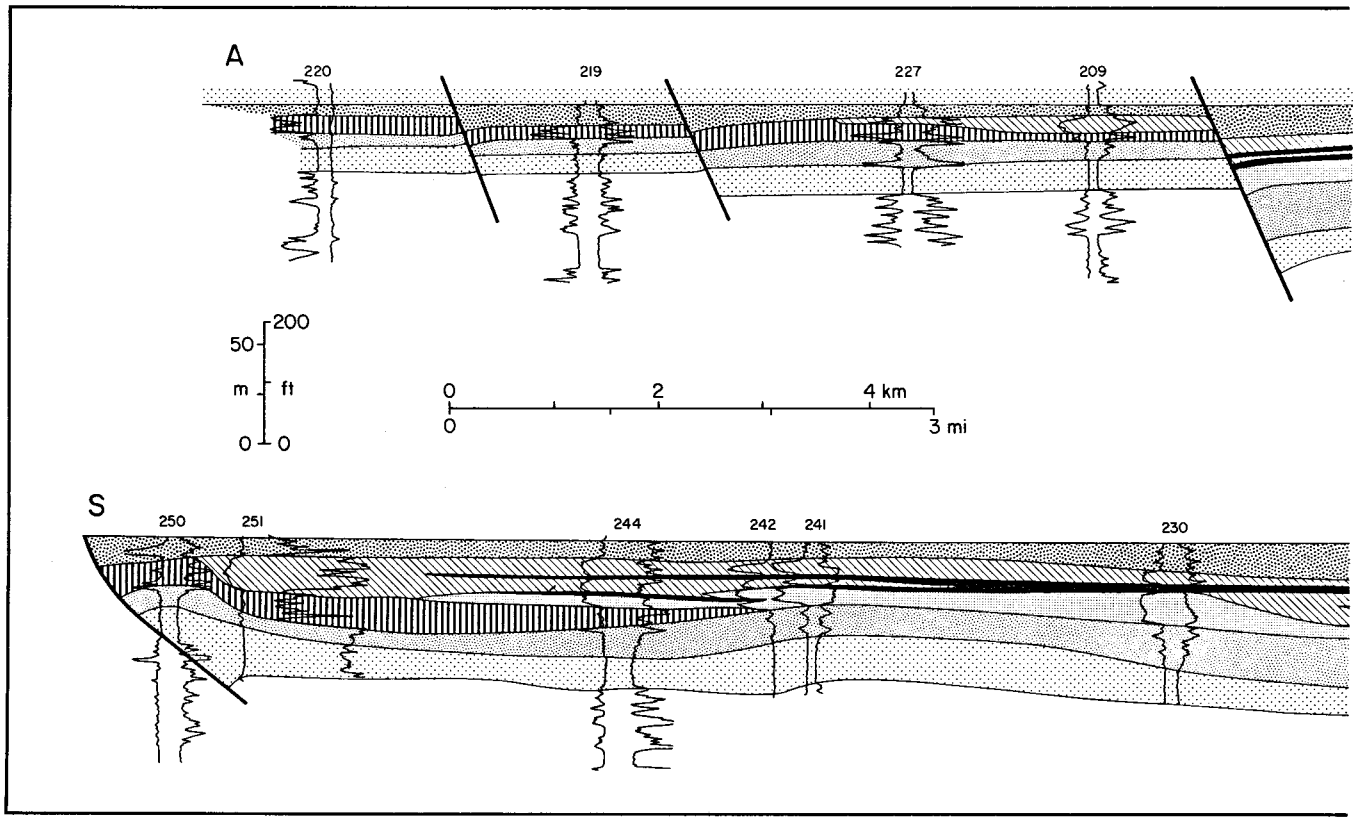


*Figure 41.* Cross sections through the T3 correlation interval. Note the thickening of the assemblage across growth faults, the relative persistence of

(2) upward decrease (fig. 33), (3) central increase, (4) central decrease (fig. 35), and (5) uniformly low values (fig. 34) — whereas pattern 6 is irregular and a composite (fig. 32) of the other types.

In their simplest form, patterns 1 and 2 reflect upward-coarsening and upward-fining sequences; pattern 3 usually represents original pore trends or tight streaks associated with the upper and lower sandstone boundaries; pattern 5 represents late-stage cementation, occlusion of primary porosity, and drastic reduction of permeability; pattern 6 is usually associated with thick amalgamated sandstones, each having variable internal properties. Higher porosities and permeabilities near the sandstone margin, shown by pattern 4, are difficult to explain. Perhaps they reflect alteration and leaching by ground water. They also may represent an inverse relation to original textural properties such that clean, well-sorted sands were tightly cemented, whereas moderately sorted sands were less affected by cementation. In any case, pattern 4 is the least common.

## Pore Properties and Stratification

Judging from limited published data (Mast and Potter, 1963; Pryor, 1973) and available core analyses, porosity and permeability are indirectly related to internal stratification because sedimentary structures are partly controlled by grain size. Mast and Potter (1963), among others, found that permeability is highest parallel to stratification and grain-fabric orientation; therefore, high vertical permeabilities may indicate fracturing across bedding surfaces. In modern sands, a relative ranking of permeabilities from highest to lowest corresponds to (1) foresets and large-scale troughs, (2) horizontal and low-angle, parallel-inclined stratification, and (3) small-scale troughs and ripple cross-stratification. Similar conclusions can be drawn from the data of Hewitt and Morgan (1965), Polasek and Hutchinson (1967), and Dodge and others (1971). These relations, however, should be considered in the context of properties of surrounding sediments because the effective permeability of a given unit is largely determined by the lower permeabilities of the bounding sediments (Pryor, 1973).

# *FREQUENCY AND ARRANGEMENT OF FLOW BARRIERS*

According to Polasek and Hutchinson (1967), fluid movement is largely determined by the distribution of sand and shaly sand rather than by permeability variations within a sand. Therefore, gross arrangement

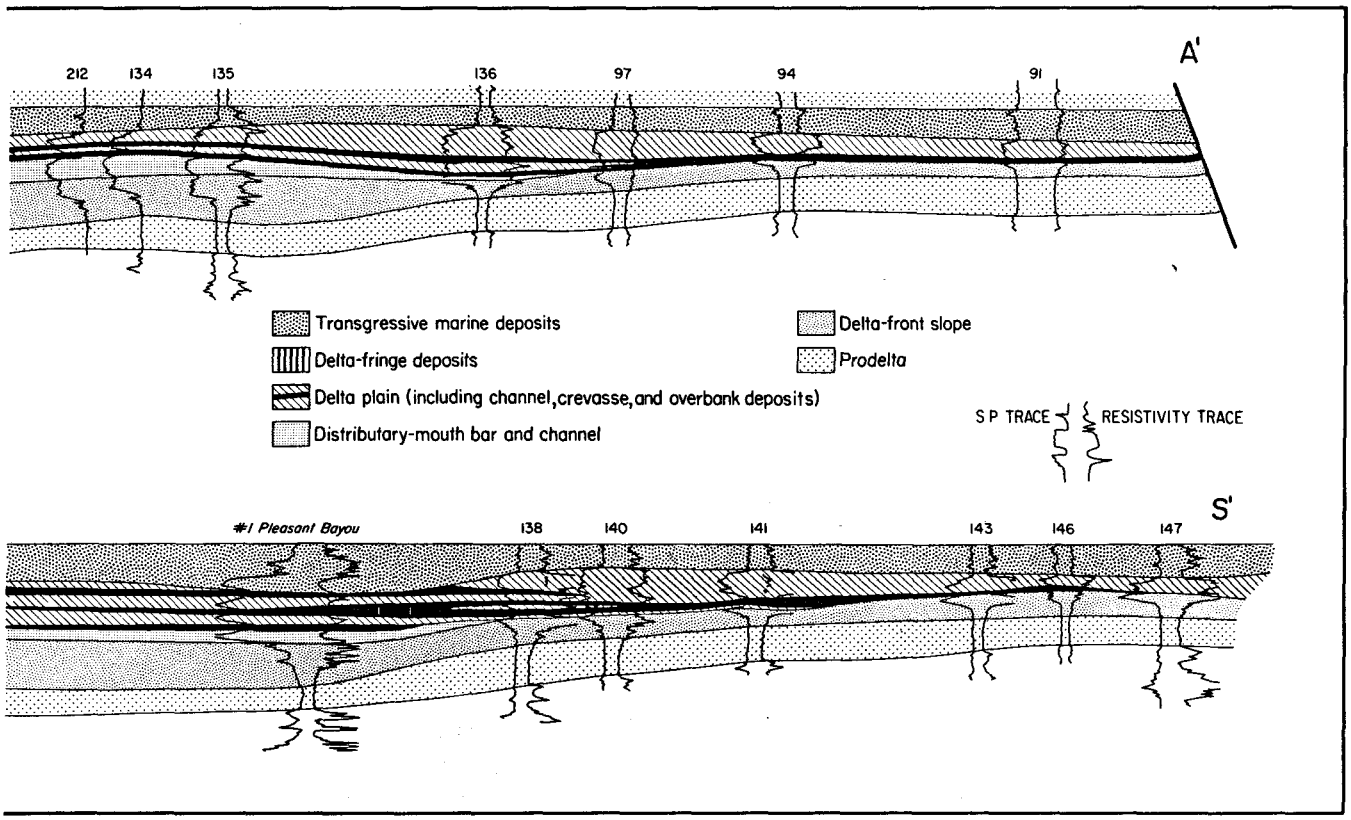


the distributary-mouth-bar and channel facies, and the presence of mudstone drapes, which inhibit vertical fluid flow in the delta-plain deposits.

of sediment types predicted from sedimentary models may aid in evaluating reservoir performance.

The distribution of pore spaces and flow barriers can be related to the depositional environment interpreted from SP and short-normal resistivity curves (Sneider and others, 1977). Establishing these relationships allows better prediction of flow barriers, of their effect on reservoir production, and of the probable locations of isolated segments within a sand body that remain undrained during primary production.

Porosity and permeability variations in fluvial sandstones are slightly more predictable in fine-grained, mixed-load or suspended-load channels than in coarse-grained, bed-load channels because channel deposits of mixed-load and suspended-load streams typically fine upward. The high percentage of silt and clay transported by these streams gives rise to a broad range of grain sizes; these grains are mixed and sorted at various stages of stream discharge. Resulting assemblages of sedimentation units are commonly graded, or at least capped, by numerous clay drapes that are preserved as discontinuous shale partings. The frequency of shale layers and the proportion of silt and clay gradually increase upward, resulting in upward decreases in porosity and permeability and in vertical continuity.

In contrast, streams transporting coarse-grained sediment do not exhibit systematic vertical changes in size; hence, the relative positions of major permeability changes are uncertain. According to Pryor's (1973) data, abrupt decreases in porosity and permeability occur at the tops and bottoms of coarse-grained channel deposits. The lower permeabilities near the channel base are caused by intercalated mud formed by rapid fall during flood stage. These slack-water deposits within the thalweg are commonly eroded or completely removed during subsequent stages of flashy discharge, but some are preserved as thin shale lenses or wedges. Coarse-grained river deposits usually are poorly sorted and contain large-scale sedimentary structures. These conditions lead to tortuous flow paths because dip directions in the master bedding and sedimentary structures are variable and often opposite.

Percent sand, sand thickness, and transmissivity (product of reservoir thickness and permeability) decrease toward the margins of fluvial and distributary channels. Transmissivity varies greatly within the sand body (Houser and Neasham, 1976) because of changes in grain fabric and because of truncations and other bedding disruptions.

The commonly recognized upward-coarsening sequence attendant with delta progradation provides a basis for predicting gross internal properties of delta-front and delta-margin sands. For the purpose of this discussion, a practical distinction is made between complete and incomplete progradational sequences. The

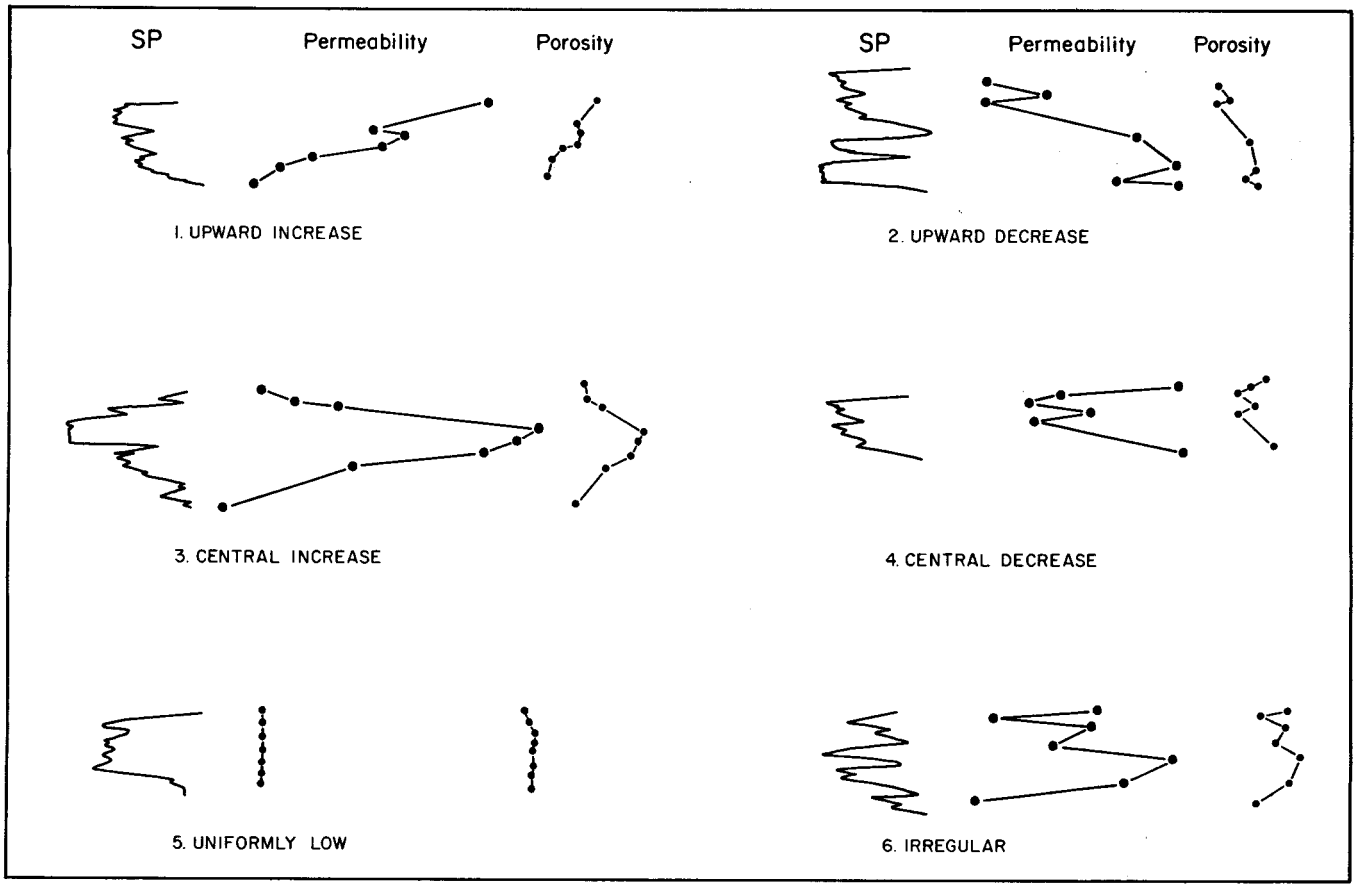


*Figure 42.* Generalized patterns of vertical changes in pore properties within a sand body.

former are characterized by superposition of distributary-channel sands over sands of delta-front or distributary-mouth origin. The latter are characterized by delta-front sands overlain by shelf or delta-plain muds because of distributary abandonment. The significance of this difference is that the number and thickness of shale interbeds decrease upward in a complete progradational sequence, whereas delta-front sands may be overlain as well as underlain by interbedded sands and shales in an incomplete sequence.

Sorting improves and sand percent and sand-bed thickness increase upward in delta-front and delta-fringe deposits. Both sands are highly continuous, but delta-fringe sands have poor vertical permeability because of numerous laterally extensive clay beds. Sands become more poorly sorted, sand beds thin, and grain sizes decrease away from distributary channels. These physical changes cause a reduction in the bulk permeability of delta-fringe deposits (Houser and Neasham, 1976).

Vertical trends of porosity and permeability in barriers and strandplains are somewhat analogous to those found in delta fronts and distributary-mouth bars because of upward-coarsening textures, but they are different in at least two respects. First, the strong wave action and sediment sorting along barrier and strandplain shorelines produce cleaner and better sorted sands, and practically no mud is deposited on the upper shoreface and beach. Second, the lateral continuity of thick barrier and strandplain sand bodies far exceeds that of most delta fronts and distributary-mouth bars (tables 1 and 2). Consequently, in their unaltered state, barriers and strandplains possess the greatest lateral and vertical continuity of all the common sandstone types.

Outer shelf and slope sands are best developed in submarine channel and fan complexes. The distribution of low-permeability zones in these deep-water sandstones is similar to the spatial patterns in deltaic deposits. The thickest and cleanest sands are associated with submarine channel deposits that are laterally restricted and vertically separated by shaly intervals. Thin-bedded sands associated with the submarine fan deposits are remarkably uniform in thickness and laterally continuous over broad areas. However, vertical continuity in these sandstones is extremely low because the thickness of the interbedded shales is comparable to or greater than that of the sand layers. Turbidites are also characterized by some contorted and bioturbated zones having extremely low permeabilities. Except for the thick channel sands, deeply buried turbidites generally make poor reservoirs for production of liquids.

# IMPLICATIONS FOR GEOPRESSURED FLUID PRODUCTION

In their ability to meet energy production requirements, sand bodies can be ranked according to sand volume, lateral continuity, and internal heterogeneity. Ideal reservoirs consist of large, laterally extensive sand bodies having minimal flow interference from internal permeability barriers. Some natural reservoirs approach this high standard, but most are less than ideal because of external and internal discontinuities. In theory, barrier and strandplain sandstones oriented parallel to the regional structural fabric approximate the ideal reservoir. These deposits also have high permeabilities in the upper part of the sand body, an added advantage for production of gravity-segregated fluids such as oil and gas.

Fluvial sandstones oriented normal to the regional structural fabric are the second most favorable. These meanderbelt systems may contain substantial quantities of sand interconnected throughout the valley-fill network. Distributary-channel sands and associated delta-front and distributary-mouth-bar sands oriented normal to depositional strike rank a close third. The channel and bar-finger sands are commonly thicker and narrower than alluvial channels, although they exhibit similar pore properties. Favorable production potential decreases markedly toward the delta fringe and distal delta front.

Submarine channels and fans oriented normal to the regional structural fabric provide the least volume and lateral continuity of the common sandstone types. A disadvantage of these and other channel sandstones is that highest permeabilities are often associated with the coarsest grain sizes and the largest sedimentary structures found near the channel base. Although channel sands make excellent reservoirs when completely filled with hydrocarbons, they are less suitable when only partially filled because reservoir continuity and permeabilities decrease toward the top of the sand body. However, basal channel sands are suitable for solution gas production if gravity segregation of the fluids is unimportant.

This relative ranking of sand bodies is greatly simplified, and undoubtedly there are many exceptions. However, the ranking can serve as a guide to drainage efficiency on the basis of shale content. In general, upper shoreface and beach sands should provide greater lateral continuity, fewer restrictions to flow, and consequently greater drainage efficiency than distal delta-front sands. Inhomogeneities within the sand body account in part for the poor agreement between reservoir volumes estimated from geological maps and those calculated from production data.

# ACKNOWLEDGMENTS

This work was funded by the U.S. Department of Energy, Division of Geothermal Energy, under Contract No. DE-AC08-79ET27111. Clarence Albers performed a detailed micropaleontological analysis of selected samples of the GCO-DOE Pleasant Bayou cores. We appreciate the support provided by personnel at the Bureau of Economic Geology who assisted in preparing this report. L. Frank Brown, Jr., Shirley P. Dutton, Robert J. Finley, Graham E. Fogg, and Stephen C. Ruppel reviewed the manuscript and made many helpful suggestions. The report was typed by Margaret T. Chastain and Dorothy C. Johnson and typeset by Phyllis J.Hopkins under the direction of Lucille Harrell. Illustrations were prepared by John T. Ames, Mark T. Bentley, Thomas M. Byrd, Margaret R. Day, Margaret L. Evans, Richard P. Flores, Jeffrey Horowitz, and Jamie McClelland under the direction of Dan F. Scranton. Text illustration photography was done by James A. Morgan. The report was edited by Jean Trimble and designed by Jamie S. Haynes.

# REFERENCES

Alpay, O. A., 1972, A practical approach to defining reservoir heterogeneity: Journal of Petroleum Technology, v. 24, p. 841-848.

Bebout, D. G., Loucks, R. G., and Gregory, A. R., 1978, Frio sandstone reservoirs in the deep subsurface along the Texas Gulf Coast: The University of Texas at Austin, Bureau of Economic Geology Report of Investigations No. 91, 92 p.

—— 1980, Geological aspects of Pleasant Bayou geopressured geothermal test well, Austin Bayou prospect, Brazoria County, Texas, *in* Dorfman, M. H., and Fisher, W. L., eds., Proceedings, fourth geopressured geothermal energy conference: The University of Texas at Austin, Center for Energy Studies, p. 11-45.

Bebout, D. G., Weise, B. R., Gregory, A. R., and Edwards, M. B., 1982, Wilcox sandstone reservoirs in the deep subsurface along the Texas Gulf Coast: their potential for production of geopressured geothermal energy: The University of Texas at Austin, Bureau of Economic Geology Report of Investigations No. 117, 125 p.

Berg, R. R., and Davies, D. K., 1968, Origin of Lower Cretaceous muddy sandstone at Bell Creek field, Montana: American Association of Petroleum Geologists Bulletin, v. 52, p. 1888-1898.

Berg, R. R., and Findley, R. L., 1973, Deep-water interpretation of upper Wilcox sandstones from core study, Katy field, Texas: Gulf Coast Association of Geological Societies Transactions, v. 23, p. 259-265.

Berg, R. R., Marshall, W. D., and Shoemaker, P. W., 1979, Structural and depositional history, McAllen Ranch field, Hidalgo County, Texas: Gulf Coast Association of Geological Societies Transactions, v. 29, p. 24-83.

Berg, R. R., and Powers, B. K., 1980, Morphology of turbidite-channel reservoirs, lower Hackberry (Oligocene), southeast Texas: Gulf Coast Association of Geological Societies Transactions, v. 30, p. 41-48.

Berg, R. R., and Tedford, F. J., 1977, Characteristics of Wilcox gas reservoirs, Northeast Thompsonville field, Jim Hogg and Webb Counties, Texas: Gulf Coast Association of Geological Societies Transactions, v. 27, p. 6-19.

Bernard, H. A., Major, C. F., Jr., Parrot, B. S., and LeBlanc, R. J., 1970, Recent sediments of southeast Texas—a field guide to the Brazos alluvial and deltaic plains and Galveston barrier island complex: The University of Texas at Austin, Bureau of Economic Geology Guidebook 11, 83 p.

Boardman, C. R., 1980, Implications of geopressured aquifer volumes obtained from pressure and production records of selected Gulf Coast geopressured gas fields: C. K. Geo-Energy, Las Vegas, Report to the U.S. Department of Energy, unpaginated.

Bouma, A. H., 1962, Sedimentology of some flysch deposits—a graphic approach to facies interpretations: Amsterdam, Elsevier, 168 p.

——— 1968, Distribution of minor structures in Gulf of Mexico sediments: Gulf Coast Association of Geological Societies Transactions, v. 18, p. 26-33.

Boyd, D. R., and Dyer, B. R., 1966, Frio barrier bar system of South Texas: American Association of Petroleum Geologists Bulletin, v. 50, p. 170-178.

Brown, L. F., Jr., Brewton, J. L., Evans, T. J., McGowen, J. H., White, W. A., Groat, C. G., and Fisher, W. L., 1980, Environmental geologic atlas of the Texas Coastal Zone—Brownsville-Harlingen area: The University of Texas at Austin, Bureau of Economic Geology, 140 p.

Casey, S. R., and Cantrell, R. B., 1941, Davis sand lens, Hardin field, Liberty County, Texas, *in* Stratigraphic type oil fields: American Association of Petroleum Geologists Special Publication, p. 564-599.

Chierici, G. L., Clucci, G. M., Sclocchi, G., and Terzi, L., 1978, Water drive from interbedded shale compaction in super-pressured gas reservoirs—model study: Journal of Petroleum Technology, v. 30, p. 937-944.

Chuber, S., 1972, Milbur (Wilcox) field, Milam and Burleson Counties, Texas: American Association of Petroleum Geologists Memoir 16, p. 399-405.

Coleman, J. M., and Garrison, L. E., 1977, Geological aspects of marine slope stability, northwestern Gulf of Mexico: Marine Geotechnology, v. 2, p. 9-44.

Conatser, W. E., 1971, Grand Isle: a barrier island in the Gulf of Mexico: Geological Society of America Bulletin, v. 82, p. 3049-3068.

Craft, B. C., and Hawkins, M. F., 1959, Applied petroleum reservoir engineering: Englewood Cliffs, New Jersey, Prentice-Hall, 437 p.

Curtis, D. M., 1970, Miocene deltaic sedimentation, Louisiana Gulf Coast, *in* Deltaic sedimentation, modern and ancient: Society of Economic Paleontologists and Mineralogists Special Publication 15, p. 293-308.

DePaul, G. J., 1980, Environment of deposition of upper Wilcox sandstones, Katy gas field, Waller County, Texas: Gulf Coast Association of Geological Societies Transactions, v. 30, p. 61-70.

Dickinson, K. A., Berryhill, H. L., Jr., and Holmes, C. W., 1972, Criteria for recognizing ancient barrier coastlines, *in* Rigby, J. K., and Hamblin, W. K., eds., Recognition of ancient sedimentary environments: Society of Economic Paleontologists and Mineralogists Special Publication 16, p. 192-214.

Dodge, C. F., Holler, D. P., and Meyer, R. L., 1971, Reservoir heterogeneities of some Cretaceous sandstones: American Association of Petroleum Geologists Bulletin, v. 55, p. 1814-1828.

Dodge, M. M., and Posey, J. S., 1981, Structural cross sections, Tertiary formations, Texas Gulf Coast: The University of Texas at Austin, Bureau of Economic Geology Cross Sections.

Doyle, J. D., 1979, Depositional patterns of Miocene facies, Middle Texas Coastal Plain: The University of Texas at Austin, Bureau of Economic Geology Report of Investigations No. 99, 25 p.

Duggan, J. O., 1972, The Anderson "L"—an abnormally pressured gas reservoir in South Texas: Journal of Petroleum Technology, v. 24, p. 132-138.

Edwards, M. B., 1980, The Live Oak delta complex: an unstable shelf-edge delta in the deep Wilcox trend of South Texas: Gulf Coast Association of Geological Societies Transactions, v. 30, p. 71-79.

——— 1981, Upper Wilcox Rosita delta system of South Texas: growth-faulted shelf-edge deltas: American Association of Petroleum Geologists Bulletin, v. 65, p. 54-73.

Fisher, W. L., and Brown, L. F., Jr., 1972, Clastic depositional systems—a genetic approach to facies analysis: The University of Texas at Austin, Bureau of Economic Geology, 211 p.

Fisher, W. L., Brown, L. F., Jr., Scott, A. J., and McGowen, J. H., 1969, Delta systems in the exploration for oil and gas: The University of Texas at Austin, Bureau of Economic Geology, 185 p.

Fisher, W. L., and McGowen, J. H., 1967, Depositional systems in Wilcox Group of Texas and their relationship to occurrence of oil and gas: Gulf Coast Association of Geological Societies Transactions, v. 17, p. 105-125.

Fisk, H. N., 1955, Sand facies of recent Mississippi delta deposits: Proceedings, fourth World Petroleum Congress, section 1-C, p. 377-398.

——— 1959, Padre Island and the Laguna Madre Flats, coastal South Texas, *in* Russell, R. H., chm., Proceedings, second Coastal Geology Conference, Louisiana State University, p. 103-151.

——— 1961, Bar-finger sands of Mississippi delta, *in* Peterson, J. A., and Osmond, J. C., eds., Geometry of sandstone bodies: American Association of Petroleum Geologists, p. 29-52.

Frazier, D. E., 1967, Recent deltaic deposits of the Mississippi River; their development and chronology: Gulf Coast Association of Geological Societies Transactions, v. 17, p. 287-315.

——— 1974, Depositional episodes: their relationship to the Quaternary stratigraphic framework in the northwestern portion of the Gulf Basin: The University of Texas at Austin, Bureau of Economic Geology Geological Circular 74-1, 28 p.

Frazier, D. E., and Osanik, A., 1961, Point-bar deposits, Old River Locksite, Louisiana: Gulf Coast Association of Geological Societies Transactions, v. 11, p. 121-137.

Freeman, J. C., 1949, Strandline accumulation of petroleum, Jim Hogg County, Texas: American Association of Petroleum Geologists Bulletin, v. 33, p. 1260-1270.

Fulton, K. J., 1975, Subsurface stratigraphy, depositional environments, and aspects of reservoir continuity—Rio Grande delta, Texas: University of Cincinnati, Ph.D. dissertation, 330 p.

Galloway, W. E., 1968, Depositional systems of the lower Wilcox Group—north-central Gulf Coast Basin: Gulf Coast Association of Geological Societies Transactions, v. 18, p. 275-289.

Galloway, W. E., Hobday, D. K., and Magara, K., 1982, Frio Formation of the Texas Gulf Coast Basin—depositional

systems, structural framework, and hydrocarbon origin, migration, distribution, and exploration potential: The University of Texas at Austin, Bureau of Economic Geology Report of Investigations No. 122, 78 p.

Garg, S. K., 1980, Shale recharge and production behavior of geopressured reservoirs: Geothermal Research Council Transactions, v. 4, p. 325-328.

Gotautas, V. A., Gordon, G. E., Johnson, J., and Lee, C., 1972, Southwest Lake Arthur field, Cameron Parish, Louisiana, *in* King, R. E., ed., Stratigraphic oil and gas fields—classification, exploration methods, and case histories: American Association of Petroleum Geologists Memoir 16, p. 389-398.

Gould, H. R., 1970, The Mississippi delta complex, *in* Morgan, J. P., ed., Deltaic sedimentation, modern and ancient: Society of Economic Paleontologists and Mineralogists Special Publication 15, p. 3-30.

Gregory, J. L., 1966, A lower Oligocene delta in the subsurface of southeastern Texas: Gulf Coast Association of Geological Societies Transactions, v. 16, p. 227-241.

Halbouty, M. T., and Barber, T. D., 1961, Port Acres and Port Arthur fields, Jefferson County, Texas: Gulf Coast Association of Geological Societies Transactions, v. 11, p. 225-234.

Hartman, J. A., 1972, G2 channel sandstone, Main Pass, Block 35 field, offshore Louisiana: American Association of Petroleum Geologists Bulletin, v. 56, p. 554-558.

Hartman, J. A., and Paynter, D. D., 1979, Drainage anomalies in Gulf Coast Tertiary sandstones: Journal of Petroleum Technology, v. 31, p. 1313-1322.

Hewitt, C. H., and Morgan, J. T., 1965, The Fry in situ combustion test—reservoir characteristics: Journal of Petroleum Technology, v. 17, p. 337-342.

Houser, J. F., and Neasham, J. W., 1976, Bed continuity and permeability variations of recent deltaic sediments (abs.): American Association of Petroleum Geologists Bulletin, v. 60, p. 681.

Hutchinson, C. A., Jr., Dodge, C. F., and Polasek, T. L., 1961, Identification, classification and prediction of reservoir nonuniformities affecting production operations: Journal of Petroleum Technology, v. 13, p. 223-229.

Law, J., 1944, A statistical approach to the interstitial heterogeneity of sand reservoirs: Journal of Petroleum Technology, T. P. 1732, p. 1-20.

LeBlanc, R. J., Jr., 1977, Distribution and continuity of sandstone reservoirs, parts 1 and 2: Journal of Petroleum Technology, v. 29, p. 776-804.

Loucks, R. G., 1979, Sandstone distribution and potential for geopressured geothermal energy production in the Vicksburg Formation along the Texas Gulf Coast: The University of Texas at Austin, Bureau of Economic Geology Geological Circular 79-4, 27 p.

Loucks, R. G., Richmann, D. L., and Milliken, K. L., 1981, Factors controlling reservoir quality in Tertiary sandstones and their significance to geopressured geothermal production: The University of Texas at Austin, Bureau of Economic Geology Report of Investigations No. 111, 41 p.

Martyn, P. F., and Sample, C. H., 1941, Oligocene stratigraphy of East White Point field, San Patricio and Nueces Counties, Texas: American Association of Petroleum Geologists Bulletin, v. 25, p. 1967-2009.

Mast, R. F., and Potter, P. E., 1963, Sedimentary structures, sand-shape fabrics, and permeability: Journal of Geology, part 2, v. 71, p. 548-565.

Milliken, K. L., Land, L. S., and Loucks, R. G., 1981, History of burial diagenesis determined from isotopic geochemistry, Frio Formation, Brazoria County, Texas: American Association of Petroleum Geologists Bulletin, v. 65, p. 1397-1413.

Morton, R. A., and Donaldson, A. C., 1978, The Guadalupe River and delta of Texas—a modern analogue for some ancient fluvial-deltaic systems, *in* Miall, A. D., ed., Fluvial sedimentology: Canadian Society of Petroleum Geologists Memoir 5, p. 773-787.

Morton, R. A., and McGowen, J. H., 1980, Modern depositional environments of the Texas Coast: The University of Texas at Austin, Bureau of Economic Geology Guidebook 20, 167 p.

Morton, R. A., Winker, C. D., and Garcia, D. D., 1980, Seismic studies in Austin-Pleasant Bayou and Cuero Prospects—a summary of research activities: The University of Texas at Austin, Bureau of Economic Geology, Report to the U.S. Department of Energy, 57 p.

Nanz, R. H., Jr., 1954, Genesis of Oligocene sandstone reservoir, Seeligson field, Jim Wells and Kleberg Counties, Texas: American Association of Petroleum Geologists Bulletin, v. 38, p. 96-117.

Oomkens, E., 1970, Depositional sequences and sand distribution in the postglacial Rhône delta complex, *in* Morgan, J. P., ed., Deltaic sedimentation, modern and ancient: Society of Economic Paleontologists and Mineralogists Special Publication 15, p. 198-212.

Overbey, W. K., Jr., and Henniger, B. R., 1971, History, development, and geology of oil fields in Hocking and Perry Counties, Ohio: American Association of Petroleum Geologists Bulletin, v. 55, p. 183-203.

Paine, W. R., 1971, Petrology and sedimentation of the Hackberry sequence of southwest Louisiana: Gulf Coast Association of Geological Societies Transactions, v. 21, p. 37-55.

Polasek, T. L., and Hutchinson, C. A., Jr., 1967, Characterization of nonuniformities within a sandstone reservoir from a fluid mechanics standpoint: Proceedings, seventh World Petroleum Congress, v. 2, p. 397-407.

Pryor, W. A., 1973, Permeability-porosity patterns and variations in some Holocene sand bodies: American Association of Petroleum Geologists Bulletin, v. 57, p. 162-189.

Ramagost, B. P., and Farshad, F. F., 1981, P/Z abnormally pressured gas reservoirs: Society of Petroleum Engineers Fall Technical Conference, SPE10125, 6 p.

Scruton, P. C., 1960, Delta building and the deltaic sequence, *in* Recent sediments, northwestern Gulf of Mexico: American Association of Petroleum Geologists, p. 82-102.

Simons, D. B., Richardson, E. V., and Nordin, C. F., 1965, Sedimentary structures generated by flow in alluvial channels: Society of Economic Paleontologists and Mineralogists Special Publication 12, p. 34-52.

Smith, D. A., 1980, Sealing and non-sealing faults in Louisiana Gulf Coast salt basin: American Association of Petroleum Geologists Bulletin, v. 64, p. 145-172.

Sneider, R. M., Richardson, F. H., Paynter, D. D., Eddy, R. E., and Wyant, I. A., 1977, Predicting reservoir rock geometry and continuity in Pennsylvanian reservoirs, Elk City Field, Oklahoma: Journal of Petroleum Technology, v. 29, p. 851-866.

Solis Iriarte, R. F., 1980, Late Tertiary and Quaternary depositional systems in the subsurface of central coastal Texas: The University of Texas at Austin, Ph.D. dissertation, 155 p.

Southard, J. B., 1971, Representation of bed configurations in depth-velocity-size diagrams: Journal of Sedimentary Petrology, v. 41, p. 903-915.

Stuart, C. A., 1970, Geopressures: supplement to Proceedings, second Symposium on Abnormal Subsurface Pressure: Louisiana State University, 121 p.

Visher, G. S., Saitta, B. S., and Phares, R. S., 1971, Pennsylvanian delta patterns and petroleum occurrences in eastern Oklahoma: American Association of Petroleum Geologists Bulletin, v. 55, p. 1206-1230.

Walker, R. G., 1979, Facies models: Geological Association of Canada Reprint Series No. 1, 211 p.

Wallace, W. E., 1969, Water production from abnormally pressured gas reservoirs in south Louisiana: Journal of Petroleum Technology, v. 21, p. 969-982.

Warren, J. E., Skiba, F. F., and Price, S. H., 1961, An evaluation of the significance of permeability measurements: Journal of Petroleum Technology, v. 13, p. 739-744.

Weise, B. R., Jirik, L. A., Hamlin, H. S., Hallam, S. L., Edwards, M. B., Schatzinger, R. A., Tyler, N., and Morton, R. A., 1981, Geologic studies of geopressured and hydropressured zones in Texas: supplementary tasks: The University of Texas at Austin, Bureau of Economic Geology, Report prepared for Gas Research Institute, 120 p.

Williams, C. E., Travis, L. R., and Hoover, E. M., 1974, Depositional environments interpreted from stratigraphic, seismic and paleo-environmental analysis, upper Wilcox, Katy field, Texas: Gulf Coast Association of Geological Societies Transactions, v. 24, p. 129-137.

Winker, C. D., 1979, Late Pleistocene fluvial-deltaic deposition, Texas Coastal Plain and shelf: The University of Texas at Austin, Master's thesis, 187 p.

Winker, C. D., Morton, R. A., Ewing, T. E., and Garcia, D. D., in press, Depositional setting, structural style, and sandstone distribution in three geopressured geothermal areas, Texas Gulf Coast: The University of Texas at Austin, Bureau of Economic Geology Report of Investigations.

Woltz, D., 1980, Block 25 Field, Chandeleur Sound, St. Bernard Parish, Louisiana: Gulf Coast Association of Geological Societies Transactions, v. 30, p. 243-249.

Wood, A. W., 1962, Northeast Thompsonville field, *in* Contributions to geology of South Texas: South Texas Geological Society, p. 241-245.

Young, L. F., Jr., 1966, Northeast Thompsonville field, South Texas, key to future exploration for downdip Wilcox production: American Association of Petroleum Geologists Bulletin, v. 50, p. 505-517.

# APPENDIX A: Metric Conversion Factors

| UNIT | | CONVERSION FACTOR | | METRIC EQUIVALENT |
|---|---|---|---|---|
| foot (ft) | × | 0.305 | = | meter (m) |
| square foot ($ft^2$) | × | 0.093 | = | square meter ($m^2$) |
| cubic foot ($ft^3$) | × | 0.028 | = | cubic meter ($m^3$) |
| mile (mi) | × | 1.609 | = | kilometer (km) |
| square mile ($mi^2$) | × | 2.590 | = | square kilometer ($km^2$) |
| barrel (bbl) | × | 0.159 | = | cubic meter ($m^3$) |
| pounds per square inch (psi) | × | 6.895 | = | kilopascals (kPa) |
| degrees Fahrenheit (°F) | | (°F–32)/1.8 | = | degrees Celsius (°C) |